Acoustooptical spectrum analysis modeling

Carmody, Michael James; Powers, J. P.

ACOUSTOOPTICAL SPECTRUM ANALYSIS MODELING

Michael James Carmody

NPS 62-81-033

NAVAL POSTGRADUATE SCHOOL
Monterey, California

THESIS

ACOUSTOOPTICAL SPECTRUM ANALYSIS MODELING

by

Michael J. Carmody

June 1981

Thesis Advisor: J. P. Powers

Approved for public release; distribution unlimited

Prepared for:
Naval Electronic Systems Command (ELEX 615)
Washington, DC 20360

UNCLASSIFIED

SECURITY CLASSIFICATION OF THIS PAGE (When Data Entered)

REPORT DOCUMENTATION PAGE		READ INSTRUCTIONS BEFORE COMPLETING FORM
1. REPORT NUMBER NPS-62-81-033	2. GOVT ACCESSION NO.	3. RECIPIENT'S CATALOG NUMBER
4. TITLE (and Subtitle) Acoustooptic Spectrum Analysis Modeling		5. TYPE OF REPORT & PERIOD COVERED Thesis Report; 1 Oct 80-30 Jun 81
		6. PERFORMING ORG. REPORT NUMBER
7. AUTHOR(s) Michael J. Carmody in conjunction with John P. Powers, Thesis Advisor		8. CONTRACT OR GRANT NUMBER(s)
9. PERFORMING ORGANIZATION NAME AND ADDRESS Naval Postgraduate School Monterey, California 93940		10. PROGRAM ELEMENT, PROJECT, TASK AREA & WORK UNIT NUMBERS
11. CONTROLLING OFFICE NAME AND ADDRESS Naval Electronic Systems Command (ELEX 615) Washington, DC 20360		12. REPORT DATE June 1981
		13. NUMBER OF PAGES 114 pages
14. MONITORING AGENCY NAME & ADDRESS(if different from Controlling Office)		15. SECURITY CLASS. (of this report) Unclassified
		15a. DECLASSIFICATION/DOWNGRADING SCHEDULE

16. DISTRIBUTION STATEMENT (of this Report)

Approved for public release; distribution unlimited

17. DISTRIBUTION STATEMENT (of the abstract entered in Block 20, if different from Report)

18. SUPPLEMENTARY NOTES

19. KEY WORDS (Continue on reverse side if necessary and identify by block number)

Bragg cell, acoustooptics, Spectrum Analyzer.

20. ABSTRACT (Continue on reverse side if necessary and identify by block number)

A summary of Bragg deflection theory and various approaches to direct detection acoustooptic spectrum analysis (AOSA) modeling is presented. A suitable model is chosen and extended to include the effects of diffraction efficiency, transducer efficiency, irradiance profiles of incident laser illumination, aperture size of the Bragg cell, and the acoustic attenuation experienced by the acoustic wavetrain generated by the input r-f signal. A Fortran program is developed to model the AOSA and predict the output image

DD FORM 1 JAN 73 1473 EDITION OF 1 NOV 65 IS OBSOLETE
S/N 0102-014-6601

UNCLASSIFIED

SECURITY CLASSIFICATION OF THIS PAGE (When Data Entered)

Item 20.

plane intensity profiles. A second version of the program includes a time variable permitting dynamic simulation of the system response.

Approved for public release; distribution unlimited

Acoustooptical Spectrum Analysis Modeling

by

Michael James Carmody
Lieutenant Commander, United States Navy
B.S., St. John's University, 1971

Submitted in partial fulfillment of the
requirements for the degree of

MASTER OF SCIENCE IN ELECTRICAL ENGINEERING

from the

NAVAL POSTGRADUATE SCHOOL
June 1981

ABSTRACT

A summary of Bragg deflection theory and various approaches to direct detection acoustooptic spectrum analysis (AOSA) modeling is presented. A suitable model is chosen and extended to include the effects of diffraction efficiency, transducer efficiency, irradiance profiles of incident laser illumination, aperture size of the Bragg cell, and the acoustic attenuation experienced by the acoustic wavetrain generated by the input r-f signal. A Fortran program is developed to model the AOSA and predict the output image plane intensity profiles. A second version of the program includes a time variable permitting dynamic simulation of the system response.

TABLE OF CONTENTS

LIST OF TABLES

LIST OF FIGURES

I. INTRODUCTION

A. OVERVIEW

Assessment of emergent technologies leads to a continuing focus on acoustooptical techniques for spectral analysis and filtering/excision [Ref. 1]. Integrated optics with distinctive advantages in size and weight easily meet the requirements for radar warning receivers. Bulk wave devices offer superior dynamic range, bandwidth, and resolution over integrated optical devices. Foreseeable applications include surveillance and electronic intelligence.

An acoustooptical spectrum analyzer transforms a wideband time domain signal into an optical spatially detected frequency domain signal. Removal of narrowband interference may be accomplished by optical excision techniques, to selectively notch filter unwanted spectral components. U. S. military applications in this area could greatly benefit from the speed of response and high quality interference rejection capabilities possible with these techniques. The potential of these techniques was recognized and led to the establishment of a joint NAVELEX 350/DARPA program to examine these areas.

The technical objectives of this effort were:

1. Survey potential applications and analyze technical requirements imposed by each.
2. Analyze alternative optical excision configurations and components.

3. Develop and procure major system components.

4. Fabricate and measure alternative broadband excisor configurations to verify analytical results.

5. Fabricate and field test a brassboard model.

6. Design a preliminary advanced development model.

The principal civilian contractor for this project is PROBE Systems, Inc. PROBE, assisted by the developmental efforts at the Naval Research Laboratory (NRL) and Naval Postgraduate School (NPS), was tasked with the attainment of these objectives. NRL's specific program assistance was the development of a photodichroic optical clipper to be evaluated by PROBE. The research summarized in this thesis is a continuation of research initiated as part of the NPS contribution to the development program.

B. THESIS OBJECTIVE

The objective of this work effort was the attainment of an understanding of the principles of direct detection acousto-optical spectrum analysis. Previous work at the Naval Postgraduate School resulted in the construction by Regan [Ref. 2] of a working laboratory acoustooptical spectrum analyzer and the subsequent modification of the existing equipment by Smith [Ref. 3] to function as an acoustooptical spectrum excisor (AOSE). The acoustooptical spectral excisor utilized optical excision, the effect of an object placed in that part of the optical path where the undesirable

frequency components have been spatially spread. The optical excision research included propagation considerations and diffraction by the obstacle. The effectiveness of the optical excisor in removing interference is dependent upon these factors and more fundamentally upon the ability of the deflected beam irradiance pattern to accurately represent the input r-f signal spectral components.

C. ACOUSTOOPTICAL SPECTRAL ANALYSIS

An acoustooptical spectrum analyzer (AOSA) consists of an acoustooptical light deflector (a Bragg cell), a coherent light source (a laser), and a detector. An input r-f signal excites a piezo-electric transducer mounted on the acoustic medium on the Bragg cell. This launches an acoustic wavetrain the length of the cell which modulates the refractive index of the interaction medium by the elasto-acoustic process. The modulated interaction material functions as a moving diffraction grating for the incident laser light. A one-dimensional angular pattern of diffracted beams is produced and focused on a photodetector array. The pattern replicates the spectral content of the original r-f signal. The intensity of the individual beams is directly proportional to the r-f signal component intensity. The deflection angles of the individual beams are proportional to the r-f signal frequency component. The detector array photosites video detect the incident beam patterns and, in a square law

fashion, convert the spectral information for electronic transmission to a display oscilloscope. Figure 1 shows the NPS laboratory AOSA. Figure 2 shows a typical oscilloscope display output from the system. Korpel [Ref. 4] includes a basics discussion on the theory of Bragg cell applications for acoustooptical spectrum analysis in an overview on acoustooptics.

D. SPECIFIC GOALS

There were three initial goals for this work. The first was the study of the factors affecting the Bragg cell deflection of incident laser light. The second was the analysis of the effect of these factors on the replication of the input r-f signal spectrum in the deflected beam pattern. The third was the development of a Fortran program that would model the acoustooptic spectrum analysis process.

1. Bragg Diffraction

The study and analysis of the factors affecting Bragg deflection was focused towards an understanding of the ability of the deflected beam pattern to faithfully replicate the spectral components of the input r-f signal. This knowledge was considered essential in order to construct a viable computer simulation model. A study of Bragg diffraction and the various approaches to modeling of the deflected beam irradiance profiles was undertaken. Previous works at NPS by Regan [Ref. 2] and Smith [Ref. 3] were used as

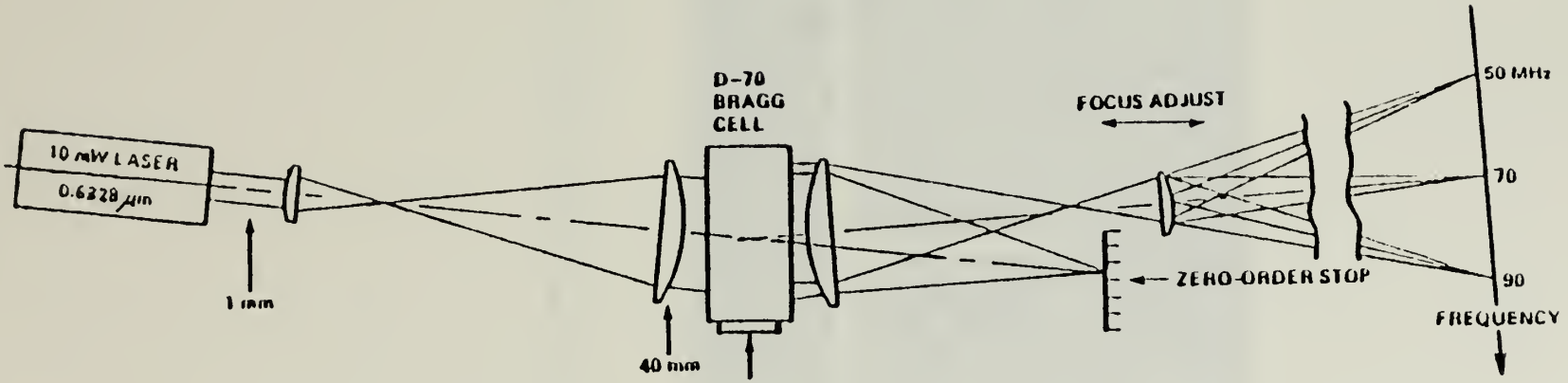

Figure 1. Direct Detection Acoustooptical Spectrum Analyzer

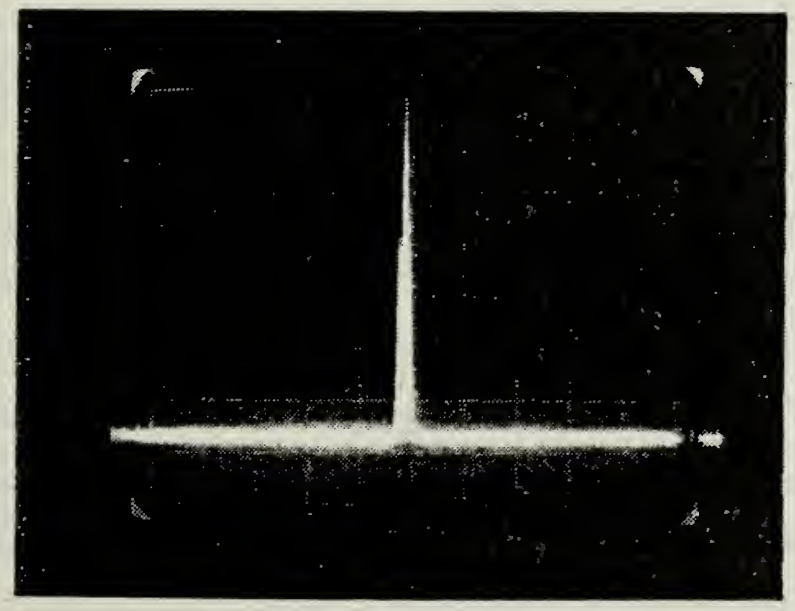

Figure 2. Oscilloscope Display of a 70 MHz Monotonic Input Signal to the NPS Acoustooptic Spectrum Analyzer

starting points. Bragg diffraction is traditionally theorized by use of complex coupled mode wave equations. The complexity of these equations rendered them unsuitable for the first order simulation sought. A study of other approaches was conducted to arrive at a method that would provide both adequate accuracy and a reasonable level of complexity.

2. Computer Model

An approach to the modeling of the AOSA was selected based on the work of Hecht [Ref. 5]. He shows the image plane intensity as the squared magnitude of the convolution of the spatial Fourier transform of an illumination function and the transform of the converted acoustic wave. Some modifications in the form of transmission factors were applied by algebraic multiplication. Hecht's illumination factor is a spatial weighting function composed of the optical amplitude profile, the optical aperture size of the Bragg cell, and the acoustic attenuation of the interaction material. The added transmission factors were the diffraction efficiency and the transducer efficiency.

A Fortran program was developed to model the AOSA given the specific physical parameters of the system and desired simulation requirements such as laser wavelength and laser beam profile. This program was used to study the quality of the replication of the r-f signal spectral components. The major thrust of this effort was to produce this model for

utilization with previously developed optical excision programs. While the program is configured to simulate various component deflectors, it was structured about the AOD-70 model Bragg deflector, manufactured by the IntraAction Corp., which is scheduled for future installation in the NPS laboratory AOSA. The AOD-70 Bragg deflector is constructed with high quality flint glass and Indium bonded Lithium Niobate stepped array transducers. It has a 50 MHz to 90 MHz bandwidth and a center frequency of 70 MHz.

During the development of the program it became apparent that the addition of a third dimension, time, to the model would significantly enhance the ability of the model to demonstrate the response of the AOSA under various simulation conditions. A second Fortran program was written, essentially a variation of the first, to provide this dynamic capability.

E. PERSPECTIVE

The application of both AOSA and AOSE techniques in wideband, high density signal environments is dependent on the accuracy of the diffracted beam profile in its replication of the input signal spectra. The classical model for determination of the diffracted beam profile is presented by Hecht [Ref. 5]. In a simplified form the diffracted beam profile is the convolution of the spatial Fourier transform of the illumination field incident on the Bragg cell and the

spatial transform of the generated acoustic wave within the cell. In detail both the illumination function and the acoustic wave are subject to modifying factors. The significant factors include diffraction efficiency, transducer efficiency, the irradiance profile of the incident laser light, the aperture size of the Bragg cell, and the acoustic attenuation experienced by the acoustic wave as it transits the cell. This thesis is an attempt to provide a more detailed model by incorporating these factors in a first order simulation to aid in the study of acoustooptic spectrum and excision techniques.

II. ACOUSTOOPTICAL SPECTRAL ANALYSIS MODELING

A. ACOUSTOOPTICAL INTERACTION THEORY

As an acoustic wave propagates in an isotropic material, it produces periodic modulation of the index of refraction by means of the elasto-acoustic effect. The interaction of incident light waves with acoustic waves is termed acousto-optical coupling and is traditionally modeled utilizing coupled wave equations. The basic theory of acoustooptical interaction in isotropic media was well developed prior to the advent of the laser. An excellent discussion of early theoretical work can be found in Ref. 6 by Born and Wolf. The advent of the laser stimulated research in acoustooptic interactions as devices were developed for the deflection and modulation of incident laser light. Development of superior acoustooptic materials and highly efficient broad-band transducers have given impetus to rapid advances in these acoustooptic applications.

Various models describing acoustooptic interaction have been proposed. A thin grating model (as it assumes a negligible depth for the sound field) was proposed by Rosenthal [Ref. 7], Korpel and associates [Ref. 8], and Lambert [Ref. 9]. The thin grating model is essentially a first order solution of the diffracted light problem. A second approach known as the physical optics model incorporates the Green's function

integral, as proposed by Gordon [Ref. 10]. An extremely rigorous model, the mathematics involved are quite complex. A third approach is termed the phenomenological geometrical optics model as proposed by Johnson [Ref. 11] and ranks midway in complexity between the thin grating and physical optics models.

For the purposes of this work a highly satisfactory approach to acoustooptical diffraction is found in a series of works by Chu, Kong, and Tamir [Refs. 12-16]. They have considered diffraction of arbitrary profiled optical beams by periodically modulated layers and have achieved closed form solutions for the resulting diffracted far-field intensity patterns. A summary of their results is presented below.

As shown in Fig. 3, a bounded beam is incident on a periodically modulated dielectric layer with permittivity of the form

$$\varepsilon(z) = \varepsilon_2(1 + M \cos 2\pi z/d) \qquad (1)$$

where

ε_2 = the relative permittivity of the slab in the absence of modulation

M = the modulation index

d = periodicity

The slab has thickness L and is bounded by a dielectric medium with relative permittivity ε_1 for $x \leq 0$ and ε_3 for $x \geq L$.

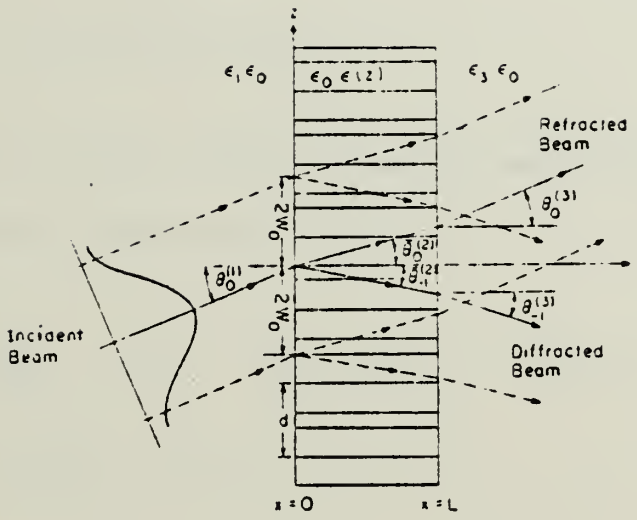

Figure 3. Bragg Diffraction Geometry (after Ref. 12)

The electric field of an incident beam may be represented as

$$E_{inc}(x,z) = \int G(\beta_o) \exp\left[j(\xi_o^{(1)} x + \beta_o z)\right] d\beta_o \tag{2}$$

with

$$\beta_o = (2\pi/\lambda)\sqrt{\varepsilon_1} \sin\theta \tag{3}$$

$$\xi_o^{(1)} = (2\pi/\lambda)\sqrt{\varepsilon_1} \cos\theta$$

$$= \sqrt{(2\pi/\lambda)^2 \varepsilon_1 - \beta_o^2} \tag{4}$$

$G(\beta_o)$ is the angular spectral amplitude of the incident beam at the entrance plane x=0.

$$G(\beta_o) = \frac{1}{2\pi} \int_{-\infty}^{\infty} E_{inc}(0,z) \exp(-j\beta_o z)\, dz$$

$$= \mathcal{F}\{E_{inc}(0,z)\} \tag{5}$$

Letting

$$E_{inc}(0,z) = F(z) \exp(jbz) \tag{6}$$

with

$$b = (2\pi/\lambda)\sqrt{\varepsilon_1} \sin\theta_o^{(1)}$$

$$= (2\pi/\lambda)\sqrt{\varepsilon_3} \sin\theta_o^{(3)} \tag{7}$$

where

$\theta_o^{(1)}$ = angle of incidence of beam axis

$\theta_o^{(3)}$ = angle of refracted beam

$F(z)$ = beam-profile at x=0

then Equation (5) becomes

$$G(\beta o) = \frac{1}{2\pi} \int F(z) \exp[-j(\beta_o - b)z]dz \tag{8}$$

Various beam profiles F(z) and their corresponding angular spectral functions $G(\beta_o)$ are listed in Table I.

For an optical beam at exactly Bragg incidence we have $\theta_o^{(1)} = \theta_B^{(1)}$ and $\theta_o^{(3)} = \theta_B^{(3)}$, and

$$b = (2\pi/\lambda)\sqrt{\varepsilon_1} \sin \theta_B^{(1)}$$

$$= (2\pi/\lambda)\sqrt{\varepsilon_3} \sin \theta_B^{(3)}$$

$$= \pi/d \tag{9}$$

The far field pattern for the Bragg deflected beam is given by

$$P(\theta) = G(\phi)\ T(\phi) \tag{10}$$

where

$$\phi = (2\pi/\lambda)\sqrt{\varepsilon_3} \sin \theta + \pi/d$$

$T(\phi)$ = is the complex transmission coefficient. A description of this coefficient may be found in Appendix C.

Thus the far-field pattern for a Bragg deflected beam is essentially the Fourier transform of the aperture field at the boundary of the layer modified slightly by a transmission factor.

While the results obtained by Chu, Kong, and Tamir are extremely useful in approaching the construction of a model for the direct detection acoustooptical spectrum analyzer, they are predicated on the periodic modulation of the layer by a single frequency acoustic wave.

TABLE I

Beam Profiles F(z) and Their Corresponding Angular Spectral Functions $G(\beta_o)$ [after Ref. 12]

Type	F(z)	$G(\beta_o)$
Gaussian	$\exp -\left(\frac{z}{2W}\right)^2$	$\frac{W_o}{\sqrt{\pi}} \exp -[(\beta_o - b)W_o]^2$
Square Wave	$P_{2W_o}(z) = \begin{cases} 1, \lvert z\rvert \leq 2W_o \\ 0, \lvert z\rvert > 2W_o \end{cases}$	$\frac{2W_o}{\pi} \frac{\sin[2(\beta_o - b)W_o]}{2(\beta_o - b)W_o}$
Triangle Wave Beam	$Q_{4W_o}(z) = \begin{cases} 1-\frac{\lvert z\rvert}{4W_o} & \lvert z\rvert \leq 4W_o \\ 0 & \lvert z\rvert > 4W_o \end{cases}$	$\frac{2W_o}{\pi}\left(\frac{\sin[2(\beta_o - b)W_o]}{2(\beta_o - b)W_o}\right)^2$
Two-side Exponential	$\exp\left(\frac{-\lvert z\rvert}{2W_o}\right)$	$\frac{2W}{\pi} \frac{1}{1+[2(\beta_o - b)W_o]^2}$
One-side Exponential	$\exp\left(-\frac{z}{4W_o}\right)U(z)$	$\frac{2W}{\pi} \frac{1}{1-j4(\beta_o - b)W_o}$
Lorenztian Beam	$\frac{1}{1+\left(\frac{4\pi z}{3W_o}\right)^2}$	$\frac{3W_o}{4} \exp\left(\frac{-3W_o}{4\pi}\right)[\beta_o - b]$

B. ACOUSTOOPTIC SPECTRUM ANALYSIS THEORY

The acoustooptic spectrum analyzer consists of only four components; a light source, Bragg cell, transform lens, and a photodetector array. The basis for acoustooptic spectrum analysis is the frequency dispersion of acoustooptic diffraction. Essentially each frequency component of the input signal will cause a deflection of the incident light beam. A typical interaction geometry is shown in Fig. 4 [Ref. 17]. A summary of the description of this interaction geometry from Ref. 17 is presented.

Two discrete frequencies are shown with corresponding acoustic wavelengths Λ_1 and Λ_2. These propagate in the x direction with velocity V_s. The medium is optically isotropic with an index of refraction n. The thickness of the ultrasonic grating along the x axis is L. A collimated beam of light of freespace wavelength λ is incident on the sound field at an angle θ_i from the z axis in the xy plane. A sound wave at frequency f interacting with the incident light wave will generate a principal diffracted beam separated from the incident beam by an angle $\theta_i + \theta_d$ by the well known Bragg law:

$$\theta_i + \theta_d = 2 \sin^{-1}\left(\frac{\lambda f}{2nV_s}\right)$$

$$= \left(\frac{\lambda}{nV_s}\right) f \qquad (11)$$

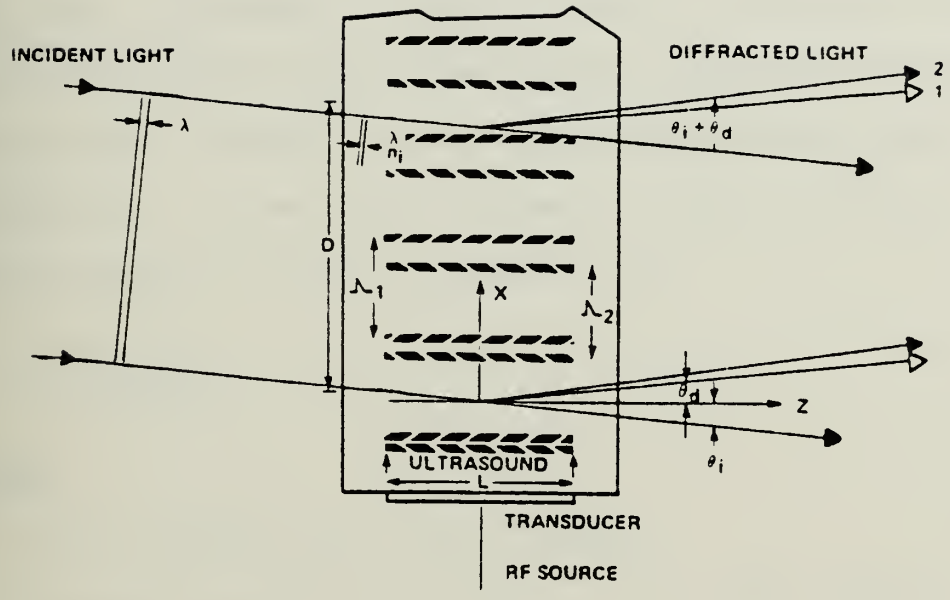

Figure 4. Bragg Cell Operation

where $\theta_i + \theta_d \leq 0.1$ rad

External to the medium

$$\theta'_i + \theta'_d \approx 2 \sin^{-1}\left(\frac{\lambda f}{2V_s}\right)$$

$$\approx \left(\frac{\lambda}{V_s}\right) f \qquad (12)$$

Thus the diffraction angle is approximately proportional to the input frequency. Figure 5 shows a classical optical ray trace diagram for the acoustooptical spectrum analyzer configuration. Figure 6 shows the corresponding optical plane schematic. In the output transform plane, position is approximately related to frequency by

$$x' \approx \left(\frac{\lambda f}{V_s}\right) F \qquad (13)$$

where

F = transform lens focal length.

At this point, by considering the input signal as a composite of frequencies each of which will cause a deflected beam in accordance with the presented interaction theory, an approach to the construction of a model may be undertaken.

Schulman [Ref. 18] and Vatz [Ref. 19] have proposed a set of optical block diagram symbols which show the process elements and indicate the mathematical function each element performs. Figure 7 shows the AOSA using these process elements.

The laser light source S_L, and beam expander lenses, T_M and T_c, are shown as providing an input to the Bragg cell

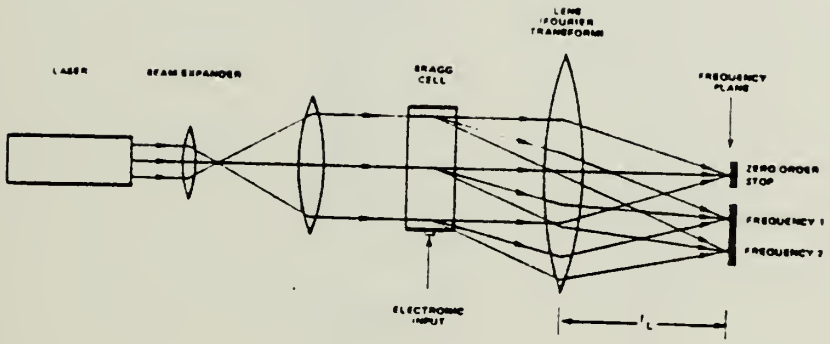

Figure 5. Classical Ray Trace Diagram for an Acoustooptical Spectrum Analyzer

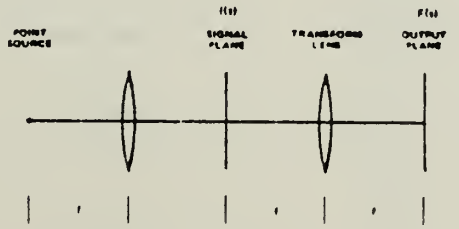

Figure 6. Optical Plane Schematic for an Acoustooptical Spectrum Analyzer

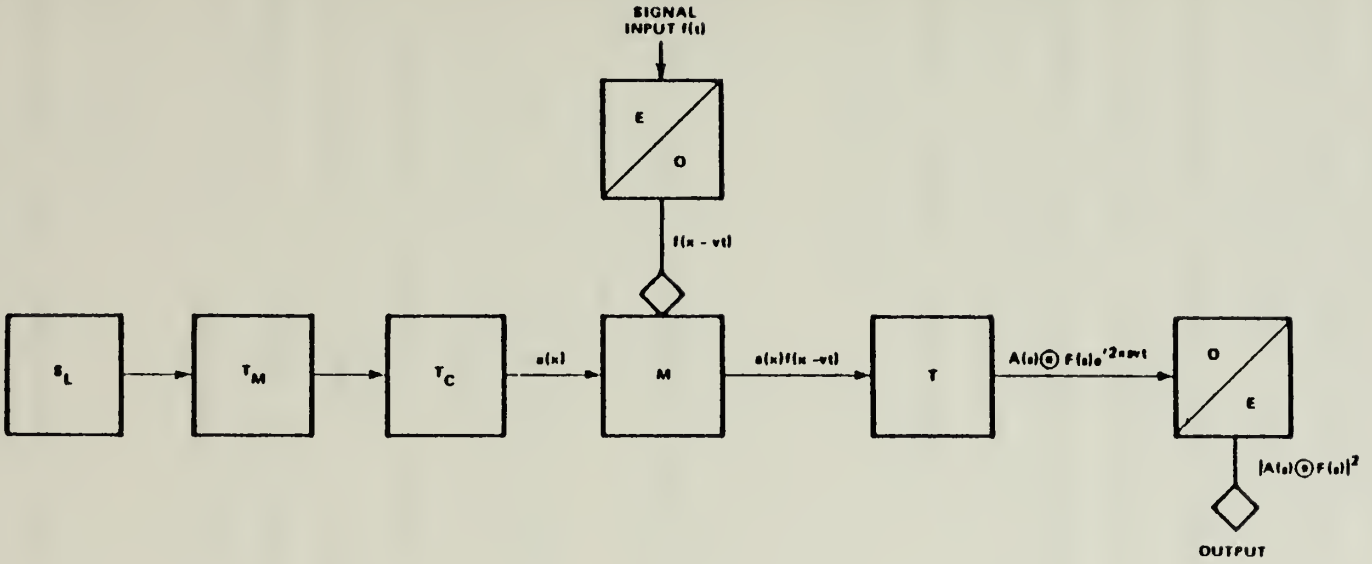

Figure 7. Block Process Element Diagram for an Acoustooptical Spectrum Analyzer [after Refs. 18 and 19]

with transverse light distribution a(x) of general form, an arbitrary profile modified by spatial noise, lens aberrations, and Bragg cell aperture. The input signal f(t) is converted to an acoustic wave in the E/O block which represents the piezo-electric transducer. This acoustic traveling wave f(x-vt) propagates through the interaction region.

In the Bragg cell interaction the light modulation can be considered a multiplication process in which the diffracted light power is proportional to the product of the light intensity and the acoustic wave power.

$$i(x) = a(x)\ f(x-vt) \tag{14}$$

where

$$x = v_s t \tag{15}$$

The transform lens T produces the Fourier transform.

$$I(s) = \mathcal{F}\{a(x)\ f(x-vt)\}$$

$$= A(s) * F(s) \exp\ [j2\pi\ S(v_s t)] \tag{16}$$

The transform is the convolution of the Fourier transform of the illumination function and the transform of the acoustic wave. The exponential factor is a Doppler frequency shift. As the detector is a square law device, the output from the AOSA is the square of the magnitude of the intensity function.

$$|A(s) * F(s)|^2 \tag{17}$$

It has been shown that the output of the AOSA is the square of the magnitude of the intensity function. The intensity function may be considered as the convolution of the spatially transformed illumination function and the spatially

transformed acoustic wave. Hecht [Ref. 20] treats the illumination function as a spatial weighting function composed of a number of factors including optical amplitude profile, aperture size, and acoustic attenuation. The AOSA frequency plane intensity distribution would thus be proportional to the squared amplitude of the Fourier transform of the weighting function with respect to the spatial frequency.

$$F(s) = \int_{-\infty}^{\infty} W(u) \exp(-j2\pi su)du \qquad (18)$$

where $u = [\frac{t}{\tau} - \frac{1}{2}]$

τ = finite period of signal analyzed

$S = f\tau$ = the normalized frequency

Further refinement in the basic model is made by the consideration of the effects of transducer efficiency and diffraction efficiency. These factors modify the frequency components in the acoustic wave.

C. AOSA MODEL CONSTRUCTION

1. Irradiance Profiles

The choice of the optical beam profile incident on the Bragg deflector is a complex decision. It would appear desirable to fill the entire deflector aperture with a uniform intensity light below the saturation level of the AOSA. The irradiance profile in this case would be that of a plane wave. A uniform intensity filling the entire aperture will maximize acoustooptic interaction and provides maximum

incident light to be contributed to the deflected beam components. Abrupt windowing will truncate the beam profile and cause sidelobes to appear. These sidelobes, if they are of sufficient magnitude, may cause erroneous components to appear at the image plane or mask low intensity components.

To reduce the sidelobe levels, a less discontinuous transition in the absorption-transmission regions is necessary. A suitable choice would be a Gaussian irradiance profile with a spherical phase wavefront. This irradiance profile commonly occurs as a laser output and has well understood propagation behavior. Smith includes a handy propagation program as part of his work [Ref. 3]. This program calculates Gaussian beam phase front radius and spot size for propagation through any number of thin lenses spaced at arbitrary distances. Since the Gaussian incident beam profile would not fill the entire aperture with uniform intensity and assuming continued operation below the AOSA saturation level, less light intensity would be available for diffraction into representative beams. This will result in the loss of sensitivity and the possibility of an inability to detect low amplitude frequency components in the presence of strong frequency components.

Other beam irradiance profiles are possible and might be employed for their specific deflected beam characteristics. Figure 8 taken from Ref. 15 shows the deflected beam profiles for various incident profiles. Such curves are useful for comparison of expected sidelobe levels.

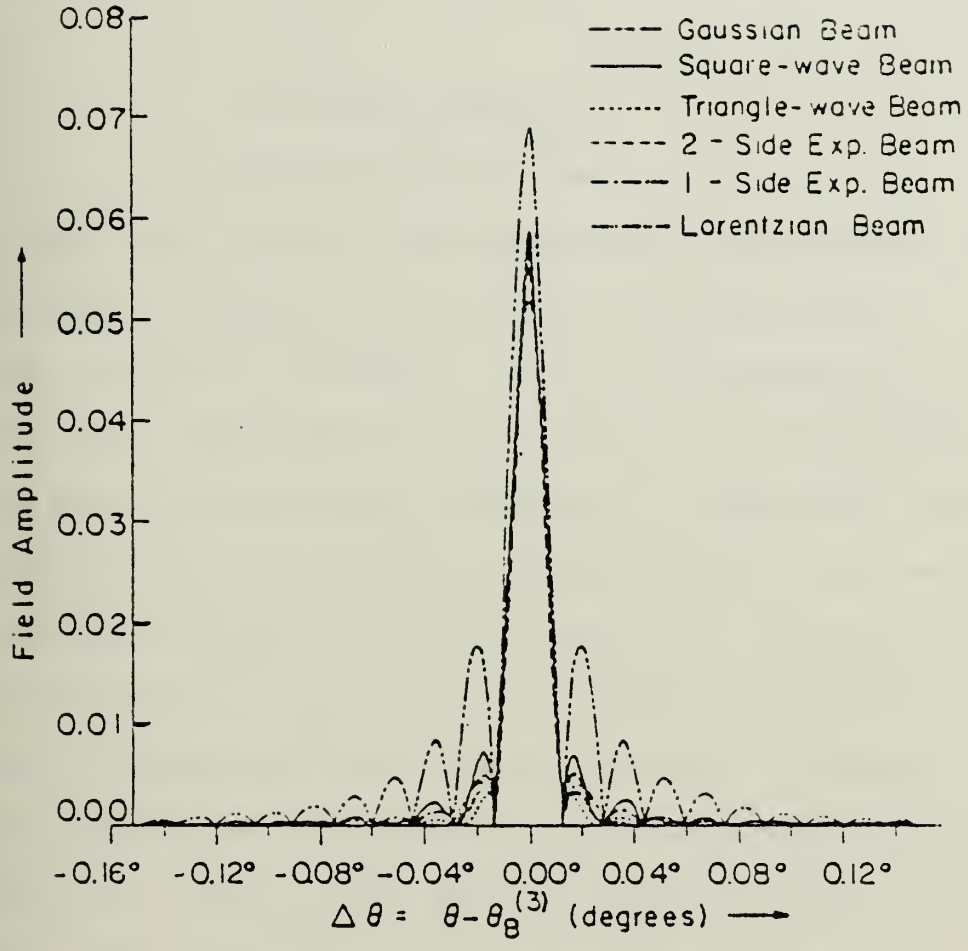

Figure 8. Bragg Deflection Beams for Various Incident Irradiance Profiles (after Ref. 15).

Hecht's [Ref. 5] implementation of the Gaussian irradiance profile is of the form:

$$w_1(t,\tau,T) = \exp\left[-4T^2\left(\frac{t}{\tau} - \frac{1}{2}\right)\right] \qquad (19)$$

where

$T = D/2W_o$

D = effective aperture

W_o = Gaussian waist size

A significant design question in the utilization of Gaussian irradiance profiles is the choice of the ratio of the aperture to the e^{-2} intensity. This is discussed also by Smith [Ref. 3]. Beam spot size is defined as the perpendicular distance from the beam centerline to the point where the irradiance has dropped by a factor of e^{-2}. To use the full information capacity of the Bragg cell, the spot size must be enlarged to illuminate the complete cell aperture. In this situation the aperture will severly truncate the Gaussian beam resulting in a profile similar to that of a sinc function. Varying the ratio of the spot size to the aperture will alter the level of the sidelobes of the profile. Smith limited his spot size to avoid sidelobes and thus isolate their effect in his study of optical excision.

Hecht expresses his spatial weighting functions in equivalent time variables. The linear relationship between the spatial and time variables and the analogous relationship between the spatial frequency and frequency provide great

flexibility in the construction of the computer program to model the AOSA. The Fourier and inverse Fourier transforms utilized in the AOSA program make no distinction as to the transforming variables.

Only plane and Gaussian irradiance profiles were included in the AOSA program. It would be a simple matter to incorporate other profiles such as the Lorentzian or triangle beams. However, the frequency with which the more exotic profiles would be encountered does not merit the addition. Figure 9 shows the comparative image plane profiles for both irradiance profiles with a monotonic 70 MHz input signal. In Figure 9 the plane wave illumination chosen completely illuminated the aperture of the Bragg cell. The Gaussian illumination used an arbitrarily chosen 3.8 millimeter spot size. Comparison shows a near 50% reduction in the level of the Gaussian sidelobes to the level of the plane wave sidelobes but with a tradeoff of a decrease in the peak intensity response. The units for the Image Plane Intensity axis in this figure and all succeeding AOSA program figures are arbitrary.

Figure 10 shows the image plane intensity for an incident Gaussian beam with a spot size of 1.945 millimeters. This is the "optimum" spot size according to Smith's criteria for sidelobe suppression. The sidelobes are barely visible but again a tradeoff results in an additional decrease in peak intensity. Use of a Guassian beam with this spot

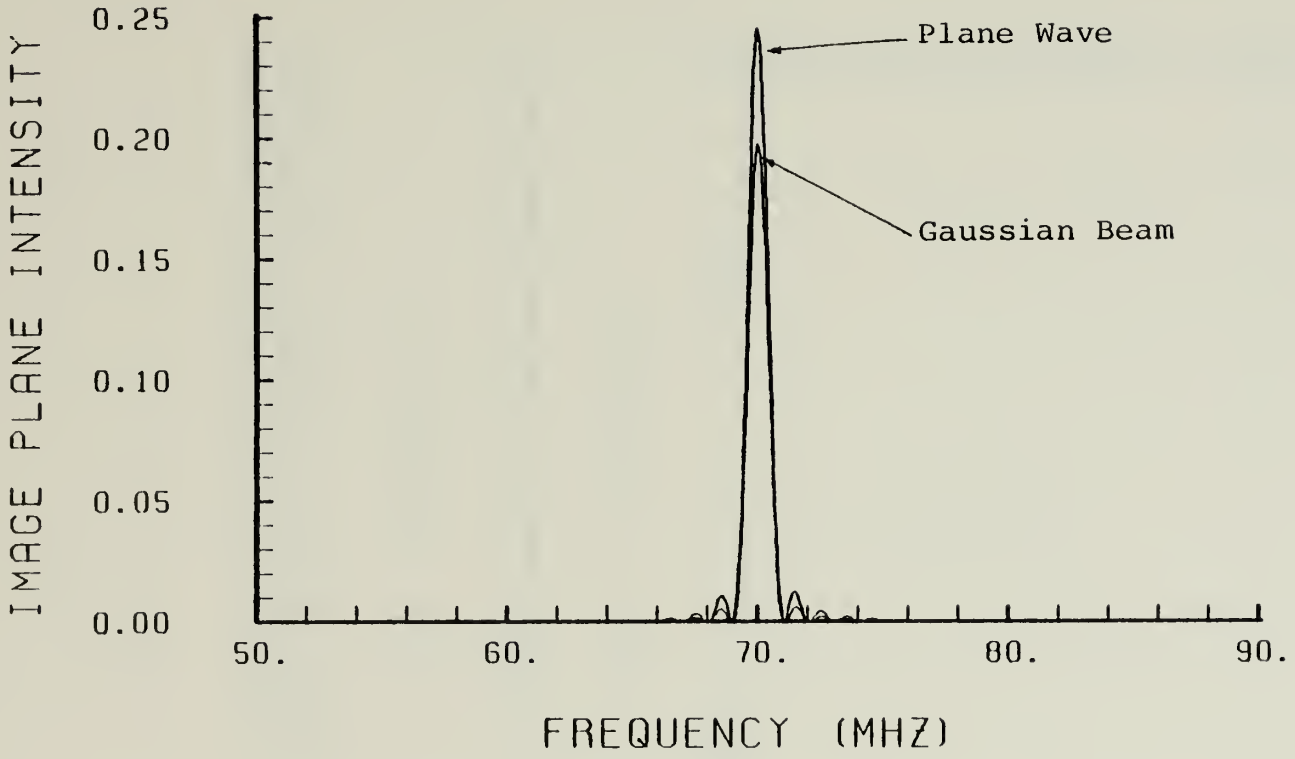

Figure 9. Comparative Image Plane Intensity Profiles (Magnitude) for Gaussian and Plane Incident Beams

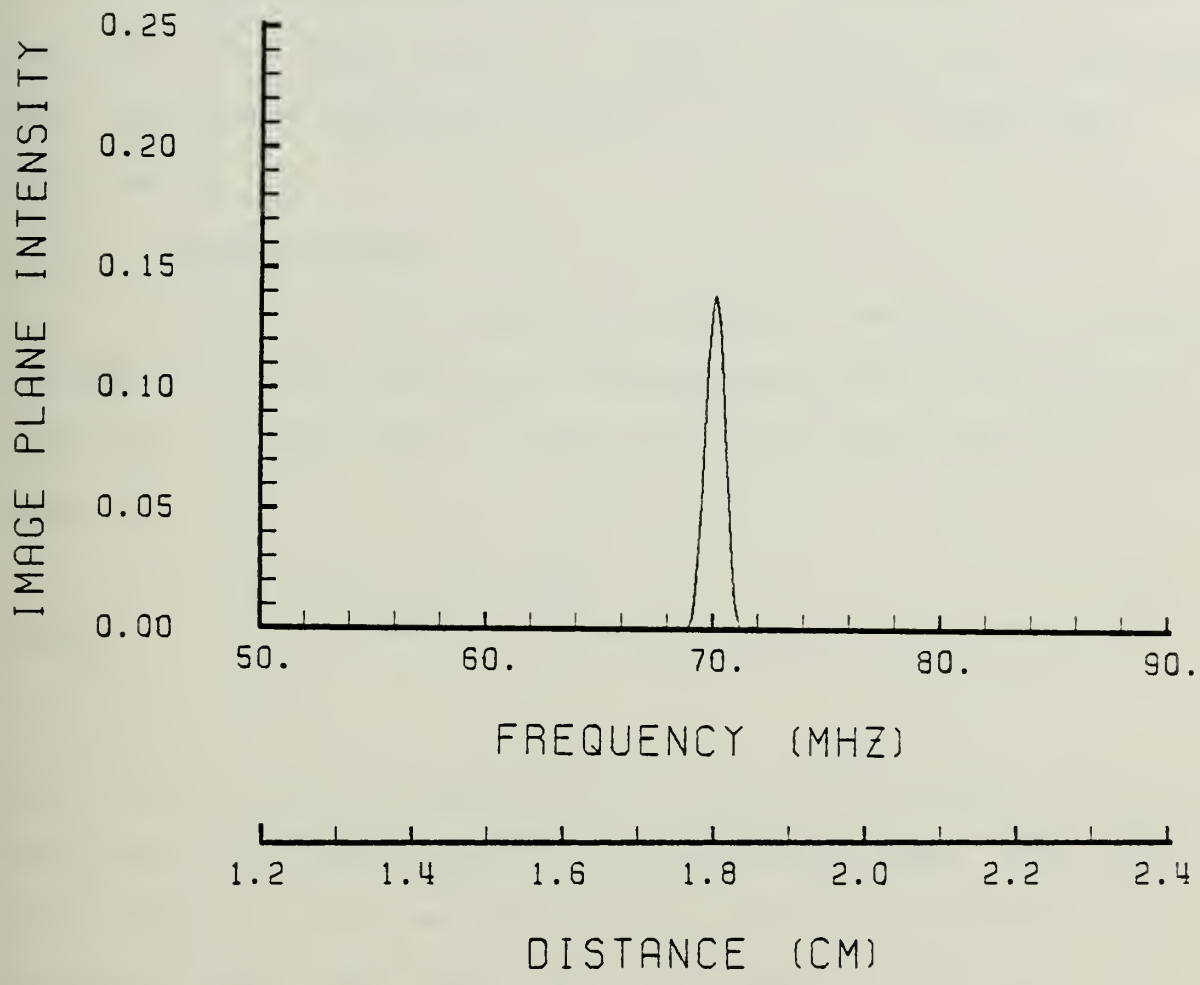

Figure 10. Image Plane Intensity Profile (Magnitude) Produced by a Monotonic 70 MHz Signal with an Incident Gaussian Beam and a Simple Transducer

size narrows the portion of the Bragg cell aperture receiving full illumination. The portion receiving the full illumination is termed the effective aperture. Its effect will be discussed in a later section. Figure 11 shows for comparison the image plane intensity profile of a fully illuminating plane wave.

2. Aperture Size

The universal feature of realistic weighting functions is that of a finite aperture corresponding to a finite period of signal τ represented by the unity amplitude window function [Ref. 5].

$$w(t,\tau) = \text{rect}\left(\frac{t}{\tau} - \frac{1}{2}\right) \tag{20}$$

where

$$\tau = D/V_s$$

Early approaches to acoustooptical spectrum analysis modeling considered the input signal as a continuous wave. The effective aperture of the selected Bragg deflector truncated the incident light, such that only the segment of acoustic wave within the optical aperture region was intercepted. That segment of acoustic wave corresponds to the finite period of signal being analyzed.

Improvements in Bragg deflector manufacturing techniques have yielded high quality, low acoustic velocity deflector crystals. These crystals are of increasingly larger dimensions. The Rayleigh limit resolution, N, is defined as the total deflection angle divided by the angular spot size.

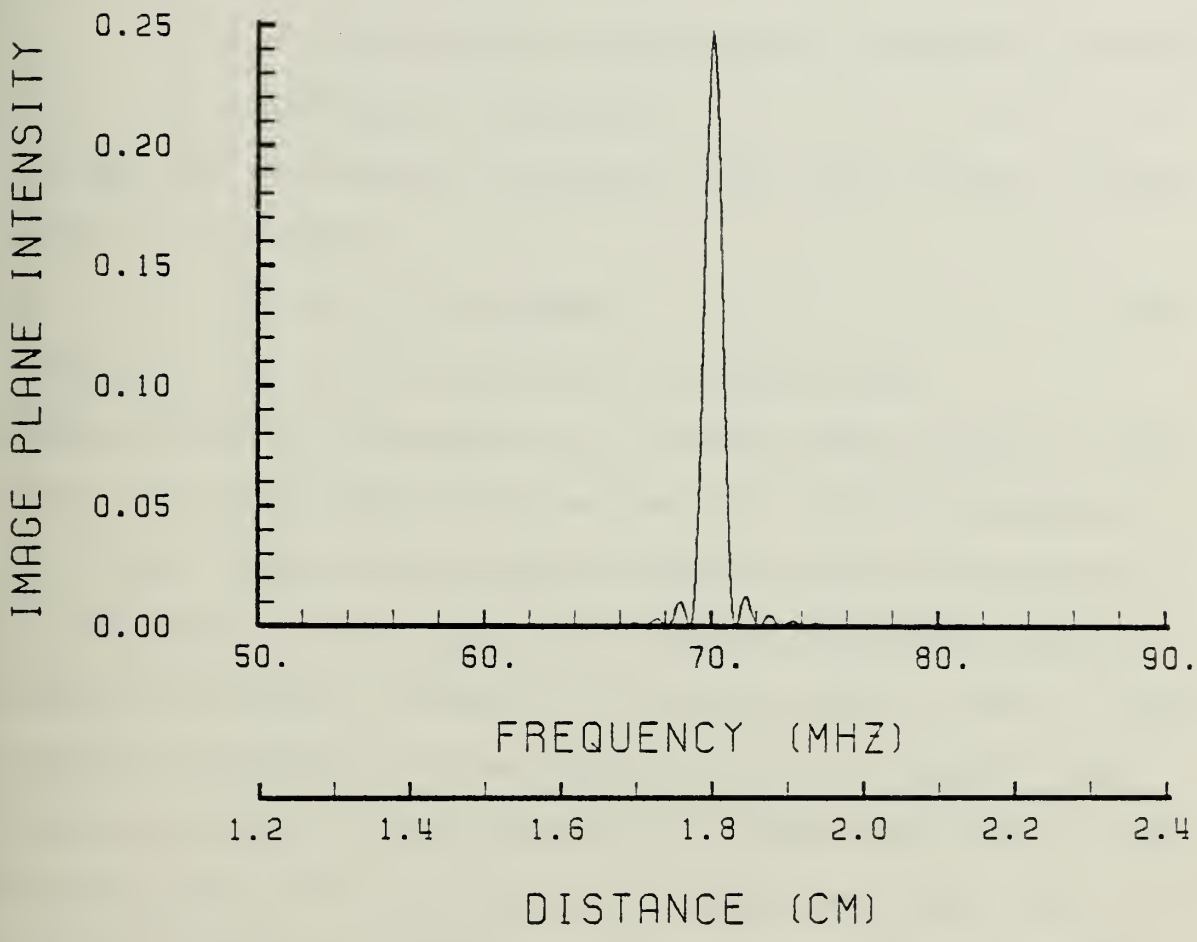

Figure 11. Image Plane Intensity Profile (Magnitude) Produced by a Monotonic 70 MHz Signal with an Incident Plane Wave and a Simple Transducer

The relation simplifies to

$$N = t_1 \times \Delta f \qquad (21)$$

where

t_1 = acoustic transit time across the optical aperture

Δf = deflector bandwidth

For the AOD-70 deflector (assuming that full aperture illumination is provided)

$$t_1 = 2.56 \times D \text{ (microsec)} \qquad (22)$$

where D is the optical aperture in centimeters.

Using the AOD-70 parameters of a 40 MHz bandwidth and a maximum t_1 of 10 microsec based on the full available aperture of 3.9 cm, calculation yields a Rayleigh resolution capacity of 400 spots. To fill the full aperture anamorphic optics such as cylindrical lenses or telescopes must be used. Using standard procedure for the detector array utilization each spot is focused to fall across two adjacent photosites. The Rayleigh resolution capacity of 400 spots provides for a maximum frequency resolution of .1 MHz for the full 40 MHz bandwidth.

Using a Gaussian beam with spot size of 1.945 millimeters to fully suppress the sidelobes in the image plane intensity profile results in an additional penalty in a decrease in the Rayleigh resolution capacity of the "time-bandwidth product," as given by Equation 21. The interaction length is no longer the Bragg cell aperture but rather the effective aperture, in this case estimated as the region

twice the spot size symmetrical about the cell spatial midpoint. This results in a smaller optical aperture, a smaller acoustic transit time, and a resultant decrease in the Rayleigh resolution. Thus, while a choice of spot size of this magnitude will suppress sidelobes, it requires a possibly unacceptable tradeoff in frequency resolution.

The larger apertures bring an additional consideration to the AOSA model construction. A typical application input signal pulse might be of one microsecond in duration while the total acoustic transit time for the AOD-70 is ten microseconds. A one microsecond pulse input to the deflector will persist in terms of the frequency spectra it contains and therefore, in the deflected beam components incident on the image plane for the full ten microsecond travel time. This effect of "time spreading" of the r-f signal is significant for its enhancement of the detection probability for short duration signals. In the application of AOSA techniques to Electronic Support Measures (ESM) receivers, this is of prime import. A 0.1 microsecond r-f signal, which is currently beyond the capability of many traditional technology base receivers, would be stretched to a 1.0 microsecond pulse greatly improving its detection probability. It should be noted that while this "time spreading" increases detection probability, it reduces the capability for accurate direct pulse width measurement, also a highly desirable factor in ESM application.

In summary the aperture size weighting function imposes three constraints on the AOSA model. The physical parameter of the optical aperture is modeled by a simple unity amplitude window function. The Rayleigh resolution and thus frequency resolution is simulated by the technique of zero padding while applying the Fourier transforms to achieve a digital record length which will yield the appropriate frequency resoltuion. Zero padding is a digital implementation technique used in Fourier analysis whereby the desired sampled signal data is entered followed by a data string of zeroes. This increases the record length to provide a desired resolution in the transformed domain without affecting the sampled data validity. The transformed domain resolution is simply the inverse of the record length. The finite signal length is modeled with a unity amplitude window function implicit in the input signal as it is digitally implemented. Since the period of signal analyzed may be shorter than the acoustic travel time of the optical aperture, it is desirable to analyze the deflection caused by interaction of the pulse acoustic segment at various points as it traverses the optical aperture. A shiftable digital array was utilized controlled by a time delay variable; zero delay corresponding to a symmetric straddling of the acoustic pulse segment about the spatial midpoint of the optical aperture. This time delay variable forms the basis for a dynamic AOSA program to be discussed in a later section.

3. Acoustic Attenuation

As the acoustic wave travels the length of the Bragg deflector, it is subject to acoustic attenuation. The amplitude of the acoustic wave decreases, with a resultant decrease in the ability to interact with the incident light wave. Hecht [Ref. 5] treats the acoustic attenuation as a spatial weighting function of the form;

$$w(t,\alpha,\tau) = \exp(-\alpha t) \tag{23}$$

where α is a frequency dependent loss factor

$$\alpha = \frac{\alpha_o f^m}{20 \log_{10} e} \tag{24}$$

with

$$\alpha_o \text{ in } \frac{dB}{\mu sec\ GH_z{}^m}$$

Values for α_o have been tabulated for common acoustooptic modes. Acoustic attenuation typically follows power law frequency dependence with exponent, m, near 2.

The AOD-70 Bragg deflector is manufactured with high quality flint glass as the interaction medium and Indium bonded Lithium Niobate for the piezo-electric transducers. The α_o values for this type of deflector range from .1 to .15 (dB/microsecond GHZ^2). A plot of the more stringent condition is shown as Figure 12. Calculation of the acoustic attenuation for the AOD-70 device parameters in terms of a normalized transmission factor was carried out. The

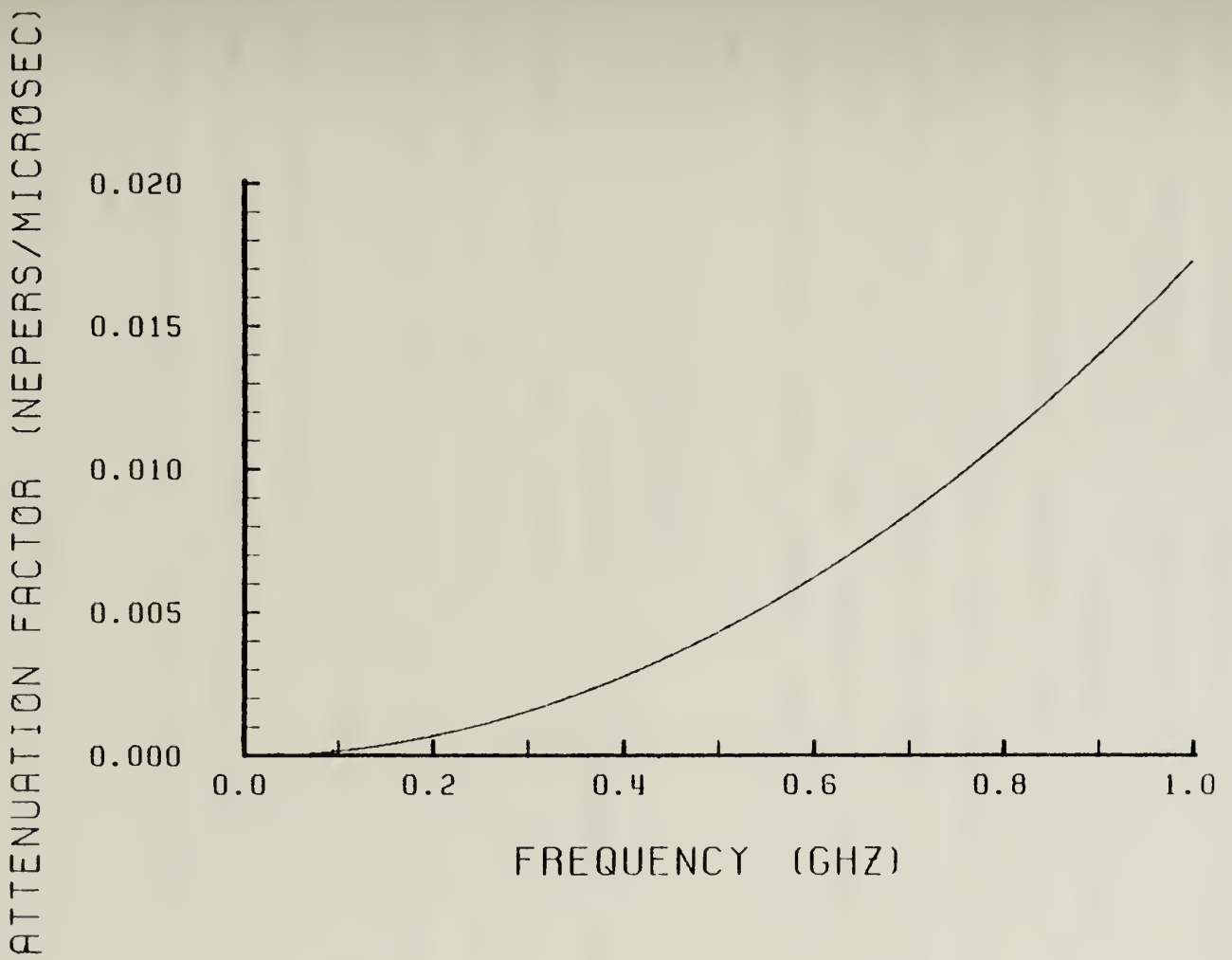

Figure 12. Attenuation Factor as a Function of Frequency for Lithium Niobate Transducer Deflector

results are plotted as Figure 13. These results show a near unity transmission for the region of concern, from 50 to 90 MHz. Since the transmission loss was negligible for this application, an acoustic attenuation factor of Hecht's form was not implemented in the AOSA programs.

If the use of the AOSA programs is envisioned in higher frequency ranges, acoustic attenuation will become a significant factor. Figure 13 shows increased loss as the frequency nears 1 GHZ. Further discussion of the effect of acoustic attenuation on weak truncations (Gaussian beam) and strong truncations (uniform optical beam) is given by Hecht [Ref. 21].

4. Diffraction Efficiency

For a simple transducer the Bragg angle cannot be exactly matched by the incident collimated light beam for all frequencies over the bandwidth of concern. As a result, for Bragg regime deflection the intensity of the diffracted beam is a function of the applied frequency. The ratio of the diffracted beam intensity to the intensity of the incident beam is defined as the diffraction efficiency. An analysis of Bragg regime deflection was conducted by Reagan in Ref. 2 and is summarized here.

Hecht [Ref. 5] expresses diffraction efficiency in a simplified form as:

$$\frac{I_1}{I_o} = \sin^2 (\eta^{1/2}) \frac{\sin^2\left[\frac{\pi}{2}\frac{L}{L_o}(FF_m - F^2)\right]}{\left[\frac{\pi}{2}\frac{L}{L_o}(FF_m - F^2)\right]} \qquad (25)$$

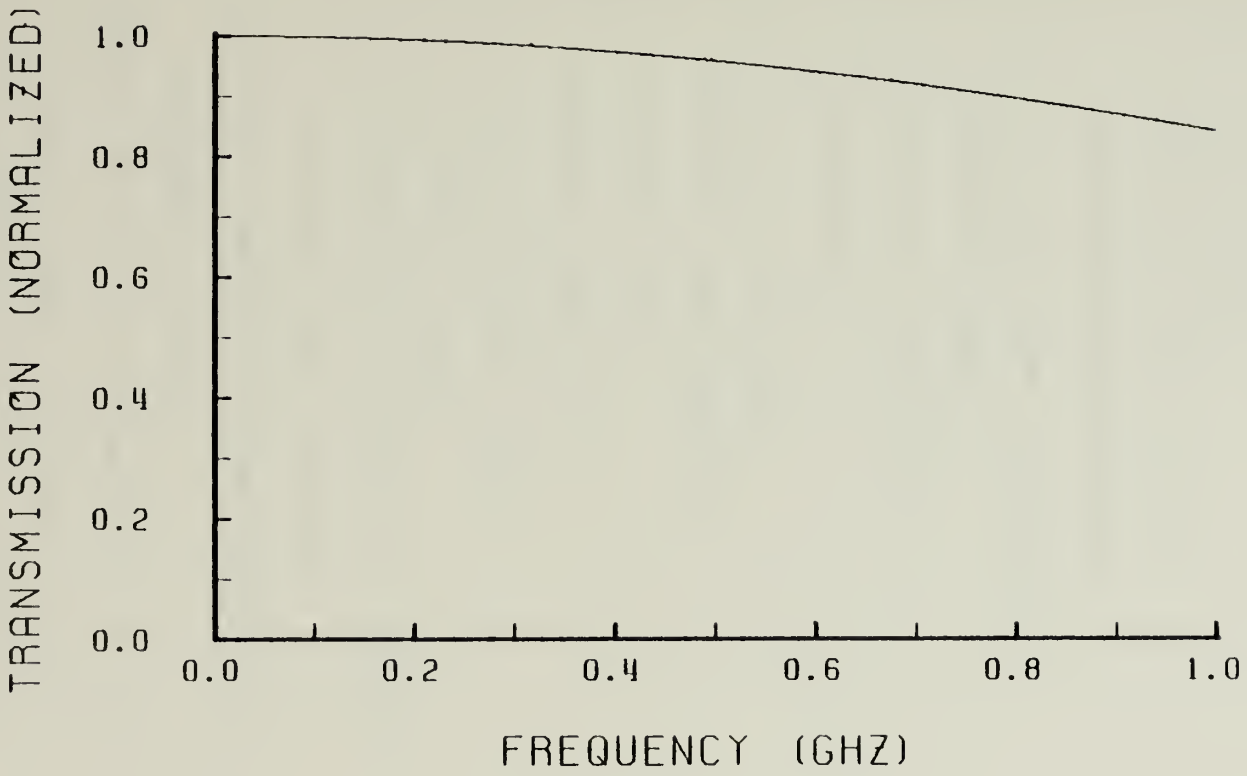

Figure 13. Normalized Transmission as a Function of Frequency for Lithium Niobate Transducer Deflector

with

$$\eta = \frac{\pi^2}{2\lambda_o^2} \frac{n^6 p^2}{\rho v^3} \frac{P_a L}{4 \cos^2 \theta_o} \tag{26}$$

and

$$L_o = n\Lambda_o^2 \cos \theta_o / \lambda_o \tag{27}$$

where: I_1 = diffracted beam intensity

I_o = undeflected beam intensity

λ_o = free space laser wavelength

n = refractive index

p = elastooptic coefficient

ρ = mass density

Λ_o = acoustic wavelength

v = acoustic wave velocity

P_a = acoustic power

H = acoustic beam height

θ_o = Bragg deflection angle

L = interaction length

L_o = characteristic interaction length

F = normalized center frequency = 1

F_m = input frequency value normalized to the center frequency value f_o

Equation 26 shows the quantity η to be constant with respect to the input signal frequency. Thus the initial sin squared term of Equation 25 may be ignored when considering the bandshape of a normal acoustooptic beam deflector. A plot of Equation 25 for various L/L_o ratios is shown as Figure 14.

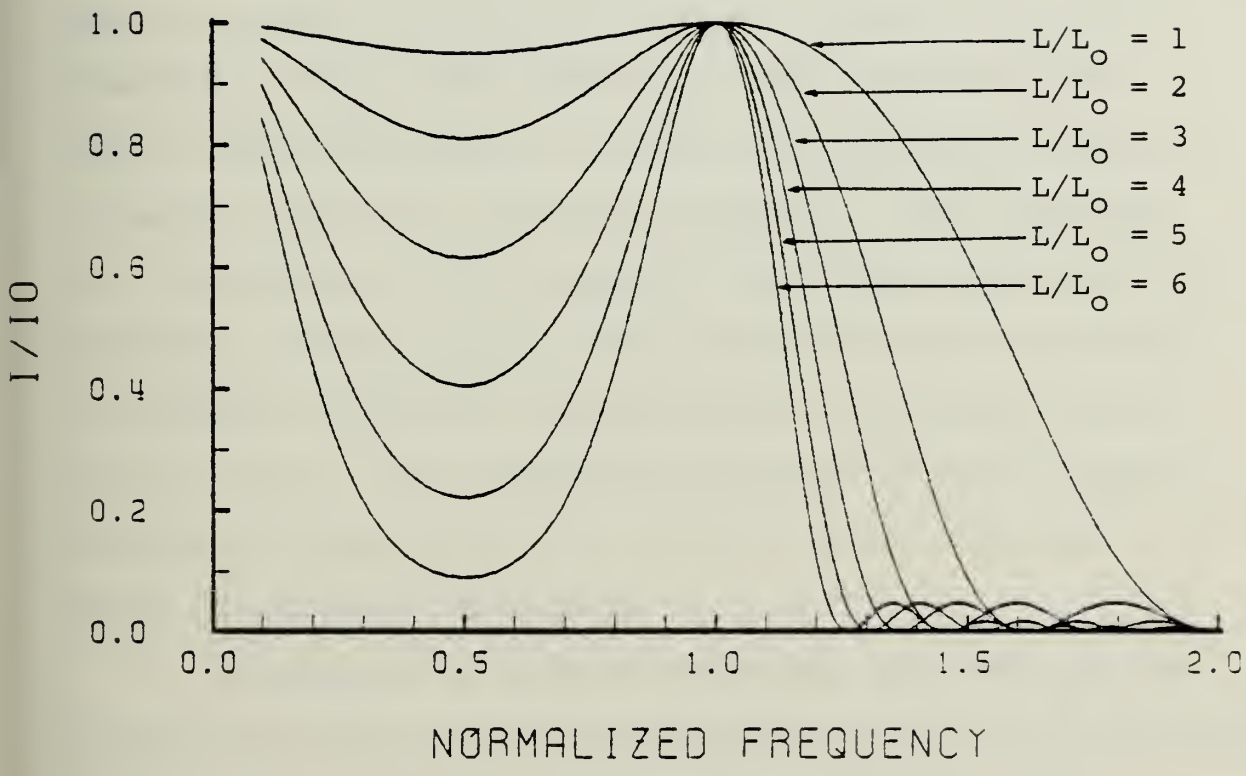

Figure 14. Diffraction Efficiency Bandshape (after Ref. 2)

The 3dB bandwidth is given by Equation 28 and is also from Ref. 5.

$$\Delta f = 1.8\ f_o\ L_o/L \tag{28}$$

For application of a Bragg regime deflector as an acoustooptical spectrum analyzer, it is desirable to maintain a bandshape as near unity and as uniform as possible over the bandwidth of concern. The characteristic interaction length is shown by Equation 27 to be constant with respect to dimensions of the Bragg deflector. The trend for AOSA applied Bragg deflectors is that of increased size with an attendant increased interaction length L. This reflects both improvement in manufacturing techniques permitting the production of high quality large deflectors and the desire for increased resolution made possible with larger interaction length. The increased interaction length, however, results in higher value L/L_o ratios with the observed effect of narrowed bandwidths.

Attempting to increase bandwidth by shortening the interaction length is of limited benefit since the diffraction shifts from the Bragg regime to the Raman-Nath regime. Raman-Nath regime diffraction is unsuitable for this application as it supports many higher order diffraction modes resulting in interference created by additional beams. Increasing the refractive index or elastooptic coefficient of the interaction medium, decreasing the acoustic beam height, or decreasing the acoustic velocity or the mass

density of medium can improve the diffraction efficiency to a limited extent. An increase of acoustic beam power will increase diffraction efficiency. The increased power also tends to heat the interaction medium, creating temperature gradients which degrade resolution and information capacity. Increased difficulty in internal reflection damping is experienced, permitting unwanted signal persistence.

The only effective manner in which to increase the bandwidth is to increase the cell's center frequency f_o. The maximum frequency which the input transducer can effectively couple to the medium is determined primarily by the bonding technique used to attach the piezo-electric strips to the interaction medium. Thus the ability to increase the center frequency is dependent on the input signal transducer. Normally Bragg deflectors are limited to operation over one octave.

In summary, for a simple transducer little can be done to improve diffraction efficiency or increase bandwidth. Beam steering, however, can significantly improve both diffraction efficiency and bandwidth. Commonly employed beam steering techniques include first order planar and stepped arrays. Figure 15 shows a typical first order stepped array. Pinnow [Ref. 22] discussed the relative merits of simple, planar and stepped array transducers. The larger dimensioned Bragg cells deflectors are almost always of the stepped array type. The AOD-70 deflector is

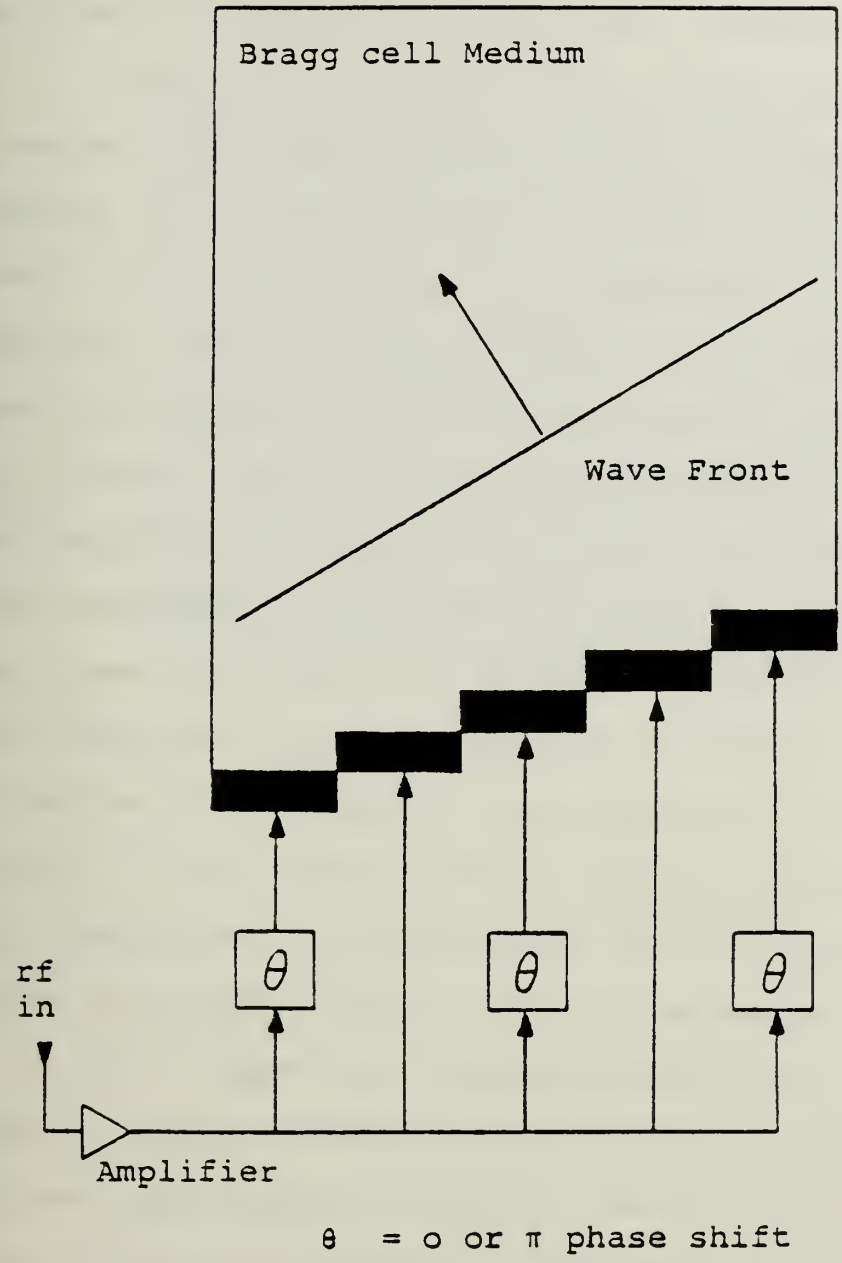

Figure 15. First-order Stepped Array Transducer

a five element stepped array. Figure 16 is the manufacturer's supplied efficiency versus frequency response curve.

The AOSA program has both a simple transducer and a stepped array approximation option. The simple transducer response is computed in accordance with isotropic theory based on the AOD-70 device full dimensions. This permits a comparison with the actual stepped array response. Figure 17 shows the computed diffraction efficiency curves for various L/L_o ratios. These were obtained by sweeping a single variable frequency over the band of concern and extracting the magnitude value for the instantaneous frequency applied. In comparison with Figure 14, which contains the bandshapes for the diffraction efficiency theory, a rippling is noticeable at the lower frequencies. This rippling is an undesirable artifact of the digital Fourier transform application. The ripple amplitude is comparatively small and falls outside of region of concern; hence it was not corrected.

The stepped array bandshape that was included in the model is an approximation based on the near uniform response that was experimentally measured for the AOD-70 device. A slight roll-off in response occurs at the endpoints of the band, but for a first order approximation a uniform window function utilizing the mean efficiency was employed.

To compare the response of the models of the two transducers, an input signal consisting of an in-phase frequency comb with 5 MHz spacing was applied. Figure 18 shows

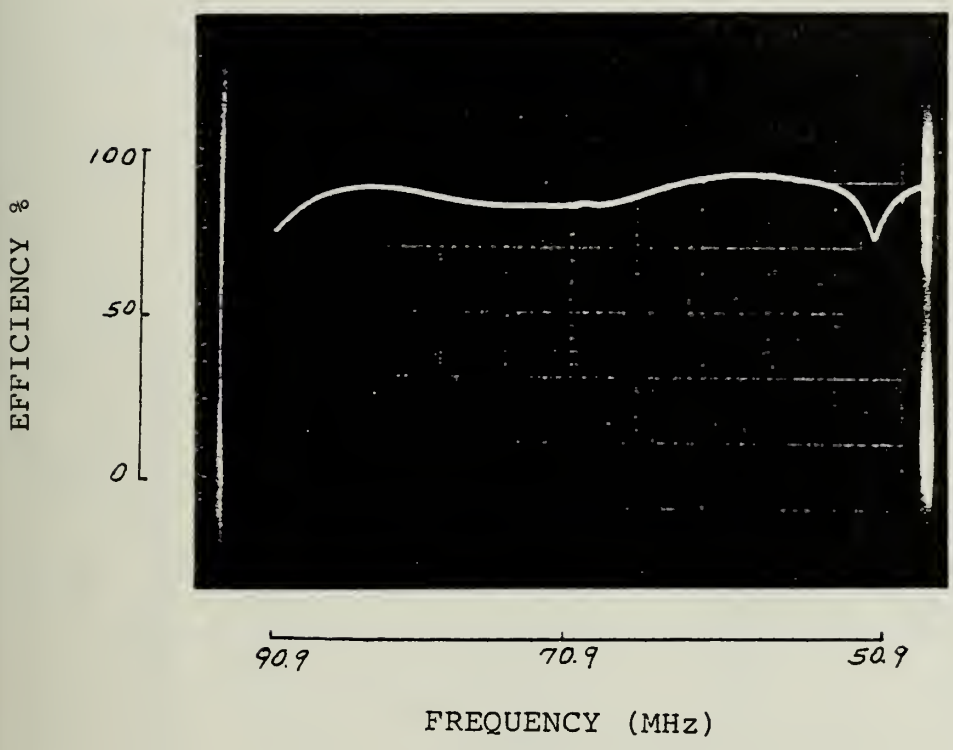

Figure 16. AOD-70 Bragg Deflector Efficiency Curve

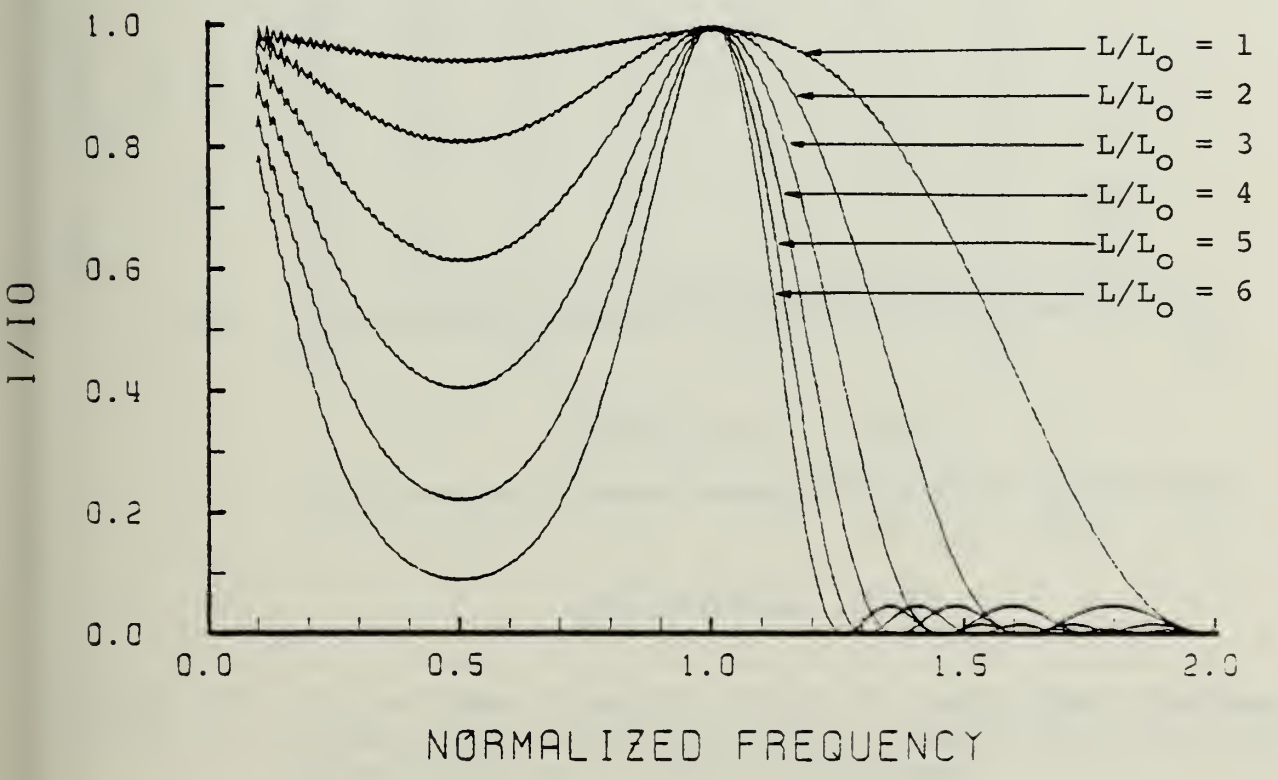

Figure 17. AOSA Implemented Diffraction Efficiency Bandshape

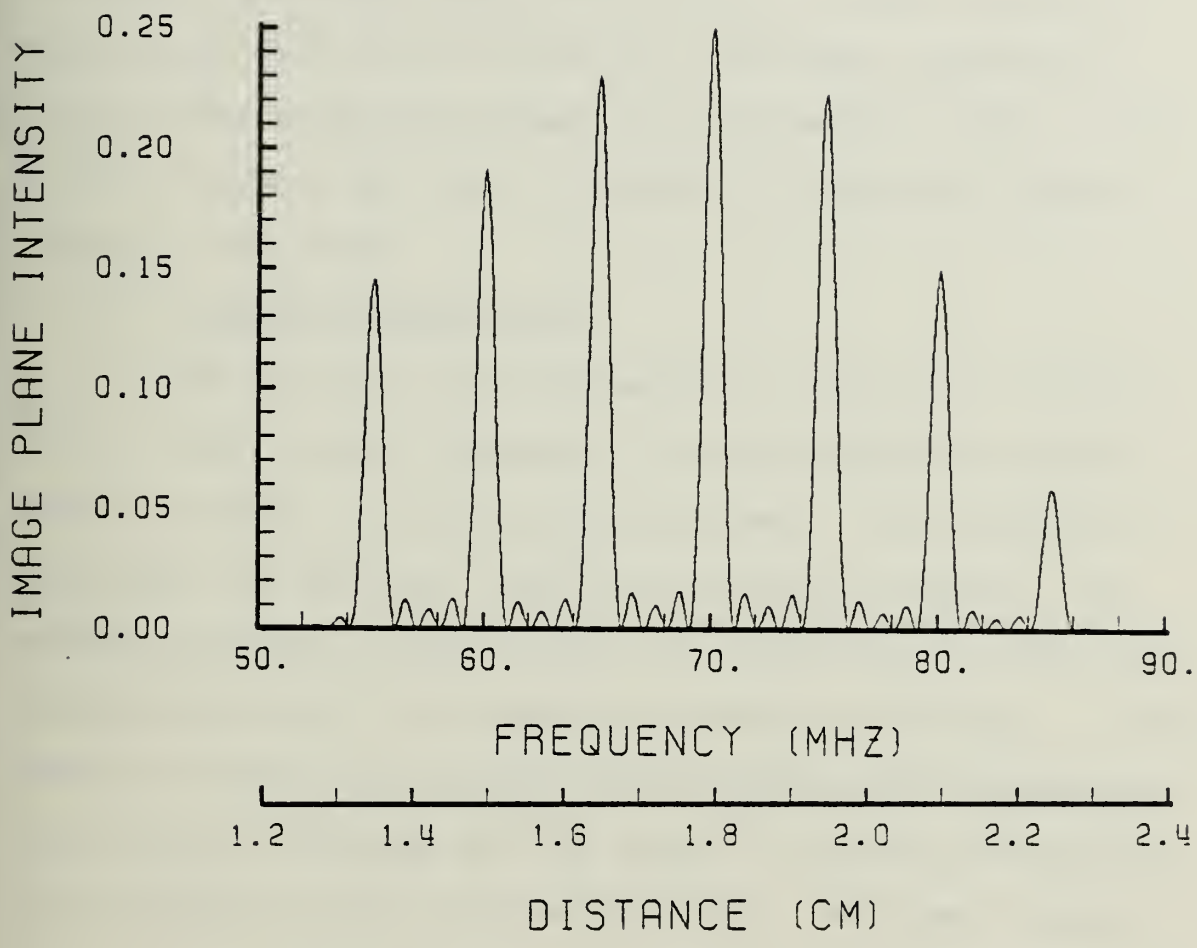

Figure 18. Image Plane Intensity Profile (Magnitude) Produced by a 5 MHz Incremental Comb Signal with an Incident Plane Wave and a Simple Transducer

the simple transducer response. Figure 19 shows the stepped array response. Comparison shows severe attenuation of the frequency components beyond 80 MHz and a lesser degree of attenuation from 50 to 60 MHz for the simple transducer. On the other hand the stepped array transducer shows a very uniform response but with a tradeoff in decreased overall intensity magnitude.

5. Transducer Efficiency

The measure of the transducer's ability to convert the r-f input signal components to representative acoustic waves is termed the transducer efficiency. The transducer efficiency is dependent upon the transducer material, the bonding technique used to fasten the transducer to the interaction medium, and the transducer impedance matching. A fundamental tradeoff relationship exists between the flatness of the frequency response and the amount of power delivered by the transducer within the desired band. The power levels used to drive the transducer are relatively low, thus we can afford a power conversion inefficiency and seek as uniform a response as possible. All transducers operate at less than unity efficiency; however, for purposes of the model, it was assumed that the desired uniform response was of paramount importance. An ideal case would provide a transducer efficiency response with little power attenuation and a uniform amplitude for all frequencies within the range of the system application. Current technology has achieved near uniform response bandshapes

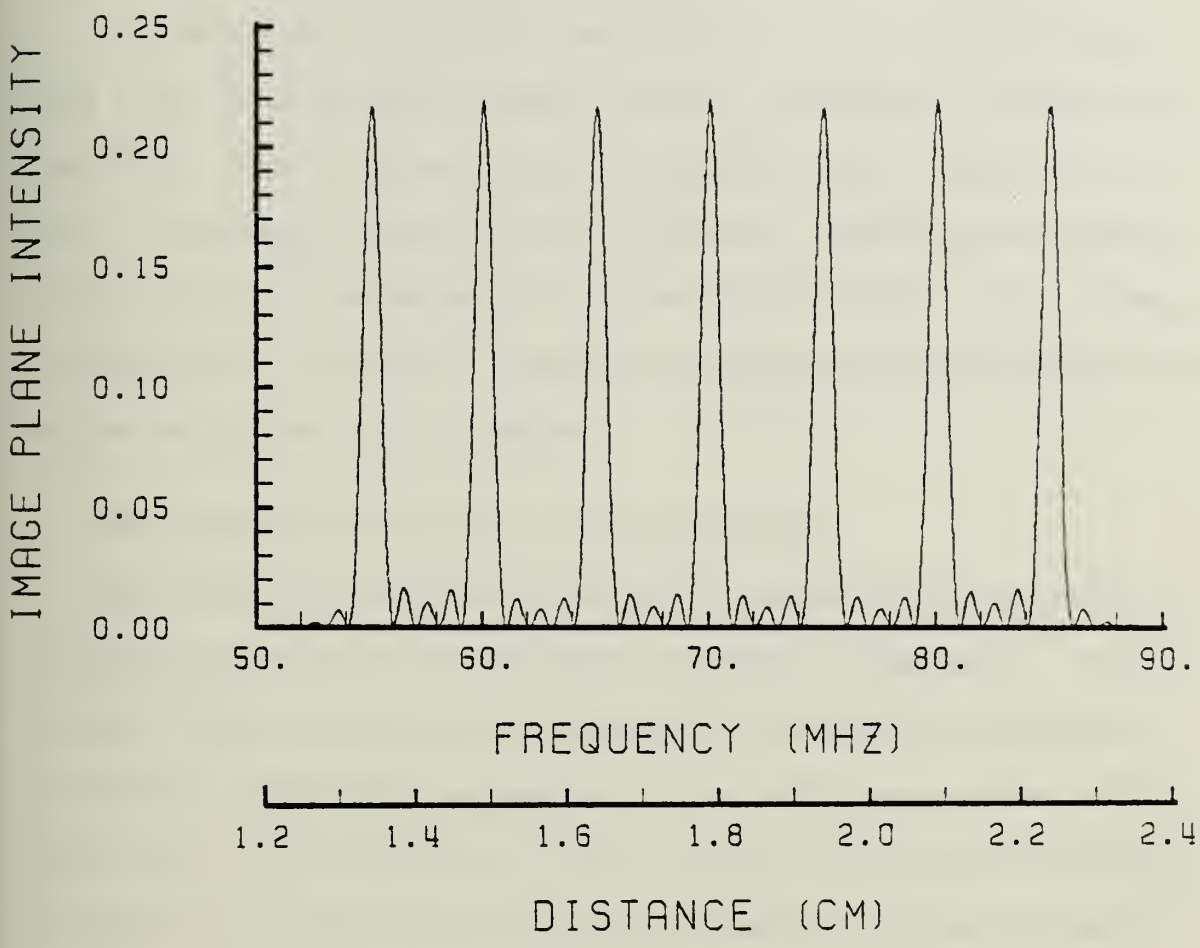

Figure 19. Image Plane Intensity Profile (Magnitude) Produced by a 5 MHz Incremental Comb Signal with an Incident Plane Wave and a Stepped Array Transducer

over bandwidths of 70 MHz, as is present in the AOD-70 cell. Chang [Ref. 23] discusses the state of current transducer technology.

Based on the above the AOSA model was implemented with a unity amplitude window for the transducer efficiency function. The program structure permits easy input of non-unity bandshapes should this be desired. Extreme broadband applications of acoustooptical spectrum analysis will result in nonuniform frequency responses requiring such modifications before using the AOSA program.

D. AOSA MODEL UTILIZATION AND EXTENSIONS

The AOSA program was designed to model direct detection acoustooptical spectrum analyzer systems in general. In its current configuration it utilizes the component parameters of the NPS laboratory system with the addition of the AOD-70 Bragg cell. The coding for the Fortran program was selected to maintain as much generality as possible, so as to permit application for analysis under other choices of components. An attempt was made to minimize the number of preliminary calculations a prospective user would have to perform prior to utilization of the program. For example, the program computes the Fourier transform lens focal distance given the deflector physical parameters, the laser characteristics, and the desired detector array spot size. A list of the required input physical parameters is given in Table II.

TABLE II

AOSA Modeling Parameters

DCELL = effective optical aperture of Bragg cell

LW = Bragg cell interaction length

VS = acoustic velocity of interaction medium

REFIND = refractive index of interaction medium

LAMBDA = laser wavelength

BW = beam width of collimated Gaussian beam (3 dB) at the Bragg cell aperture

SPOT = desired detector array spot size

PULSE = r-f signal pulse duration

TDELAY = time delay for examining signal pulse at varied points during the acoustic transit period

The remaining program variables are primarily concerned with control of the program including output formats and the various subroutines utilized within the program.

The main exception to the above is the created variable TDELAY, for time delay, which permits the user to examine the representative acoustic pulse at frozen intervals of time during its transit of the optical interaction aperture. This suggested the possibility of adding another dimension to the AOSA program, to create in effect a dynamic AOSA model which would examine the response of the acoustooptic spectrum analyzer periodically by looping through the basic static algorithm with decreasing time delays. The results are presented in a three-dimensional isometric or perspective projection. This permits the user to simulate the response of the image plane intensity as the acoustic pulse transits segments of the optical interaction region rather than at a single fixed point of time. To simplify the graphic output the present configuration of the dynamic AOSA program (called TAOSA) is set to examine the first fraction of a microsecond as the acoustic pulse enters the optical region. Computer simulations were conducted over the entire transit period and to verify the symmetry of response as the acoustic pulse exited the optical region.

Both the static and dynamic programs provide the user with options to simulate various system configurations. Types of transducers, incident beam profiles, and output in

either relative magnitude or decibel form is available. The static program offers a choice of several levels of graphical output, from a coarse line plot to two Versatec offline plotting options. Currently both programs utilize a deterministic form for the input r-f signal. The programs could be easily modified to accept sampled r-f data.

The following series of figures are typical of the outputs of the AOSA and TAOSA programs. They were selected to demonstrate the ability of the programs to model a variety of complexity in input signals, to demonstrate the quality of resolution achievable by an acoustooptical spectrum analyzer and for comparison with the known spectral content of the inputed signals.

Figure 20 is the input r-f signal magnitude for a 70 MHz monotone. Figures 21 and 22 are outputs using the decibel option of the AOSA program. Figure 21 shows the relative sidelobe levels by interaction of the monotone with an incident plane wave. For comparison Figure 22 shows the decrease in the relative sidelobe level produced by the monotone with an incident Gaussian beam of 1.045 millimeter spot size. Figures 23 and 24 show the dynamic response of the same monotone with the two wave types. The x axis on all TAOSA program graphics represents time as the acoustic pulse transits the Bragg cell aperture region. Time zero corresponds to the instant when the leading edge of the acoustic wavetrain crosses into the aperture region. Figure 23 shows the dynamic

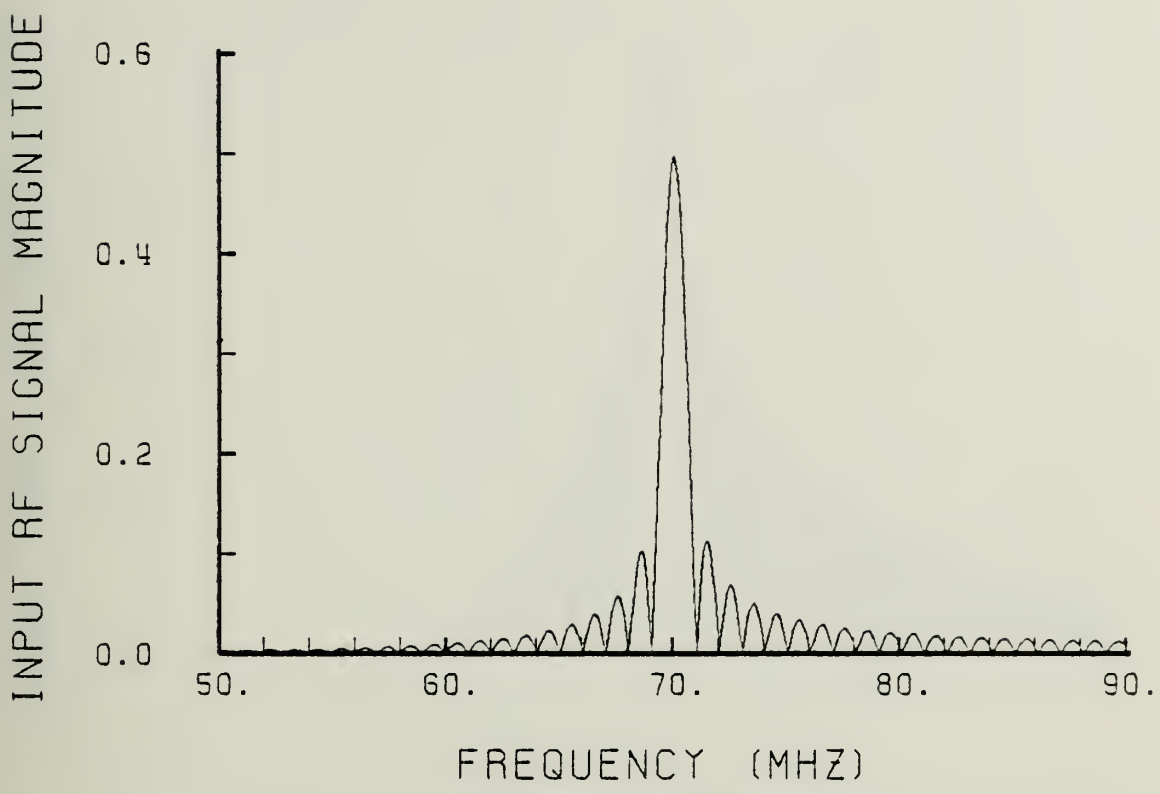

Figure 20. Input RF Signal Magnitude for a 70 MHz Monotone

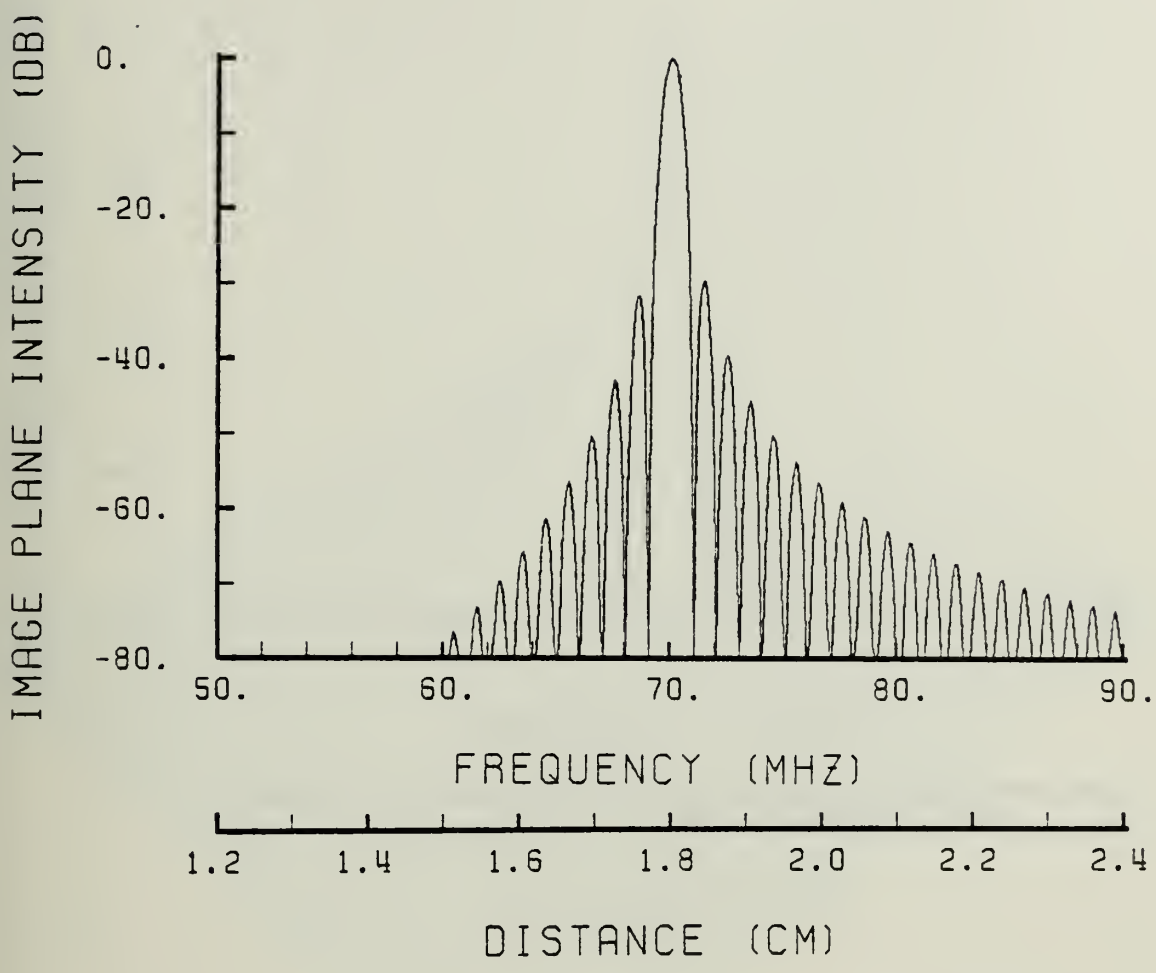

Figure 21. Image Plane Intensity Profile (Decibel) Produced by a Monotonic 70 MHz Signal with an Incident Gaussian Beam and a Stepped Array Transducer

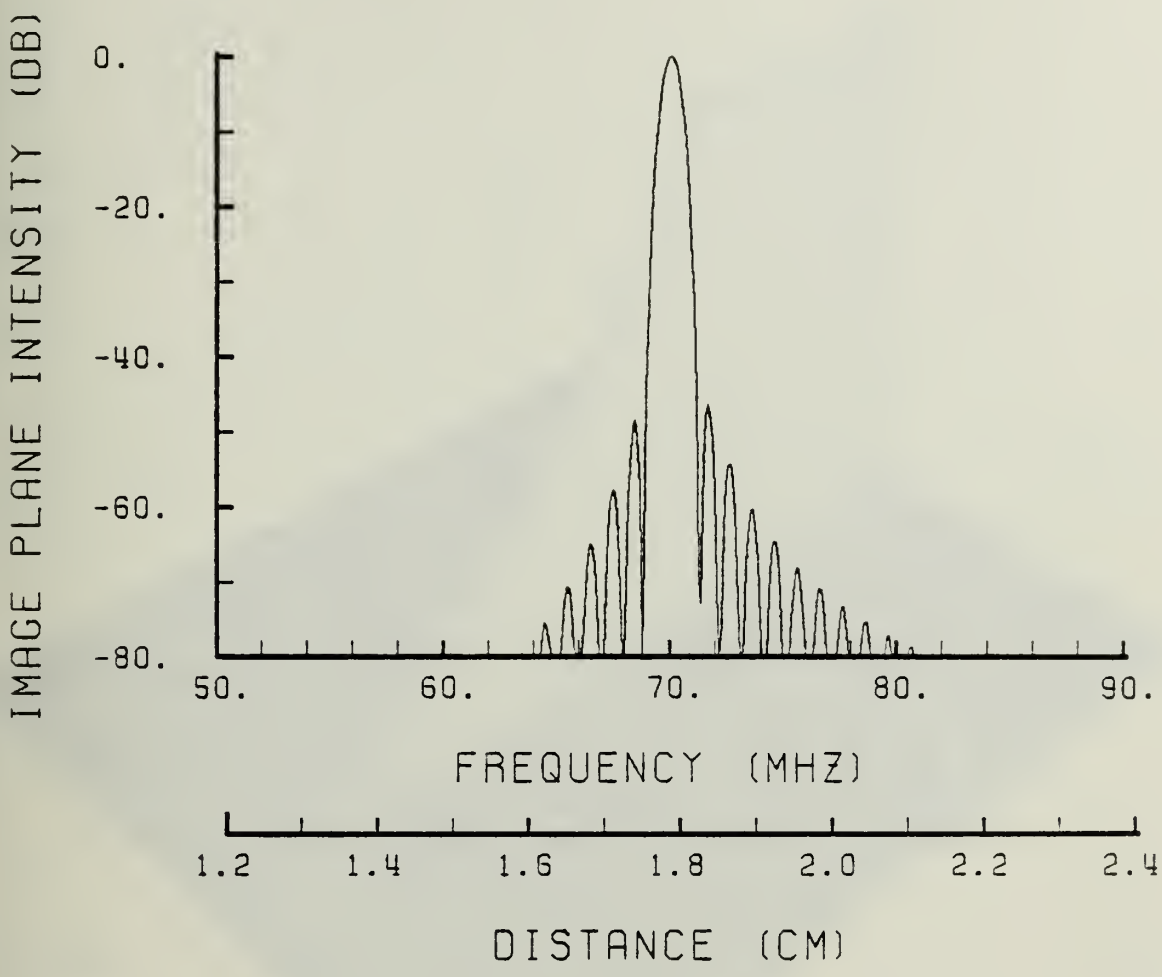

Figure 22. Image Plane Intensity Profile (Decibel) Produced by a Monotonic 70 MHz Signal with an Incident Plane Wave and a Stepped Array Transducer

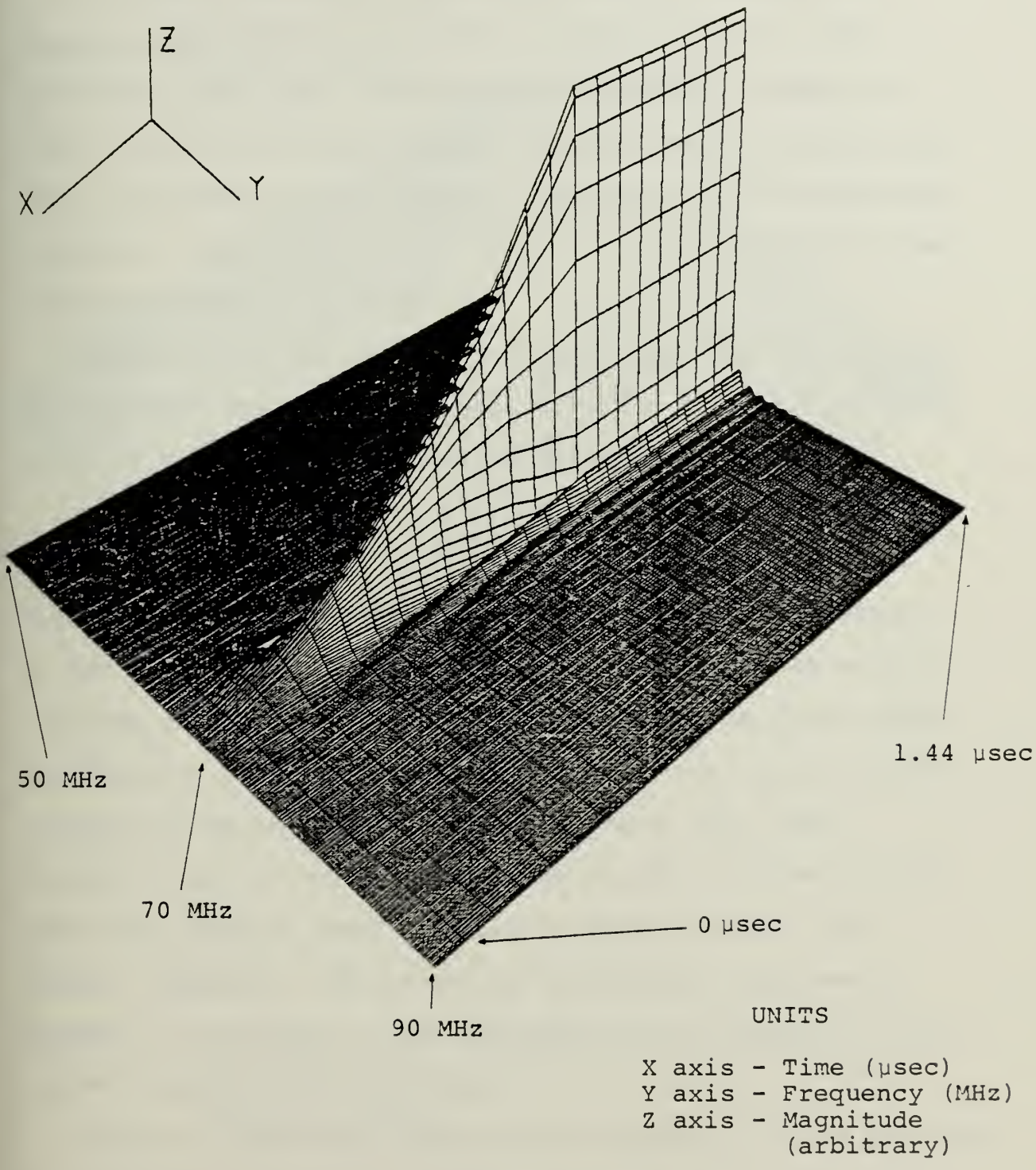

Figure 23. Image Plane Intensity Profile (Magnitude) Produced by a Monotonic 70 MHz Signal with an Incident Plane Wave and a Stepped Array Transducer (Dynamic Model)

response of the monotone with an incident plane wave. A much slower response is seen in Figure 24 showing the response produced by an incident Gaussian wave of 1.945 millimeter spot size. The Gaussian response is shown to occur later in the cell aperture transit period and to last for a relatively short time when compared to the plane wave response. The symmetric roll-off is already visible at the rightmost edge of the figure.

Figure 25 is the input r-f signal magnitude for a simple sinusoidally modulated FM signal with $\beta = 8.0$ and $f_m = 5$ MHz. β is the modulation index and is defined as

$$\beta = \frac{\Delta f}{f_m} \tag{29}$$

Figure 26 shows the image plane intensity profile produced by the interaction of the signal shown in Figure 25 with an incident plane wave. Figure 27 shows the image plane intensity profile produced by the same signal interacting with an incident Gaussian beam of 1.945 millimeter spot size. Figures 28 and 29 are the analagous dynamic program outputs. Again the Gaussian beam interaction shows a slower and smaller response. The advantage of sidelobe suppression, however, is apparent in the extremely clear presentation of the FM intermodulation products.

Figure 30 shows the image plane intensity profile produced by a linear chirp with an incident plane wave. Figure 31 shows the profile produced by the interaction with a Gaussian

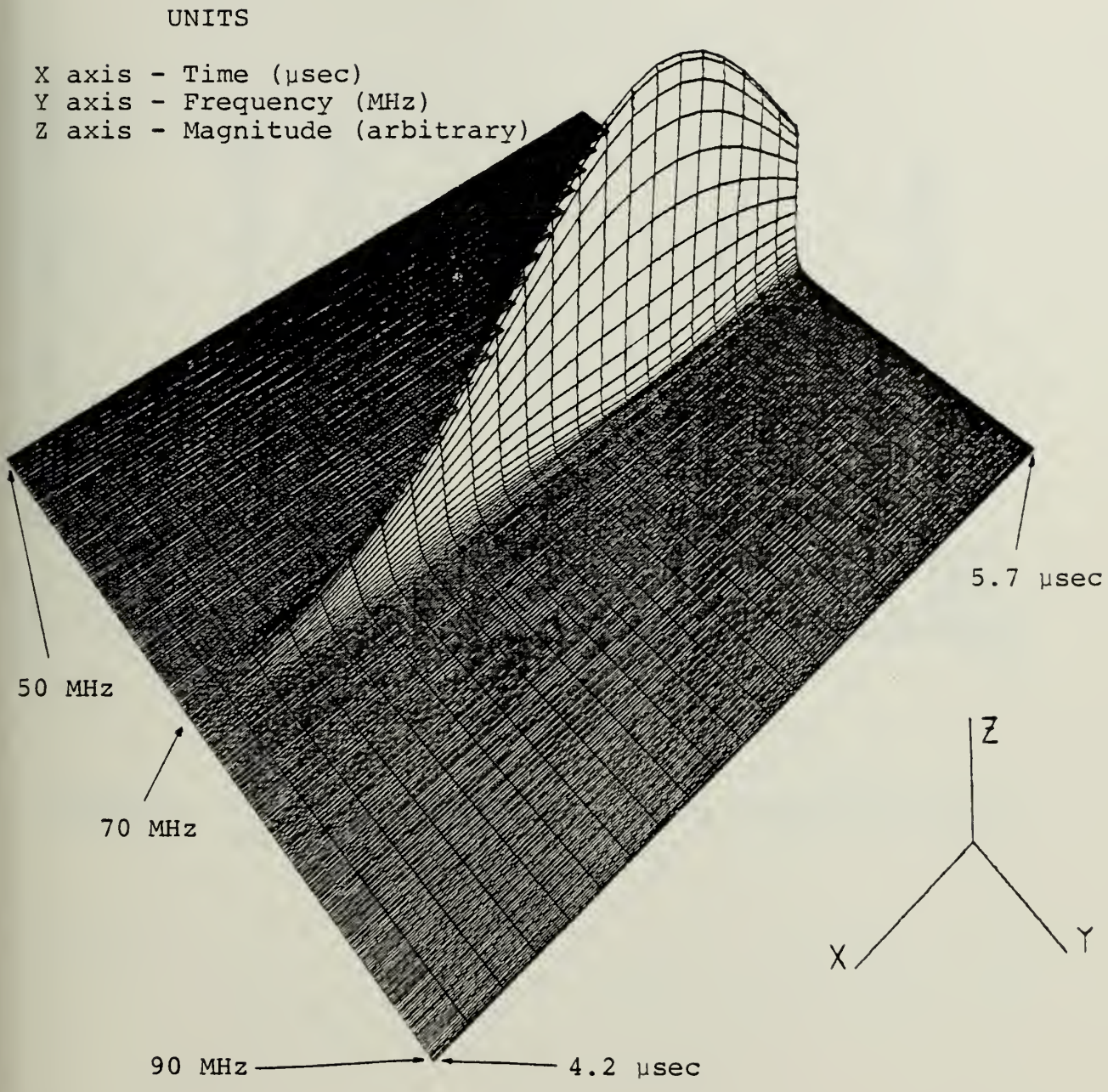

Figure 24. Image Plane Intensity Profile (Magnitude) Produced by a Monotonic 70 MHz Signal with an Incident Gaussian Beam and a Stepped Array Transducer (Dynamic Model)

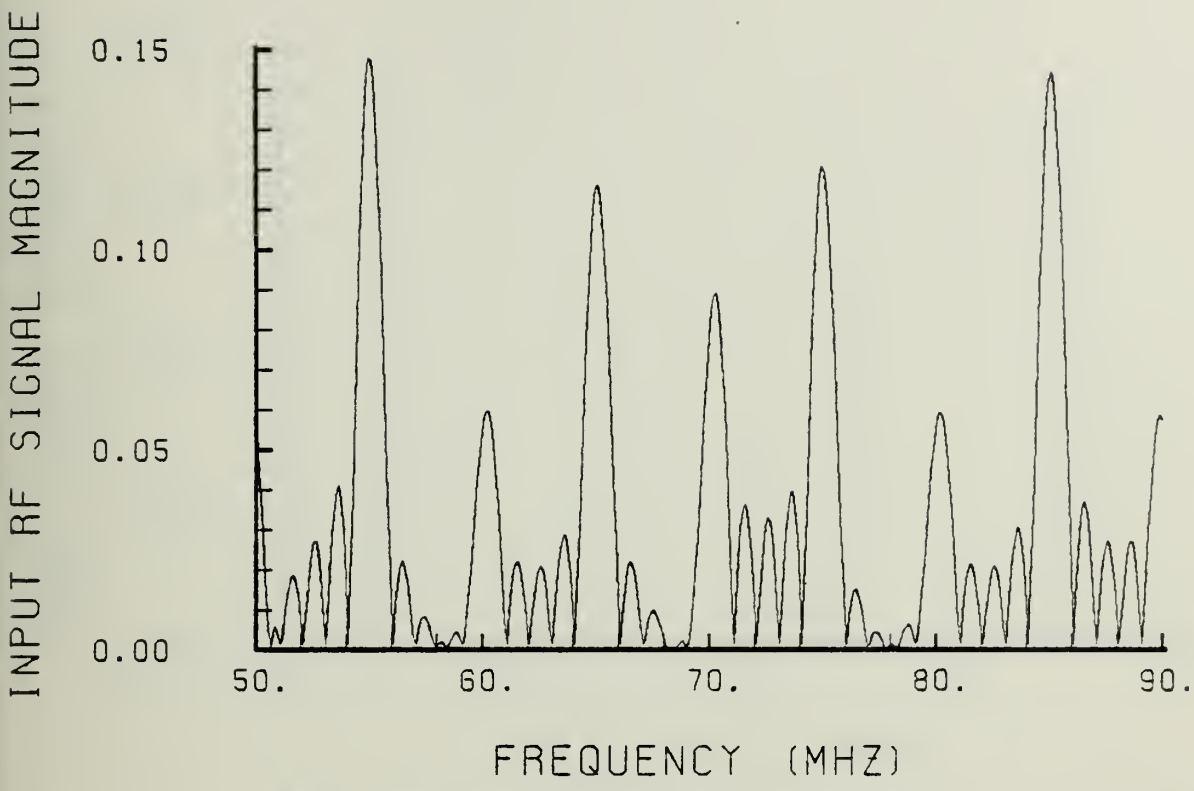

Figure 25. Input RF Magnitude for an FM Modulation Signal with $\beta = 8.0$, $f_m = 5$ MHz

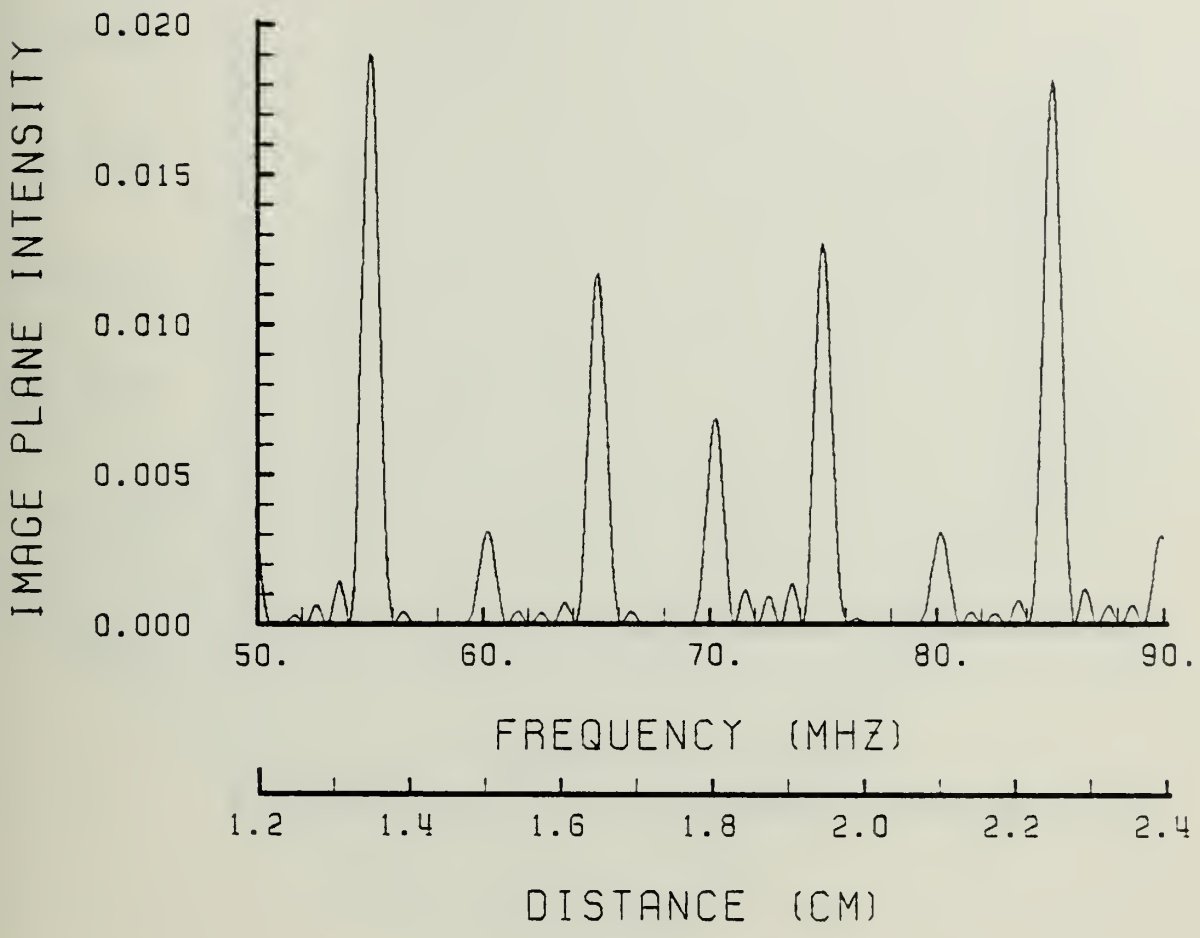

Figure 26. Image Plane Intensity Profile (Magnitude) Produced by an FM Modulation Signal, $\beta = 8.0$, $f_m = 5$ MHz, with an Incident Plane Wave and a Stepped Array Transducer

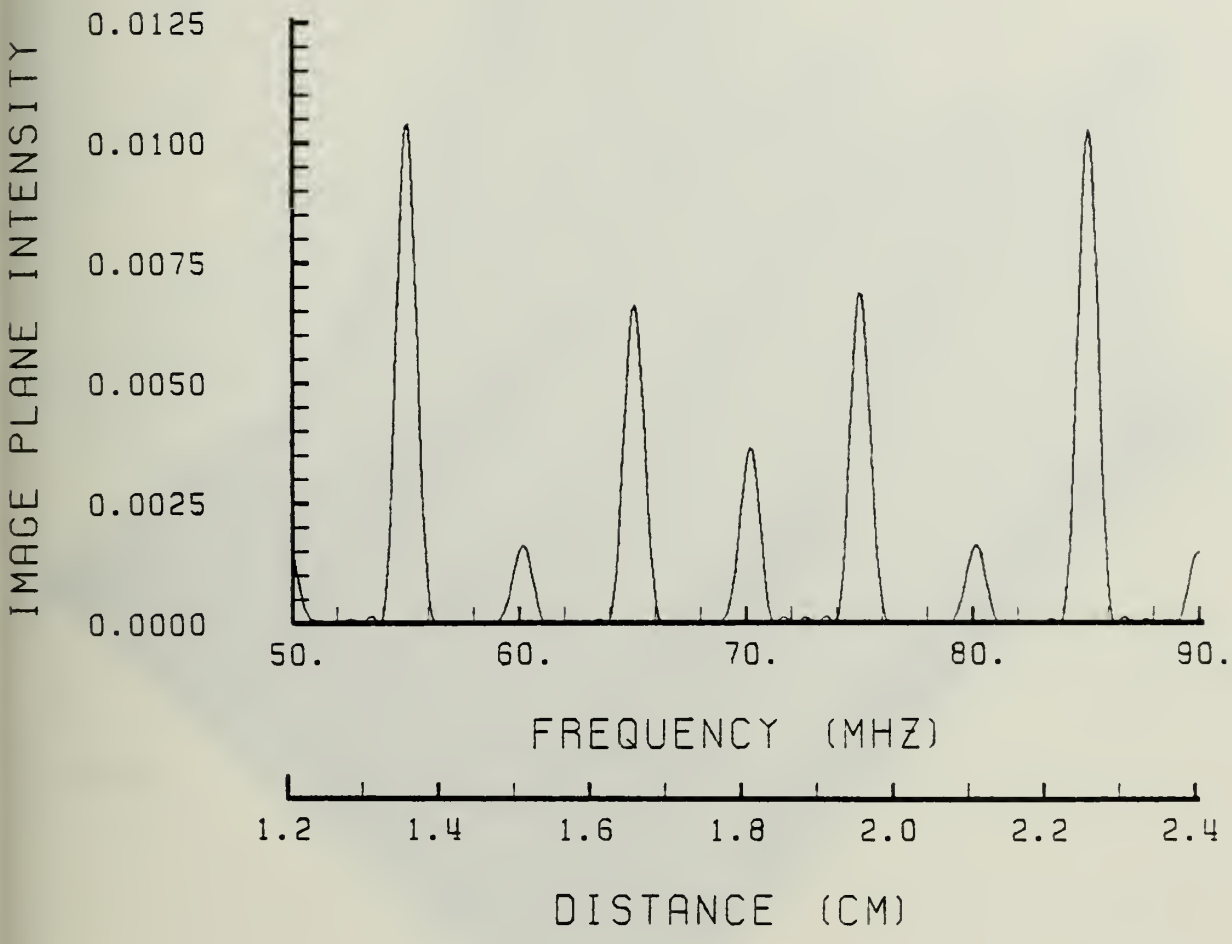

Figure 27. Image Plane Intensity Profile (Magnitude) Produced by an FM Modulation Signal, $\beta = 8.0$, $f_m = 5$ MHz, with an Incident Gaussian Beam and a Stepped Array Transducer

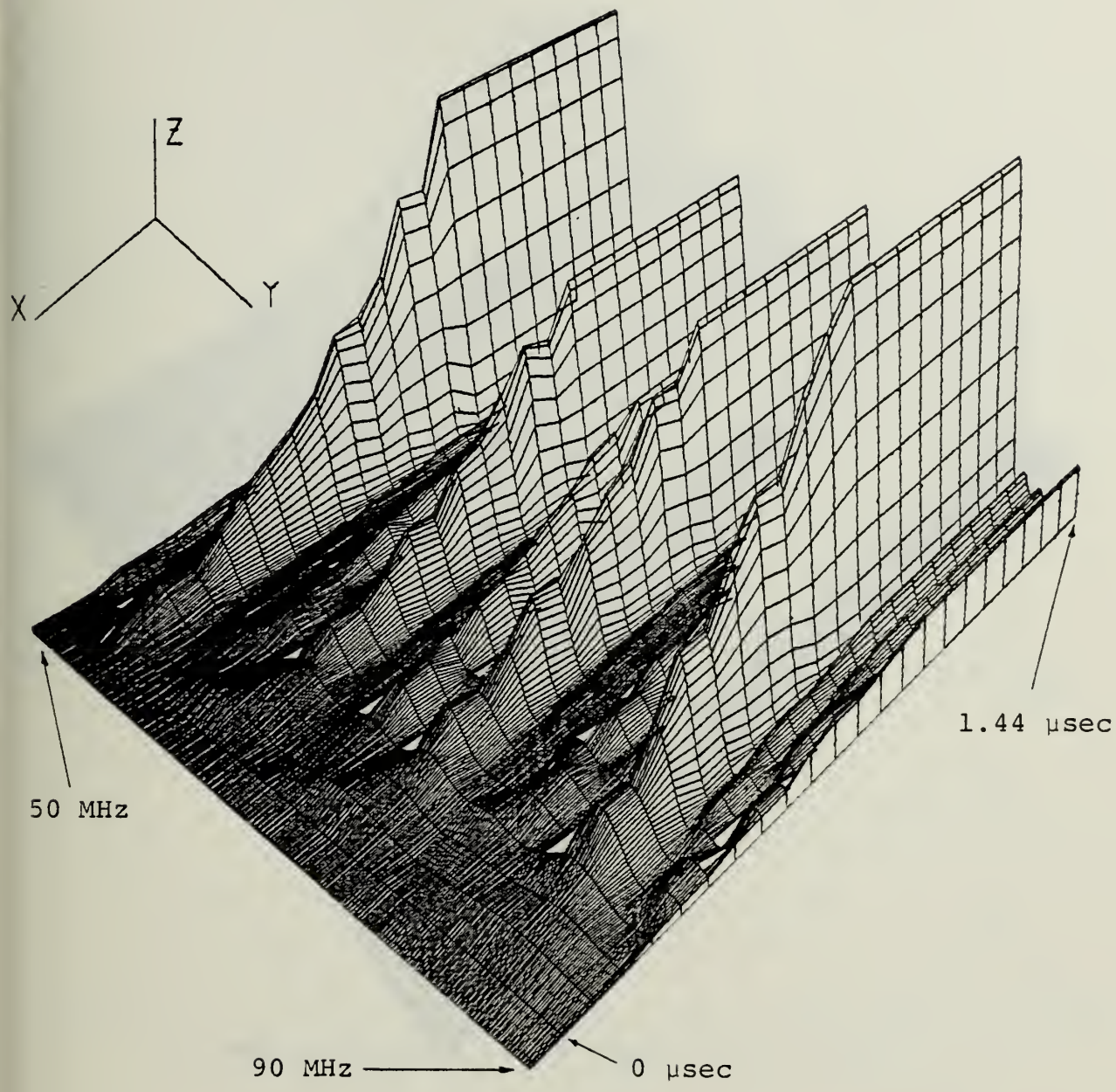

UNITS

X axis - Time (μsec)
Y axis - Frequency (MHz)
Z axis - Magnitude (arbitrary)

Figure 28. Image Plane Intensity Profile (Magnitude) Produced by an FM Modulation Signal, $\beta = 8.0$, $f_m = 5$ MHz, with an Incident Plane Wave and a Stepped Array Transducer (Dynamic Model)

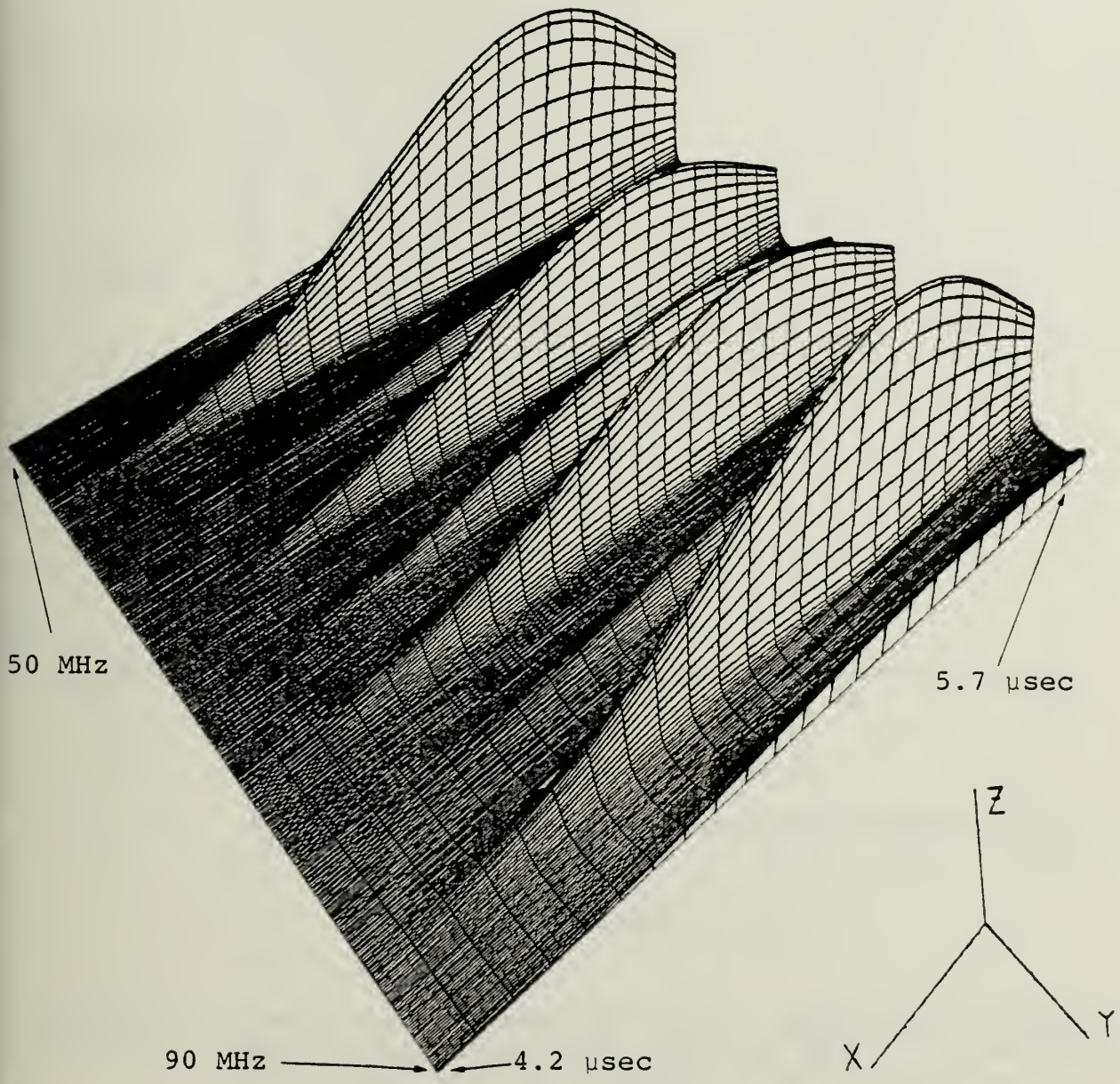

UNITS

X axis - Time (μsec)
Y axis - Frequency (MHz)
Z axis - Magnitude (arbitrary)

Figure 29. Image Plane Intensity Profile (Magnitude) Produced by an FM Modulation Signal, $\beta = 8.0$, $f_m = 5$ MHz, with an Incident Gaussian Beam and a Stepped Array Transducer (Dynamic Model)

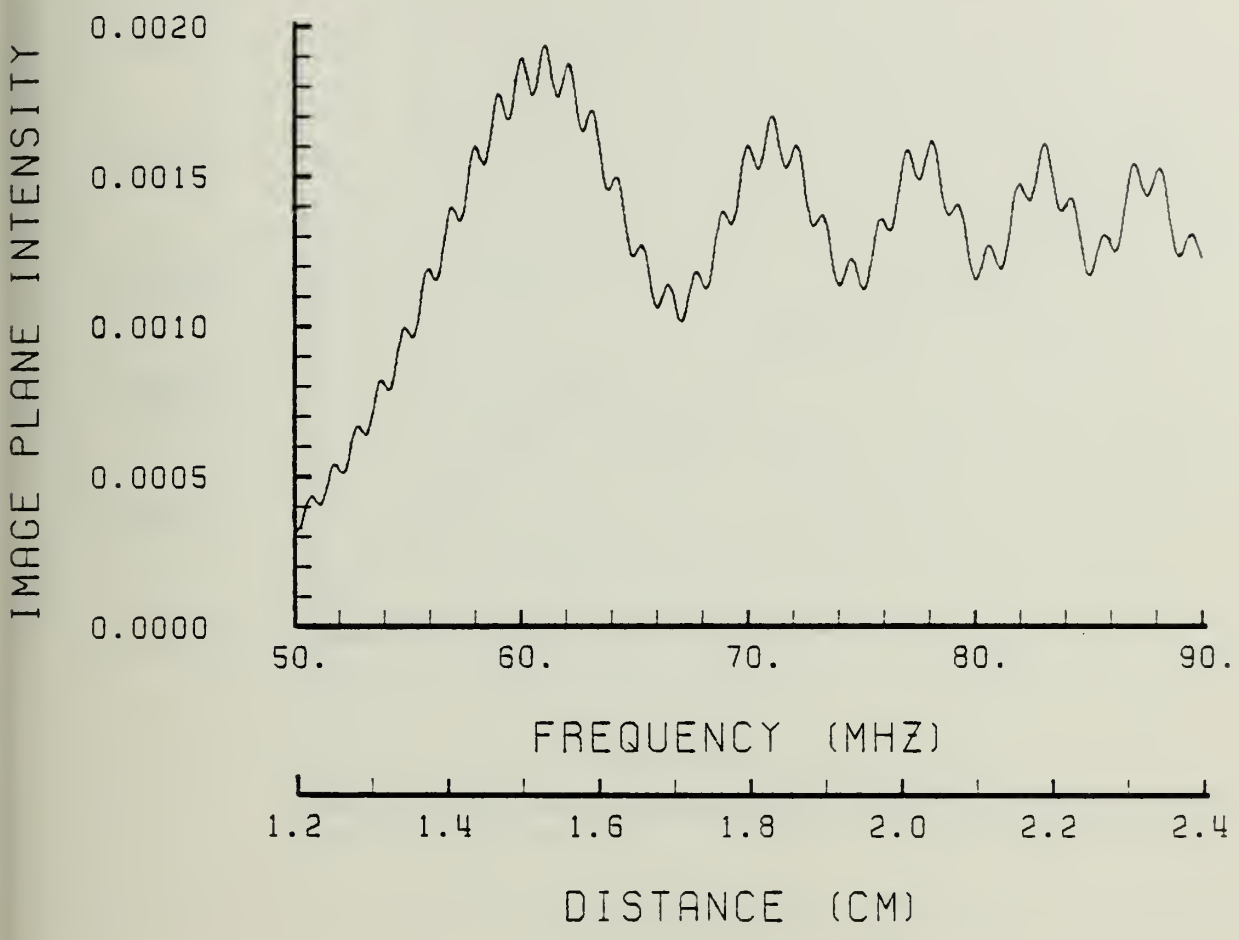

Figure 30. Image Plane Intensity Profile (Magnitude) Produced by a Linear Chirp with Δf_m = 80 MHz, f_o = 50 MHz, t = 2 μsec with an Incident Plane Wave and a Stepped Array Transducer

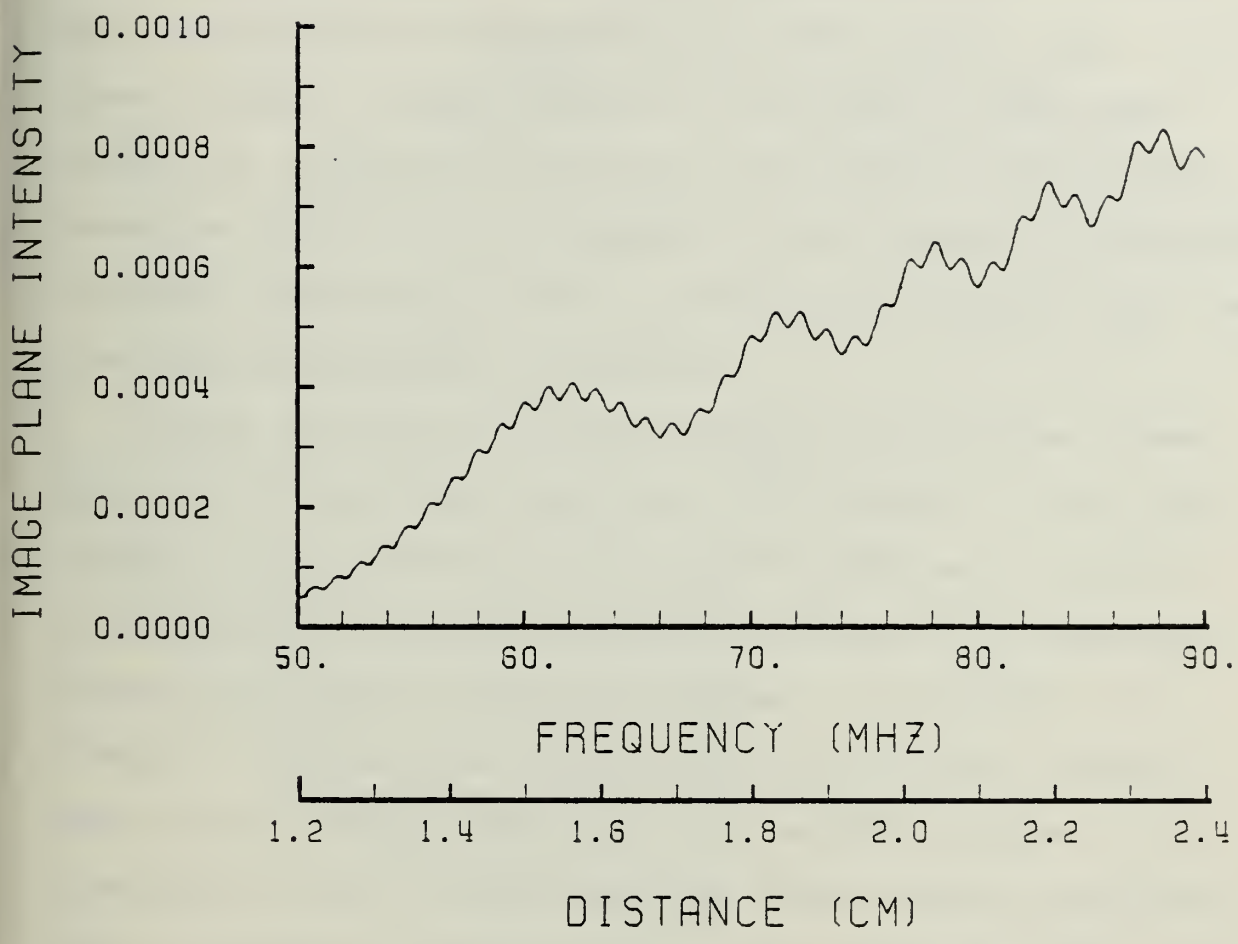

Figure 31. Image Plane Intensity Profile (Magnitude) Produced by a Linear Chirp with Δf_m = 80 MHz, f_o = 50 MHz, t = 2 μsec with an Incident Gaussian Beam and a Stepped Array Transducer

beam. For both the chirp parameters are Δf_m = 80 MHz, f_o = 50 MHz, and t = 2 microseconds. Both show high and low frequency ripples. The high frequency ripple is an artifact of the digital implementation of the linear chirp. The lower frequency ripple present is the effect of the fundamental and sidelobe interaction. The Gaussian interaction shows the effects of its inherent slower response and degraded frequency resolution in the attenuation of magnitude over the lower halfband frequency components.

Figure 32 shows the dynamic response of the same linear chirp and an incident plane wave. The severity of the interaction of the fundamental and sidelobe components, as additional frequency components enter the Bragg cell, manifests itself in a dynamic transient response. Only after a considerable interval does the response settle into a steady state displaying the expected chirp spectral profile. For comparison Figure 33 shows the same linear chirp interacting with an incident Gaussian beam of 1.945 millimeter spot size. In this case the sidelobe suppression is a distinct advantage producing a smooth steady state response almost from the onset of the interaction. It must be kept in mind that the interaction will continue to begin much later than that of the plane wave and thus the plane wave will achieve steady state earlier than the Gaussian.

The TAOSA program also has the decibel output option. Figure 34 shows the relative decibel image plane intensity of a monotone of 70 MHz interacting with a plane wave.

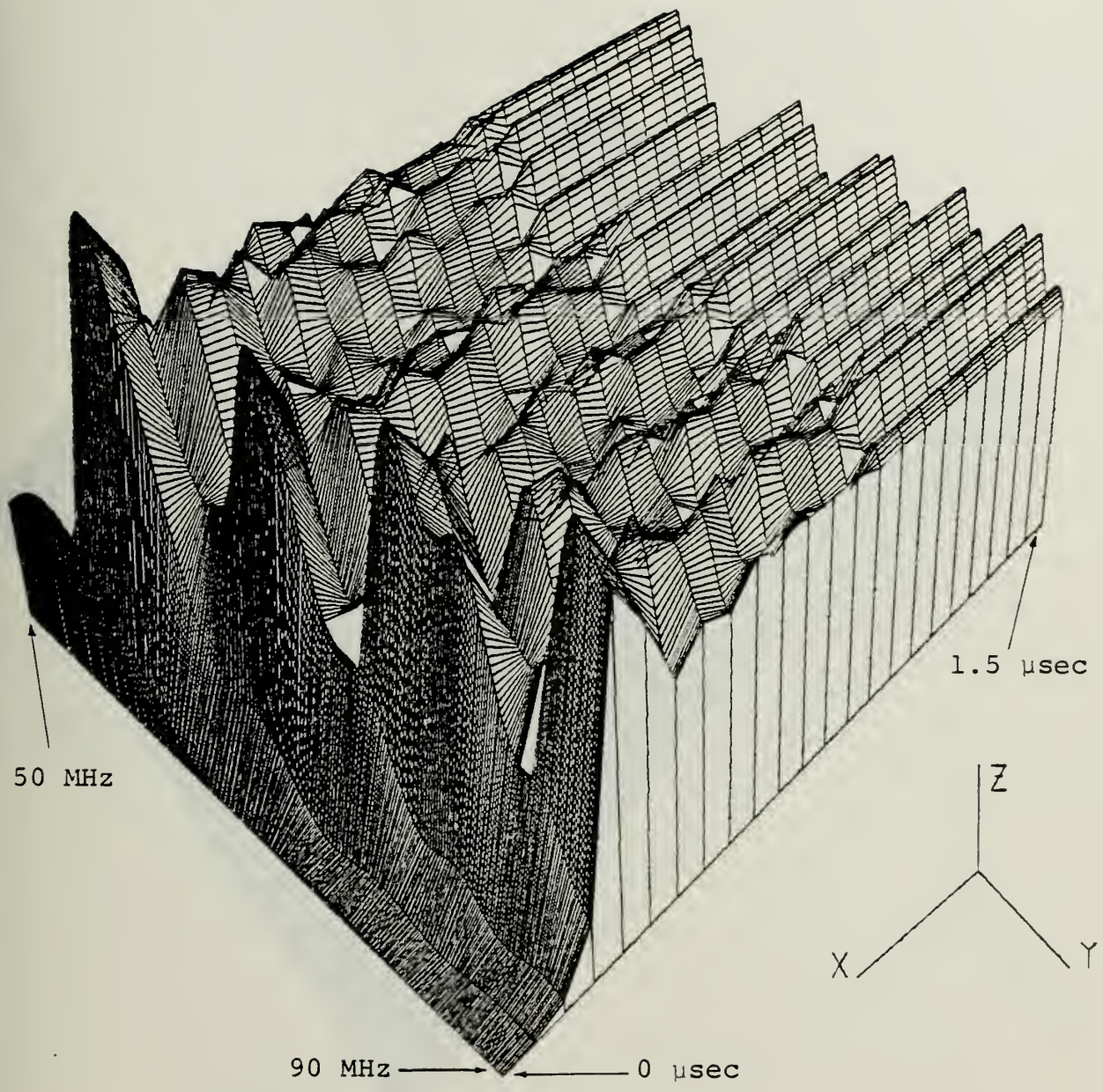

UNITS

X axis - Time (μsec)
Y axis - Frequency (MHz)
Z axis - Magnitude (arbitrary)

Figure 32. Image Plane Intensity Profile (Magnitude) Produced by a Linear Chirp with Δf_m = 80 MHz, f_o = 50 MHz, t = 2 μsec, with an Incident Plane Wave and a Stepped Array Transducer (Dynamic Model)

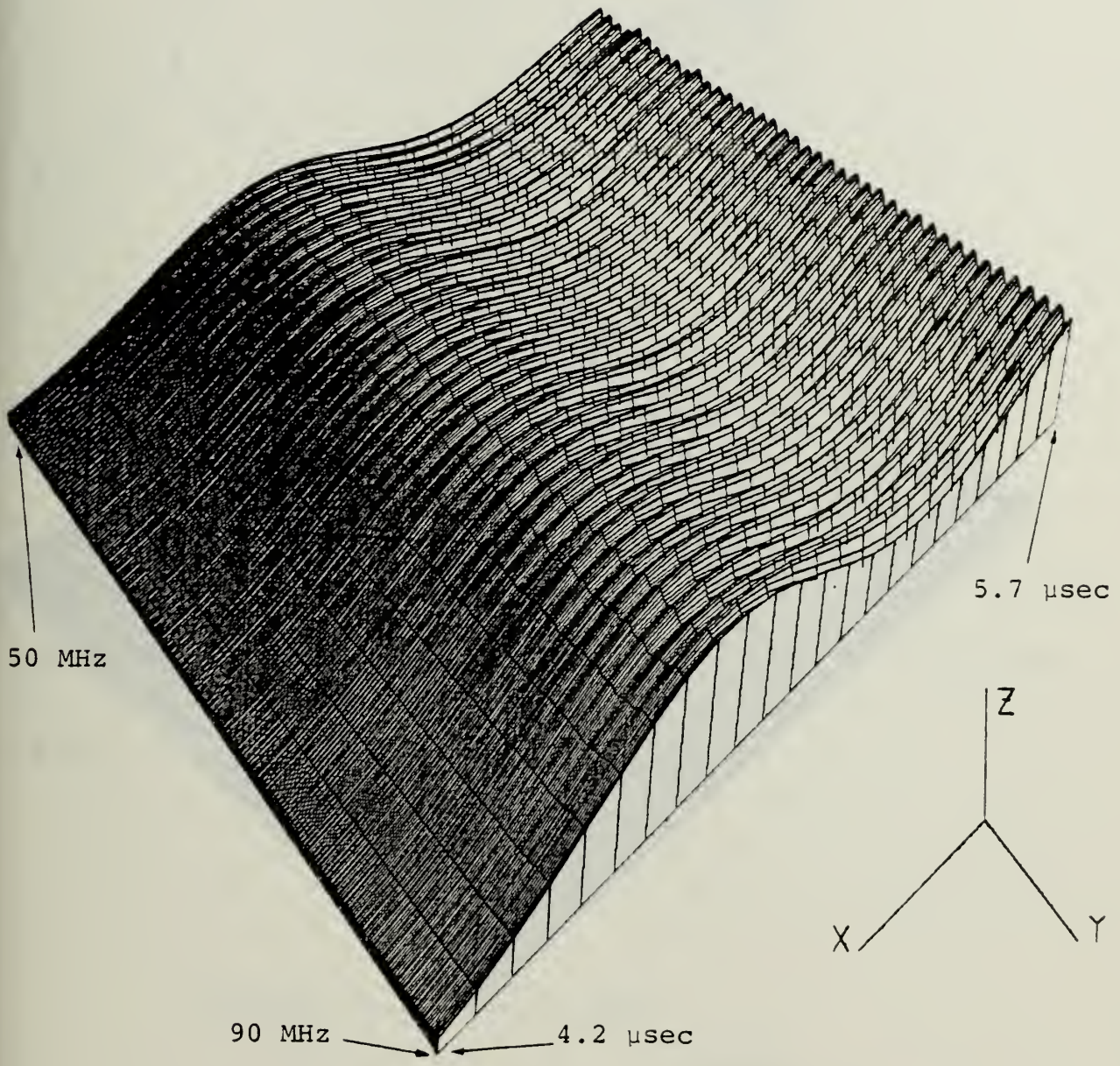

UNITS

X axis - Time (μsec)
Y axis - Frequency (MHz)
Z axis - Magnitude (arbitrary)

Figure 33. Image Plane Intensity Profile (Magnitude) Produced by a Linear Chirp with Δf_m = 80 MHz, f_o = 50 MHz, t = 2 μsec with an Incident Gaussian Beam and a Stepped Array Transducer (Dynamic Model)

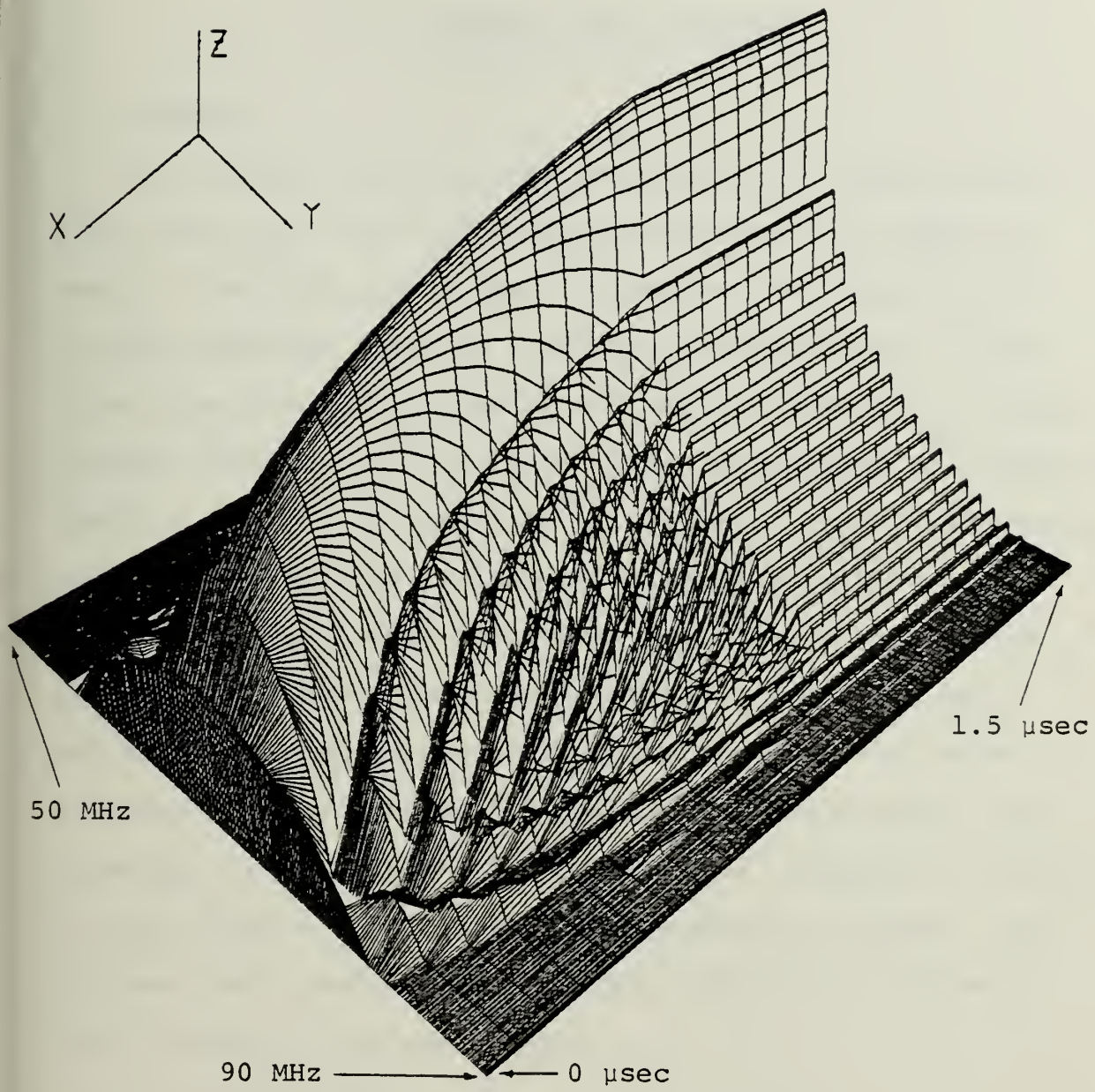

UNITS

X axis - Time (µsec)
Y axis - Frequency (MHz)
Z axis - Magnitude (relative dB)

Figure 34. Image Plane Intensity Profile (Decibel) Produced by a Monotonic 70 MHz Signal with an Incident Plane Wave and a Stepped Array Transducer (Dynamic Model)

III. SUMMARY AND CONCLUSIONS

A. SUMMARY

This thesis has presented an analysis of Bragg diffraction theory and direct detection acoustooptical spectrum analysis modeling techniques. Based on the study of the various modeling theories a suitable approach for a first order simulation was selected and used to develop a Fortran program modeling the direct detection acoustooptical spectrum analysis process. Extensions of the basic theory have been added to include the factors of diffraction efficiency, transducer efficiency, irradiance profiles of the incident laser illumination, the aperture size of the Bragg cell, and acoustic attenuation of the generated acoustic wave. A second program dynamically models the AOSA process incorporating a time variable to simulate the response of the AOSA as the acoustic wave transits the interaction region. The programs were used to model the NPS laboratory AOSA using the parameters from that system.

B. AREAS FOR FURTHER STUDY

Further effort related to this thesis is required in the following areas.

1. Nonlinearities

The theoretical basis for the AOSA model program does not take into account the nonlinear effects of crossmodulation

(the compression of one signal due to another) or intermodulation (the interaction of two or more signals). While the restriction of the operation of the AOSA to the Bragg regime eliminates much of the effects of these nonlinearities, the overall effect on the replication efficiency is still at issue. Further analysis is needed to determine if these factors seriously degrade the model's accuracy. Hecht discusses this issue in Ref. 21.

2. Time Varying Signals

The ability of the AOSA to respond to rapid time varying signals (which will depend on the speed of response of the detector array and the Bragg cell) needs to be examined. Currently the TAOSA program provides for a fixed delay for the simulation of overall system response time.

3. System Components

The physical response and performance of the AOSA systems components warrant further study. Currently only a gross simulation of the system response time can be made by insertion of a fixed time delay. Closer examination of the speed of the detector array with particular emphasis on the uniformity of photosite response is needed. Integrated optical devices for AOSA and AOSE applications will use semi-conductor lasers. These lasers will need to be examined for the system effects produced by fluctuations in intensity and variations in coherence. The current HeNe laser used in the NPS system should be examined for its intensity and coherence fluctuations and resultant effects.

C. CONCLUSIONS

Comparison of the AOSA model image plane intensity profiles with known AOSA system output spectral profiles demonstrates the AOSA program as a satisfactory first order simulation. The acoustooptical spectral analysis process yields high quality replication of the spectral content on input signals. Future coupling of the AOSA program with optical excision routines previously developed may provide additional insight into the application of acoustooptical spectral analysis and excision for use in wideband, high density signal environments.

APPENDIX A

ACOUSTOOPTIC SPECTRUM ANALYZER (AOSA) PROGRAM

This Fortran program calculates the relative Bragg deflected image plane intensity profiles for multifrequency input r-f signals to a modeled acoustooptic spectrum analyzer (AOSA). The physical parameters used in the modeling of the AOSA are discussed within the program and are summarized in Table II of the thesis.

The program provides several additional selectable variables:

ITEST - provides for graphical and numerical or graphical only output

IWAVE - provides for choice of plane or Gaussian incident light waves

ITRANS - provides for choice of simple or first order stepped array transducer simulations

IDB - provides for choice of graphical output in magnitude or relative dB formats

IGRAF - provides for choice of line printer or Versatec graphical plotting

IPLOT - provides for choice of PLOTG or DRAWP Versatec plotting subroutines

Use of these variables is discussed within the program.

Additional alterable variables exist within the program related to the Fourier transform process. It is believed that the present configuration will suffice for most general applications.

This program utilizes the PLOTG and DRAWP Versatec software subroutines, the line plot subroutine PLOTP, and FOURT, which calculates the forward and inverse Cooley-Tukey Fast Fourier Transform of multidimensional complex data. Prospective utilizers at the Naval Postgraduate School should refer to the W. R. Church Computer Center for detailed information.

```
C
C   ACOUSTO-OPTICAL SPECTRUM ANALYZER MODEL
C
      DIMENSION SINL(2,6400),WORK(12800),F(19200),TEMP1(6400),TEMP2(6400
     1),TEMP3(6400),TEMP4(6400),TEMP5(6400),TEMP6(6400),TEMP7(6400),TEMP
     28(6400),BP(6400),TT1(640),TT2(640),TT3(640),TINL(2,6400),TE(6400)
      INTEGER*4 ITB(12)/12*0/
      REAL*4 L(6400),RTB(28),STB(28),TTB(28),UTB(28),QTB(28),WTB(28),
     1ATB(28),BTB(28),CTB(28),DTB(28)
      REAL LMBDA,LFL,LZERO,LLO,LW
      ITB(2)=0
      ITB(3)=5
      ITB(4)=3
      ITB(12)=0
C
C   INITIALIZATION OF PARAMETERS UTILIZED IN THE AOSA MODEL PROGRAM
C
C              N        = NUMBER OF SAMPLES PER RECORD LENGTH
C              NP       = NUMBER OF SAMPLES PER PULSE LENGTH
C              FCO      = CENTRAL FREQUENCY OF BRAGG CELL
C              DCELL    = EFFECTIVE APPERTURE OF BRAGG CELL
C              PULSE    = PULSE LENGTH (TYPICALLY 1 MICROSECOND)
C              PERIOD   = RECORD LENGTH
C              LL       = LOWER FREQUENCY INCREMENT FOR BANDWIDTH OF CELL
C              LU       = UPPER FREQUENCY INCREMENT FOR BANDWIDTH OF CELL
C              LD       = NUMBER OF DELTAF CONTAINED IN BANDWIDTH OF CELL
C              NXL      = LOWER SPATIAL INCREMENT FOR PULSE WIDTH
C              NXU      = UPPER SPATIAL INCREMENT FOR PULSE WIDTH
C              NDL      = LOWER SPATIAL INCREMENT FOR CELL EFF APERTURE
C              NDU      = UPPER SPATIAL INCREMENT FOR CELL EFF APERTURE
C              LZERO    = CHARACTERISTIC INTERACTION LENGTH OF BRAGG CELL
C              LLO      = RATIO OF INTERACTION LENGTH TO CHARACTERISTIC
C                         INTERACTION LENGTH OF BRAGG CELL
C              LW       = INTERACTION LENGTH
C              VS       = ACOUSTIC VELOCITY
C              SPOT     = DESIRED DETECTOR ARRAY SPOT SIZE
C              LMBDA    = LASER WAVELENGTH
C              BW       = BEAM WIDTH OF COLLIMATED GAUSSIAN BEAM (3DB)
C              EFFD     = EFFECTIVE DIAMETER OF EXIT BEAM FROM BRAGG CELL
C              THETAO   = DEFLECTION ANGLE OF BRAGG CELL CENTER FREQUENCY
C              REFIND   = REFRACTIVE INDEX OF BRAGG CELL MATERIAL
C              LFL      = FOURIER TRANSFORM LENS FOCAL LENGTH
C              DELTAT   = TIME SAMPLE INCREMENT = PERIOD/N
C              DELTAF   = FREQUENCY RESOLUTION INCREMENT = 1/PERIOD
C              DELTAX   = SPATIAL RESOLUTION INCREMENT =VS*DELTAT
C              TDELAY   = TIME VARIANCE IN SECS (SHOULD BE INTEGRAL
C                         MULTIPLE OF DELTAT)
C
```

```
      N=6400
      N1=N+1
      N2=N*2
      N3=N2+1
      N4=N*3
      PI=3.141592654
      DCELL=39.0E-3
      VS=3.90E+3
      LMBDA=6.328E-7
      REFIND=2.2
      SPOT=26.0E-6
      BW=1.945E-3
      LW=5.08E-2
      TDELAY=0.0
      PULSE=1.0E-6
      PERIOD=10.*PULSE
      NP=N*PULSE/PERIOD
      DELTAT=PERIOD/N
      DELTAF=1./PERIOD
      DELTAX=VS*DELTAT
      NXL=N/2-NP/2
      NXU=N/2+NP/2
      NXO=N/2
      NXU1=NXU+1
      NXL1=NXL+1
      XO=(N/2)*DELTAX
      XSL=NXL*DELTAX
      XSU=NXU*DELTAX
      NDD=(DCELL/DELTAX)+1
      NDL=N/2-NDD/2
      NDU=N/2+NDD/2
      NDL1=NDL+1
      NDU1=NDU+1
      ND=NDU-NDL
      LXO=(N/2)*DELTAX
      LXL=NDL*DELTAX
      LXU=NDU*DELTAX
      LL=(5.0E+7)/DELTAF
      LU=(9.0E+7)/DELTAF
      LL1=LL+1
      LU1=LU+1
      LD=LU-LL
      FCO=7.0E+7
      THETAO=(LMBDA*FCO)/(2.*VS)
      LZERO=(REFIND/LMBDA)*(COS(THETAO))*((VS**2)/(FCO**2))
      LLO=LW/LZERO
      NDELAY=(TDELAY*VS)/DELTAX
C
```

```
C  SET ITEST   = 1  IF TABULAR AND GRAPHICAL OUTPUT IS DESIRED
C             = 0  IF ONLY GRAPHICAL OUTPUT IS DESIRED
C  SET IGRAF   = 1  IF VERSATEC PLOT IS DESIRED
C             = 0  IF LINE PRINTER PLOT IS DESIRED
C  SET IDB     = 1  IF ORDINATE IS COMPUTED AS MAGNITUDE/INTENSITY
C             = 0  IF ORDINATE IS COMPUTED AS RELATIVE DB
C  SET ITRANS  = 1  IF PHASED ARRAY TRANSDUCER IS UTILIZED
C             = 0  IF SIMPLE TRANSDUCER IS UTILIZED
C  SET IWAVE   = 1  FOR GAUSSIAN WAVEFRONT
C             = 0  FOR PLANE WAVEFRONT
C  SET IPLOT   = 1  FOR DRAWP SUBROUTINE IF VERSATEC SOFTWARE IS UTILIZED
C             = 0  FOR PLOTG SUBROUTINE IF VERSATEC SOFTWARE IS UTILIZED
C
      ITEST=0
      IGRAF=1
      IDB=1
      ITRANS=1
      IWAVE=1
      IPLOT=0
C
C  INPUT THE TIME DOMAIN SIGNAL
C
      DO 1 I=1,NXL
      SINL(1,I)=0.0
    1 SINL(2,I)=0.0
      DO 2 I=NXL,NXU
C  ************************************
      FW0=7.0E+7
      FW1=0.0
      FS0=5.5E+7
      FS1=6.0E+7
      FS2=6.5E+7
      FS3=7.0E+7
      FS4=7.5E+7
      FS5=8.0E+7
      FS6=8.5E+7
CCCC            MONO/MULTIPLE TONES
C     SINL(1,I)=(COS(2.*PI*FW0*I*PERIOD/N))+(COS(2.*PI*FW1*I*PERIOD/N))
CCCC            SWEEP MULTIPLE TONES
C     SINL(1,I)=(COS(2.*PI*FS0*I*PERIOD/N))+(COS(2.*PI*FS1*I*PERIOD/N))+
C    1 (COS(2.*PI*FS2*I*PERIOD/N))+(COS(2.*PI*FS3*I*PERIOD/N))+
C    2 (COS(2.*PI*FS4*I*PERIOD/N))+(COS(2.*PI*FS5*I*PERIOD/N))+
C    3 (COS(2.*PI*FS6*I*PERIOD/N))
CCCC            SIMPLE TWO TONE BEAT
C     SINL(1,I)=(COS(2.*PI*FW0*I*PERIOD/N))*(COS(2.*PI*FW1*I*PERIOD/N))
CCCC            PM MODULATION
C     SINL(1,I)=(COS((2.*PI*FW0*I*PERIOD/N)+((2.*PI*FM*I*PERIOD/N)*
C    1((I-NXL)/NP))))
```

```
C      FM=4.0E+7
CCCC              FM MODULATION
C      BBETA=8.0
C      FM=5.0E+6
C      SINL(1,I)=(COS((2.*PI*FWO*I*PERIOD/N)+(BBETA*SIN(2.*PI*
C     1FM*I*PERIOD/N))))
CCCCCC            LINEAR CHIRP
       FM=1.25E+5
       SINL(1,I)=COS((2.*PI*I*(PERIOD/N)*(FWO+(FM*(I-NXL)))))
C ***************************************
     2 SINL(2,I)=0.0
       DO 3 I=NXU1,N
       SINL(1,I)=0.0
     3 SINL(2,I)=0.0
C
C COMPUTE TIME DOMAIN SIGNAL CHARACTERISTICS
C
       DO 5 I=1,N
       TEMP1(I)=DELTAT*I
       TEMP2(I)=SINL(1,I)
       TEMP7(I)=TEMP2(I)
     5 TEMP3(I)=SQRT(((SINL(1,I))**2)+((SINL(2,I))**2))
C
C TRANSFER TIME DOMAIN SIGNAL VALUES TO TEMPORARY REGISTERS FOR
C TABULAR AND/OR GRAPHICAL OUTPUT
C
       DO 6 I=1,NP
       K=NXL+I+1
       TT1(I)=TEMP1(K)
     6 TT2(I)=TEMP2(K)
C
C COMPUTE FOURIER TRANSFORM LENS FOCAL LENGTH
C
       EFFD=DCELL
       LFL=EFFD*SPOT/LMBDA
C
C INPUT DIFFRACTION EFFICIENCY BANDPASS FUNCTION
C
       IF(ITRANS)9,16,9
     9 DO 10 I=1,LL
    10 BP(I)=0.0
       DO 11 I=LL,LU
    11 BP(I)=.87
       DO 12 I=LU1,N
    12 BP(I)=0.0
       GO TO 23
    16 DO 20 I=1,N
       IF(I*DELTAF-FCO)17,18,17
```

```
   17 AA=((PI/2.)*LLO*((I*DELTAF/FCO)-((I*DELTAF/FCO)**2)))
      BB=SIN(AA)
      CC=(BB/AA)**2
      GO TO 19
   18 CC=1.0
   19 CONTINUE
   20 BP(I)=CC
   23 CONTINUE
C
C  INPUT TRANSDUCER EFFICIENCY BANDPASS FUNCTION(TOPHAT ASSUMED)
C
      DO 24 I=1,N
   24 TE(I)=1.0
C
C  COMPUTE ACTUAL FREQUENCY SPECTRUM OF INTERACTED PULSE
C
      IF(NDELAY)25,28,25
   25 DO 26 I=1,NDELAY
   26 TEMP7(I)=0.0
   28 DO 29 I=1,N
      TINL(1,I)=TEMP7(I)
   29 TINL(2,I)=0.0
      CALL FOURT(TINL,N,1,-1,0,WORK)
      DO 30 I=LL1,LU1
   30 TEMP7(I)=SQRT(((TINL(1,I))**2)+((TINL(2,I))**2))/NP
C
C  OUTPUT TIME DOMAIN SIGNAL CHARACTERISTICS
C
      IF(ITEST)111,112,111
  111 WRITE(6,900)DELTAT,DELTAF,DELTAX
      WRITE(6,901)
      WRITE(6,902)
      WRITE(6,903)(TEMP1(I),SINL(1,I),SINL(2,I),TEMP3(I),I=NXL,NXU)
  112 IF(IGRAF)114,113,114
  113 WRITE(6,904)
      WRITE(6,905)
      CALL PLOTP(TT1,TT2,NP,0)
      WRITE(6,900)DELTAT,DELTAF,DELTAX
      GO TO 119
  114 IF(NP.LT.1599) GO TO 115
      RTB(1)=0.0
      RTB(2)=0.0
      RTB(3)=0.0
      RTB(4)=0.0
      DATA RTB(05),RTB(06),RTB(07),RTB(08)/'INPU','T RF',' SIG','NAL '/
      DATA RTB(09),RTB(10),RTB(11),RTB(12)/'VS T','IME ',',   ',',   '/
      DATA RTB(13),RTB(14),RTB(15),RTB(16)/'   ',',   ',',   ',',   '/
      DATA RTB(17),RTB(18),RTB(19),RTB(20)/4*'   '/
```

```
      DATA RTB(21),RTB(22),RTB(23),RTB(24)/4*'    '/
      DATA RTB(25),RTB(26),RTB(27),RTB(28)/4*'    '/
      IF(IPLOT)510,511,510
  510 CALL DRAWP(NP,TT1,TT2,ITB,RTB)
      GO TO 119
  511 CALL PLOTG(TT1,TT2,NP,1,1,0,'TIME',5,'INPUT RF SIGNAL MAGNITUDE',
     1 25,0.0,0.0,0.0,0.0,4.5,3.0)
      GO TO 119
  115 WRITE(6,910)
      WRITE(6,904)
      WRITE(6,905)
      CALL PLOTP(TT1,TT2,NP,0)
  119 CONTINUE
C
C CALL THE FFT SUBROUTINE TO CONVERT THE TIME DOMAIN SIGNAL TO THE
C FREQUENCY DOMAIN
C
      CALL FOURT(SINL,N,1,-1,0,WORK)
      DO 200 I=LL1,LU1
      TEMP1(I)=DELTAF*I/(1.0E+6)
  200 TEMP2(I)=SQRT(((SINL(1,I))**2)+((SINL(2,I))**2))/NP
C
C INPUT THE TRUNCATED LASER WAVEFRONT
C
      IF(IWAVE)205,210,205
  205 DO 206 I=1,NDL
  206 L(I)=0.0
      DO 207 I=NDL,NDU
      FLTI=FLOAT(I)/FLOAT(N)
  207 L(I)=EXP(-4.*((DCELL/(2.*BW))**2)*((FLTI-.5)**2))
      DO 208 I=NDU1,N
  208 L(I)=0.0
      WRITE(6,921)
      WRITE(6,923)LL0
      GO TO 240
  210 DO 221 I=1,NDL
  221 L(I)=0.0
      DO 222 I=NDL,NDU
  222 L(I)=1.0
      DO 223 I=NDU1,N
  223 L(I)=0.0
      WRITE(6,922)
      WRITE(6,923)LL0
  240 CONTINUE
      WRITE(6,930)BW
C
C TRANSFER VALUES FOR BANDWIDTH OF CONCERN (50-90 MHZ) TO TEMPORARY
C REGISTERS FOR TABULAR AND/OR GRAPHICAL OUTPUT
```

```
C
      DO 250 I=1,LD
      K=LL+I
      TEMP3(I)=TEMP1(K)
  250 TEMP4(I)=TEMP2(K)
C
C OUTPUT FREQUENCY DOMAIN SIGNAL CHARACTERISTICS
C
      IF (ITEST)260,270,260
  260 WRITE(6,904)
      WRITE(6,906)
      WRITE(6,900)DELTAT,DELTAF,DELTAX
      WRITE(6,907)
      WRITE(6,903)(TEMP1(I),SINL(1,I),SINL(2,I),TEMP2(I),I=LL1,LU1)
  270 IF(IGRAF)290,280,290
  280 IF(IDB)281,282,281
  281 WRITE(6,904)
      WRITE(6,908)
      CALL PLOTP(TEMP3,TEMP4,LD,0)
      WRITE(6,909)DELTAF
      GO TO 300
  282 CALL DBCON(TEMP4,LD,N)
      WRITE(6,904)
      WRITE(6,924)
      CALL PLOTP(TEMP3,TEMP4,LD,0)
      WRITE(6,909)DELTAF
      GO TO 300
  290 CONTINUE
  291 IF(IDB)292,293,292
  292 CONTINUE
      STB(1)=0.0
      STB(2)=0.0
      STB(3)=0.0
      STB(4)=0.0
      DATA STB(05),STB(06),STB(07),STB(08)/'INPU','T RF',' SIG','NAL '/
      DATA STB(09),STB(10),STB(11),STB(12)/'MAGN','ITUD','E VS',' FRE'/
      DATA STB(13),STB(14),STB(15),STB(16)/'QUEN','CY (','MHZ)','    '/
      DATA STB(17),STB(18),STB(19),STB(20)/4*'    '/
      DATA STB(21),STB(22),STB(23),STB(24)/4*'    '/
      DATA STB(25),STB(26),STB(27),STB(28)/4*'    '/
      IF(IPLOT)512,513,512
  512 CALL DRAWP(LD,TEMP3,TEMP4,ITB,STB)
      GO TO 300
  513 CALL PLOTG(TEMP3,TEMP4,LD,1,1,0,'FREQUENCY (MHZ)',15,'INPUT RF SIG
     1NAL MAGNITUDE',25,0.0,0.0,0.0,0.0,4.5,3.0)
      GO TO 300
  293 ATB(1)=0.0
      ATB(2)=0.0
```

```
      ATB(3)=0.0
      ATB(4)=0.0
      DATA ATB(05),ATB(06),ATB(07),ATB(08)/'INPU','T RF',' SIG','NAL '/
      DATA ATB(09),ATB(10),ATB(11),ATB(12)/'MAGN','ITUD','E IN',' REL'/
      DATA ATB(13),ATB(14),ATB(15),ATB(16)/'ATIV','E DB',' VS ','    '/
      DATA ATB(17),ATB(18),ATB(19),ATB(20)/'    ','FREQ','UENC','Y (M'/
      DATA ATB(21),ATB(22),ATB(23),ATB(24)/'HZ) ','   ','   ','   '/
      DATA ATB(25),ATB(26),ATB(27),ATB(28)/'    ','   ','   ','   '/
      CALL DBCON(TEMP4,LD,N)
      IF(IPLOT)514,515,514
  514 CALL DRAWP(LD,TEMP3,TEMP4,ITB,ATB)
      GO TO 300
  515 CALL PLOTG(TEMP3,TEMP4,LD,1,1,0,'FREQUENCY (MHZ)',15,'INPUT RF SIG
     1NAL MAGN (DB)',25,0.0,0.0,0.0,0.0,4.5,3.0)
  300 CONTINUE
C
CC APPLY TRANSDUCER EFFICIENCY BANDPASS FUNCTION
C
      DO 320 I=1,N
      DD=SINL(1,I)
  320 SINL(1,I)=DD*TE(I)
C
CC CALL INVERSE FFT SUBROUTINE TO CONVERT THE FREQUENCY DOMAIN SIGNAL
CC TO THE TIME DOMAIN
C
      CALL FOURT(SINL,N,1,1,1,WORK)
C
CC SCALE SHIFT TO SPATIAL DOMAIN AND TRANSFER SPATIAL VALUES TO TEMP
C REGISTERS FOR TABULAR OR GRAPHICAL OUTPUT
C
      DO 360 I=1,N
C FACTOR OF 100 TO CONVERT TO CM
      TEMP1(I)=I*DELTAX*100.
      TEMP2(I)=SINL(1,I)/N
      TEMP3(I)=SINL(2,I)/N
  360 TEMP4(I)=(((TEMP2(I))**2)+((TEMP3(I))**2))/NP
      DO 370 I=1,NP
      K=NXL+I
      TEMP5(I)=TEMP1(K)
  370 TEMP6(I)=SINL(1,K)/N
C
CC OUTPUT SPATIAL SIGNAL VALUES
C
      IF(ITEST)380,390,380
  380 WRITE(6,912)
      WRITE(6,900)DELTAT,DELTAF,DELTAX
      WRITE(6,913)
      WRITE(6,903)(TEMP1(I),TEMP2(I),TEMP3(I),TEMP4(I),I=NXL,NXU)
```

```
  390 IF(IGRAF)410,400,410
  400 WRITE(6,904)
      WRITE(6,911)
      CALL PLOTP(TEMP5,TEMP6,NP,0)
      GO TO 430
  410 IF(NP.LT.1599) GO TO 420
      TTB(1)=0.0
      TTB(2)=0.0
      TTB(3)=0.0
      TTB(4)=0.0
      DATA TTB(05),TTB(06),TTB(07),TTB(08)/'INPU','T RF',' SIG','NAL '/
      DATA TTB(09),TTB(10),TTB(11),TTB(12)/'VS D','ISTA','NCE ','(CM)'/
      DATA TTB(13),TTB(14),TTB(15),TTB(16)/'    ','    ','    ','    '/
      DATA TTB(17),TTB(18),TTB(19),TTB(20)/'    ','    ','    ','    '/
      DATA TTB(21),TTB(22),TTB(23),TTB(24)/'    ','    ','    ','    '/
      DATA TTB(25),TTB(26),TTB(27),TTB(28)/'    ','    ','    ','    '/
      IF(IPLOT)516,517,516
  516 CALL DRAWP(NP,TEMP5,TEMP6,ITB,TTB)
      GO TO 430
  517 CALL PLOTG(TEMP5,TEMP6,NP,1,1,0,'DISTANCE (CM)',13,'INPUT RF SIGNA
     1L MAGNITUDE',25,0.0,0.0,0.0,0.0,4.5,3.0)
      GO TO 430
  420 WRITE(6,914)
      WRITE(6,904)
      WRITE(6,911)
      CALL PLOTP(TEMP5,TEMP6,NP,0)
  430 CONTINUE
C
CC  SHIFT SIGNAL SPATIAL VALUES TO 3*N REGISTER FOR TIME VARIANCE
C
      DO 460 I=1,N
  460 F(I)=0.0
      DO 470 I=N1,N2
      K=I-N1+1
  470 F(I)=SINL(1,K)/N
      DO 480 I=N3,N4
  480 F(I)=0.0
C
CC  APPLY TIME VARIANCE, SHIFT PRODUCT TO TEMPORARY REGISTER FOR
C   INTERACTION WITH LASER WAVEFRONT
C
      DO 490 I=1,N
      K=N+I-NDELAY
  490 TEMP1(I)=F(K)
C
CC  INTERACTION OF ACOUSTIC AND OPTICAL WAVEFRONTS
C
      DO 500 I=1,N
```

```
      SINL(1,I)=TEMP1(I)*L(I)
  500 SINL(2,I)=0.0
C
C CALL FFT SUBROUTINE TO CONVERT THE SPATIAL INTERACTION TO THE
C FREQUENCY DOMAIN
C
      CALL FOURT(SINL,N,1,-1,0,WORK)
      DO 600 I=LL1,LU1
      TEMP1(I)=DELTAF*I/(1.0E+6)
C FACTOR OF 100 TO CONVERT TO CM
      TEMP2(I)=(((LFL*LAMBDA*DELTAF)*(I))/(VS))*100.
  600 TEMP4(I)=(SQRT(((SINL(1,I))**2)+((SINL(2,I))**2))/NP)**2
C
C APPLY DIFFRACTION EFFICIENCY BANDPASS FUNCTION
C
      DO 605 I=LL1,LU1
  605 TEMP4(I)=TEMP4(I)*BP(I)
C
C TRANSFER VALUES OF FUNCTION INREGION OF CONCERN TO TEMPORARY
C REGISTERS FOR TABULAR AND/OR GRAPHICAL OUTPUT
C
      DO 610 I=1,LD
      TEMP5(I)=((LFL*LMBDA*DELTAF*I)/(VS))*100.
      K=LL+I
      TEMP6(I)=TEMP1(K)
      TEMP7(I)=TEMP7(K)
  610 TEMP8(I)=TEMP4(K)
C
C OUTPUT IMAGE PLANE INTENSITY, DEFLECTION DISTANCE, AND FREQUENCY
C
      IF(ITEST)620,630,620
  620 WRITE(6,904)
      WRITE(6,915)
      WRITE(6,916)
      WRITE(6,917)(TEMP2(I),TEMP1(I),SINL(1,I),SINL(2,I),TEMP4(I),I=LL1,
     1LU1)
  630 IF(IGRAF)650,640,650
  640 IF(IDB)641,642,641
  641 WRITE(6,904)
      WRITE(6,918)
      CALL PLOTP(TEMP6,TEMP8,LD,0)
      WRITE(6,904)
      WRITE(6,919)
      CALL PLOTP(TEMP5,TEMP8,LD,0)
      GO TO 660
  642 CALL DBCON(TEMP8,LD,N)
      WRITE(6,904)
      WRITE(6,925)
```

```
      CALL PLOTP(TEMP6,TEMP8,LD,0)
      WRITE(6,904)
      WRITE(6,926)
      CALL PLOTP(TEMP5,TEMP8,LD,0)
      GO TO 660
  650 CONTINUE
  651 IF(IDB)652,653,652
  652 QTB(1)=0.0
      QTB(2)=0.0
      QTB(3)=0.0
      QTB(4)=0.0
      DATA QTB(05),QTB(06),QTB(07),QTB(08)/'IMAG','E PL','ANE ','INTE'/
      DATA QTB(09),QTB(10),QTB(11),QTB(12)/'NSIT','Y VS',' FRE','QUEN'/
      DATA QTB(13),QTB(14),QTB(15),QTB(16)/'CY (','MHZ)','    ','    '/
      DATA QTB(17),QTB(18),QTB(19),QTB(20)/'    ','    ','    ','    '/
      DATA QTB(21),QTB(22),QTB(23),QTB(24)/'    ','    ','    ','    '/
      DATA QTB(25),QTB(26),QTB(27),QTB(28)/'    ','    ','    ','    '/
      IF(IPLOT)518,519,518
  518 CALL DRAWP(LD,TEMP6,TEMP8,ITB,QTB)
      GO TO 520
  519 CALL PLOTG(TEMP6,TEMP8,LD,1,1,0,'FREQUENCY (MHZ)',15,'IMAGE PLANE
     1INTENSITY',21,0.0,0.0,0.0,0.0,4,5,3.0)
      UTB(1)=0.0
      UTB(2)=0.0
      UTB(3)=0.0
      UTB(4)=0.0
      DATA UTB(05),UTB(06),UTB(07),UTB(08)/'IMAG','E PL','ANE ','INTE'/
      DATA UTB(09),UTB(10),UTB(11),UTB(12)/'NSIT','Y VS',' DEF','LECT'/
      DATA UTB(13),UTB(14),UTB(15),UTB(16)/'ION ','DIST','ANCE','(CM)'/
      DATA UTB(17),UTB(18),UTB(19),UTB(20)/'    ','    ','    ','    '/
      DATA UTB(21),UTB(22),UTB(23),UTB(24)/'    ','    ','    ','    '/
      DATA UTB(25),UTB(26),UTB(27),UTB(28)/'    ','    ','    ','    '/
  520 CONTINUE
      IF(IPLOT)522,523,522
  522 CALL DRAWP(LD,TEMP5,TEMP8,ITB,UTB)
      GO TO 660
  523 CALL PLOTG(TEMP5,TEMP8,LD,1,1,0,'POSITION (CM)',13,'IMAGE PLANE IN
     1TENSITY',21,0.0,0.0,0.0,0.0,4.5,3.0)
      GO TO 660
  653 CALL DBCON(TEMP8,LD,N)
      BTB(1)=0.0
      BTB(2)=0.0
      BTB(3)=0.0
      BTB(4)=0.0
      DATA BTB(05),BTB(06),BTB(07),BTB(08)/'IMAG','E PL','ANE ','INTE'/
      DATA BTB(09),BTB(10),BTB(11),BTB(12)/'NSIT','Y IN',' REL','ATIV'/
      DATA BTB(13),BTB(14),BTB(15),BTB(16)/'E DB',' VS ','    ','    '/
      DATA BTB(17),BTB(18),BTB(19),BTB(20)/'    ','FREQ','UENC','Y (M'/
```

```
      DATA BTB(21),BTB(22),BTB(23),BTB(24)/'HZ) ',' ',' ',' '/
      DATA BTB(25),BTB(26),BTB(27),BTB(28)/' ',' ',' ',' '/
      IF(IPLOT)524,525,524
  524 CALL DRAWP(LD,TEMP6,TEMP8,ITB,BTB)
      GO TO 530
  525 CALL PLOTG(TEMP6,TEMP8,LD,1,1,0,'FREQUENCY (MHZ)',15,'IMAGE PLANE
     1INTENSITY (DB)',26,0.0,0.0,0.0,0.0,4.5,3.0)
      CTB(1)=0.0
      CTB(2)=0.0
      CTB(3)=0.0
      CTB(4)=0.0
      DATA CTB(05),CTB(06),CTB(07),CTB(08)/'IMAG','E PL','ANE ','INTE'/
      DATA CTB(09),CTB(10),CTB(11),CTB(12)/'NSIT','Y IN',' REL','ATIV'/
      DATA CTB(13),CTB(14),CTB(15),CTB(16)/'E DB',' VS ',' ',' '/
      DATA CTB(17),CTB(18),CTB(19),CTB(20)/' ','POSI','TION',' (CM'/
      DATA CTB(21),CTB(22),CTB(23),CTB(24)/')',' ',' ',' '/
      DATA CTB(25),CTB(26),CTB(27),CTB(28)/' ',' ',' ',' '/
  530 CONTINUE
      IF(IPLOT)531,532,531
  531 CALL DRAWP(LD,TEMP5,TEMP8,ITB,CTB)
      GO TO 660
  532 CALL PLOTG(TEMP5,TEMP8,LD,1,1,0,'POSITION (CM)',13,'IMAGE PLANE IN
     1TENSITY (DB)',26,0.0,0.0,0.0,0.0,4.5,3.0)
  660 CONTINUE
C
CC OUTPUT TRUE SPECTRUM OF INTERACTED PULSE
C
      IF(IGRAF)700,690,700
  690 IF(IDB)691,692,691
  691 WRITE(6,904)
      WRITE(6,920)
      CALL PLOTP(TEMP6,TEMP7,LD,0)
      GO TO 710
  692 CALL DBCON(TEMP7,LD,N)
      WRITE(6,904)
      WRITE(6,927)
      CALL PLOTP(TEMP6,TEMP7,LD,0)
      GO TO 710
  700 IF(IDB)701,702,701
  701 WTB(1)=0.0
      WTB(2)=0.0
      WTB(3)=0.0
      WTB(4)=0.0
      DATA WTB(05),WTB(06),WTB(07),WTB(08)/'MAGN','ITUD','E OF',' INT'/
      DATA WTB(09),WTB(10),WTB(11),WTB(12)/'ERAC','TED ','PULS','E VS'/
      DATA WTB(13),WTB(14),WTB(15),WTB(16)/' FRE','QUEN','CY (','MHZ)'/
      DATA WTB(17),WTB(18),WTB(19),WTB(20)/' ',' ',' ',' '/
      DATA WTB(21),WTB(22),WTB(23),WTB(24)/' ',' ',' ',' '/
```

```
      DATA WTB(25),WTB(26),WTB(27),WTB(28)/'    ','    ','    ','    '/
      IF(IPLOT)540,541,540
  540 CALL DRAWP(LD,TEMP6,TEMP7,ITB,WTB)
      GO TO 710
  541 CALL PLOTG(TEMP6,TEMP7,LD,1,1,0,'FREQUENCY (MHZ)',15,'INTERACTED P
     1ULSE MAGNITUDE',26,0.0,0.0,0.0,0.0,4.5,3.0)
      GO TO 710
  702 CALL DBCON(TEMP7,LD,N)
      DTB(1)=0.0
      DTB(2)=0.0
      DTB(3)=0.0
      DTB(4)=0.0
      DATA DTB(05),DTB(06),DTB(07),DTB(08)/'MAGN','ITUD','E OF',' INT'/
      DATA DTB(09),DTB(10),DTB(11),DTB(12)/'ERAC','TED ','PULS','E IN'/
      DATA DTB(13),DTB(14),DTB(15),DTB(16)/' REL','ATIV','E DB',' VS '/
      DATA DTB(17),DTB(18),DTB(19),DTB(20)/'    ','    ','FREQ','UENC'/
      DATA DTB(21),DTB(22),DTB(23),DTB(24)/'Y (M','HZ) ','    ','    '/
      DATA DTB(25),DTB(26),DTB(27),DTB(28)/'    ','    ','    ','    '/
      IF(IPLOT)544,545,544
  544 CALL DRAWP(LD,TEMP6,TEMP7,ITB,DTB)
      GO TO 710
  545 CALL PLOTG(TEMP6,TEMP7,LD,1,1,0,'FREQUENCY (MHZ)',15,'INTERACTED P
     1ULSE MAG (DB)',25,0.0,0.0,0.0,0.0,4.5,3.0)
  710 CONTINUE
  900 FORMAT('0','DELTAT=',E12.5,10X,'DELTAF=',E12.5,10X,'DELTAX=',E12.5
     1,///)
  901 FORMAT('0','INPUT PULSE CHARACTERISTICS',//)
  902 FORMAT('0',4X,'TIME',18X,'REAL',15X,'IMAGINARY',14X,'MAGNITUDE'
     1,////)
  903 FORMAT(E12.5,7X,F15.8,7X,F15.8,7X,F15.8)
  904 FORMAT('1')
  905 FORMAT('0','INPUT PULSE SHAPE',//)
  906 FORMAT('0','FOURIER TRANSFORM COEFFICIENTS',//)
  907 FORMAT('0',1X,'FREQUENCY',16X,'REAL',14X,'IMAGINARY',14X,'MAGNITUD
     1E',///)
  908 FORMAT('0','INPUT PULSE SPECTRUM, MAGNITUDE VS FREQUENCY(MHZ)',///
     1)
  909 FORMAT('0','DELTAF=',E12.5,//)
  910 FORMAT('0','NUMBER OF INPUT WAVEFORM SAMPLES INSUFFICIENT FOR VERS
     1ATEC PLOT')
  911 FORMAT('0','ACOUSTIC PULSE SHAPE VS DISTANCE(X=VS*T)',///)
  912 FORMAT('0','SIGNAL PULSE SPATIAL CHARACTERISTICS',//)
  913 FORMAT('0',2X,'DISTANCE',16X,'REAL',15X,'IMAGINARY',14X,'MAGNITUDE
     1',////)
  914 FORMAT('0','NUMBER OF SPATIAL VALUES INSUFFICIENT FOR VERSATEC PLO
     1T',//)
  915 FORMAT('0','SPATIAL FREQUENCY CHARACTERISTICS',//)
  916 FORMAT('0','DEFLECT DIST',8X,'FREQUENCY',15X,'REAL',17X,'IMAGINARY
```

```
     1',12X,'MAGNITJDE SQ',////)
  917 FORMAT(E12.5,7X,E12.5,7X,F15.8,7X,F15.8,7X,F15.8)
  918 FORMAT('0','IMAGE PLANE INTENSITY VS FREQUENCY (MHZ)',//)
  919 FORMAT('0','IMAGE PLANE INTENSITY VS DEFLECTION DISTANCE',//)
  920 FORMAT('0','INTERACTED PULSE SPECTRUM',///)
  921 FORMAT('0','GAUSSIAN LASER WAVEFRONT UTILIZED',/)
  922 FORMAT('0','PLANE LASER WAVEFRONT UTILIZED',/)
  923 FORMAT('0','INTERACTION LENGTH RATIO=',E12.5,//)
  924 FORMAT('0','INPUT PULSE SPECTRUM(RELATIVE DB) VS FREQUENCY(MHZ)',/
     1//)
  925 FORMAT('0','IMAGE PLANE INTENSITY(RELATIVE DB) VS FREQUENCY(MHZ)',
     1///)
  926 FORMAT('0','IMAGE PLANE INTENSITY(RELATIVE DB) VS POSITION',//)
  927 FORMAT('0','INTERACTED PULSE SPECTRUM(RELATIVE DB)',//)
  928 FORMAT('0','GAUSSIAN BEAM VALUES',//)
  929 FORMAT(E12.5,1X,E12.5,1X,E12.5,1X,E12.5,1X,E12.5,1X,E12.5)
  930 FORMAT('0','GAUSSIAN BEAMWIDTH =',E12.5,//)
      CALL PLOT(0.0,0.0,999)
      STOP
      END
      SUBROUTINE DBCON(DATA,NN,N)
      DIMENSION DATA(N)
      TL=0.0
      DO 3 I=1,NN
      TS=DATA(I)
      IF(TS.GE.TL)GO TO 2
      GO TO 3
    2 TL=TS
    3 CONTINUE
      DO 7 I=1,NN
      DATA(I)=(80.)+(10.*ALOG(DATA(I)/TL))
      IF(DATA(I).LE.(0.))GO TO 5
      GO TO 6
    5 DATA(I)=0.0
    6 DATA(I)=DATA(I)-80.
    7 CONTINUE
      RETURN
      END
```

APPENDIX B

DYNAMIC ACOUSTOOPTIC SPECTRUM ANALYZER PROGRAM

The dynamic acoustooptic spectrum analyzer program (TAOSA) is essentially a variation of the AOSA Fortran program. It computes the time delay to shift the acoustic pulse outside of the optical interaction aperture and then incrementally decreases this delay to simulate the action of the pulse as it transits the optical interaction region. The system response time may be simulated by adding a fixed time delay.

The variables used in the program are discussed both within the program and in Appendix A. An additional variable, TINT, is added as an acceleration factor that varies the increment size based on the level of intensity of the incident laser beam.

The results are presented as a three-dimensional isometric or perspective plot. Perspective users at the Naval Postgraduate School should refer to the W. R. Church Computer Center for detailed information on the three-dimensional plotting routine PLT3D1 in use.

```
C
C   ACOUSTO-OPTICAL SPECTRUM ANALYZER DYNAMIC MODEL
C
      DIMENSION WK(24,400,3),D(24,400),SINL(2,6400),WORK(12800),F(19200)
     1,TEMP1(6400),TEMP2(6400),TEMP3(6400),TEMP4(6400),TEMP5(6400),BP(64
     200),KX(3000),KY(3000),Y(400),X(24),SIZE(2),FF(2),DINL(2,6400),TE(6
     3400)
      REAL*8 TTL(12),DTL(12),STL(12)
      REAL*4 L(6400)
      LOGICAL*1 IDN(24,400)
      REAL LMBDA,LFL,LZERO,LLO,LW
      DATA TTL(01),TTL(02),TTL(03)/'IMAGE PL','ANE INTE','NSITY VS'/
      DATA TTL(04),TTL(05),TTL(06)/' POSITIO','N AND TI','ME      '/
      DATA TTL(07),TTL(08),TTL(09)/'       (','RELATIVE',' INTENSI'/
      DATA TTL(10),TTL(11),TTL(12)/'TY)    ',',        ','        '/
      DATA DTL(01),DTL(02),DTL(03)/'IMAGE PL','ANE INTE','NSITY VS'/
      DATA DTL(04),DTL(05),DTL(06)/' POSITIO','N AND TI','ME      '/
      DATA DTL(07),DTL(08),DTL(09)/'       (','DB RELAT','IVE)    '/
      DATA DTL(10),DTL(11),DTL(12)/'        ',',       ','        '/
C
C  INITIALIZATION OF PARAMETERS UTILIZED IN THE AOSA MODEL PROGRAM
C
C            N        = NUMBER OF SAMPLES PER RECORD LENGTH
C            NP       = NUMBER OF SAMPLES PER PULSE LENGTH
C            FCO      = CENTRAL FREQUENCY OF BRAGG CELL
C            DCELL    = EFFECTIVE APPERTURE OF BRAGG CELL
C            PULSE    = PULSE LENGTH (TYPICALLY 1 MICROSECOND)
C            PERIOD   = RECORD LENGTH
C            LL       = LOWER FREQUENCY INCREMENT FOR BANDWIDTH OF CELL
C            LU       = UPPER FREQUENCY INCREMENT FOR BANDWIDTH OF CELL
C            LD       = NUMBER OF DELTAF CONTAINED IN BANDWIDTH OF CELL
C            NXL      = LOWER SPATIAL INCREMENT FOR PULSE WIDTH
C            NXU      = UPPER SPATIAL INCREMENT FOR PULSE WIDTH
C            NDL      = LOWER SPATIAL INCREMENT FOR CELL EFF APERTURE
C            NDU      = UPPER SPATIAL INCREMENT FOR CELL EFF APERTURE
C            LZERO    = CHARACTERISTIC INTERACTION LENGTH OF BRAGG CELL
C            LLO      = RATIO OF INTERACTION LENGTH TO CHARACTERISTIC
C                       INTERACTION LENGTH OF BRAGG CELL
C            LW       = INTERACTION LENGTH
C            VS       = ACOUSTIC VELOCITY
C            SPOT     = DESIRED DETECTOR ARRAY SPOT SIZE
C            LMBDA    = LASER WAVELENGTH
C            BW       = BEAM WIDTH OF COLLIMATED GAUSSIAN BEAM (3DB)
C            EFFD     = EFFECTIVE DIAMETER OF EXIT BEAM FROM BRAGG CELL
C            THETAO   = DEFLECTION ANGLE OF BRAGG CELL CENTER FREQUENCY
C            REFIND   = REFRACTIVE INDEX OF BRAGG CELL MATERIAL
C            LFL      = FOURIER TRANSFORM LENS FOCAL LENGTH
C            WZERO    = MINIMUM SPOT SIZE
```

```
C             DELTAT  = TIME SAMPLE INCREMENT = PERIOD/N
C             DELTAF  = FREQUENCY RESOLUTION INCREMENT = 1/PERIOD
C             DELTAX  = SPATIAL RESOLUTION INCREMENT =VS*DELTAT
C             TDELAY  = TIME VARIANCE IN SECS (SHOULD BE INTEGRAL
C                       MULTIPLE OF DELTAT)
C             TINT    = TIME INTERVAL ACCELERATION FACTOR
C
      N=6400
      N1=N+1
      N2=N*2
      N3=N2+1
      N4=N*3
      PI=3.141592654
      DCELL=39.0E-3
      VS=3.90E+3
      LMBDA=6.328E-7
      REFIND=2.2
      SPOT=26.0E-6
      BW=1.945E-3
      LW=5.08E-2
      PULSE=1.0E-6
      PERIOD=10.*PULSE
      NP=N*PULSE/PERIOD
      DELTAT=PERIOD/N
      DELTAF=1./PERIOD
      DELTAX=VS*DELTAT
      NXL=N/2-NP/2
      NXU=N/2+NP/2
      NXL1=NXL+1
      NXU1=NXU+1
      NDD=(DCELL/DELTAX)+1
      NDL=N/2-NDD/2
      NDU=N/2+NDD/2
      NDL1=NDL+1
      NDU1=NDU+1
      LL=(5.0E+7)/DELTAF
      LU=(9.0E+7)/DELTAF
      LL1=LL+1
      LU1=LU+1
      LD=LU-LL
      FC0=7.0E+7
      SCALE=0.0
      TL=0.0
      THETA0=(LMBDA*FC0)/(2.*VS)
      LZERO=(REFIND/LMBDA)*(COS(THETA))*((VS**2)/(FC0**2))
      LL0=LW/LZERO
C
C INITIATE PARAMETERS FOR PLT3D1 ROUTINE
```

```
C
      NROW=24
      NCOL=400
      ALPHA=30.
      BETA=45.
      FF(1)=0.0
      FF(2)=FF(1)
      SIZE(1)=6.0
      SIZE(2)=SIZE(1)
      NKXY=3000
      LINES=0
C
CC SET IWAVE  = 1 FOR GAUSSIAN WAVEFRONT
CC            = 0 FOR PLANE WAVEFRONT
CC SET IDB    = 1 IF INTENSITY VALUES ARE TO DE DISPLAYED IN MAGNITUDE
CC            = 0 IF INTENSITY VALUES ARE TO BE DISPLAYED IN RELATIVE DB
CC SET ITRANS = 1 IF PHASED ARRAY TRANSDUCER IS UTILIZED
CC            = 0 IF SIMPLE TRANSDUCER IS UTILIZED
C
      IWAVE=1
      IDB=1
      ITRANS=1
C
CC INITIALIZE D ARRAY VALUES AT ZERO
C
      DO 1 JI=1,NROW
      DO 1 JJ=1,NCOL
      D(JI,JJ)=0.0
    1 CONTINUE
C
CC INITIATE LOOP TO PROVIDE MULTIPLE TIME VARIANCE FOR DYNAMIC MODEL
C
      IF(IWAVE)550,551,550
  550 TINT=-3.92E-6
      GO TO 552
  551 TINT=5.0E-7
  552 CONTINUE
      TDELAY=((NDD/2)*DELTAT)+TINT
      DO 800 II=1,NROW
      TDELAY=TDELAY-(40.0*DELTAT)
C
CC INPUT THE TIME DOMAIN SIGNAL
C
      DO 2 I=1,NXL
      SINL(1,I)=0.0
    2 SINL(2,I)=0.0
      DO 3 I=NXL,NXU
C ***************************************************************
```

```
      FW0=7.0E+7
      FW1=0.0
CCCC                  SIMPLE MONO/MULTIPLE TONES
      SINL(1,I)=(COS(2.*PI*FW0*I*PERIOD/N))+(COS(2.*PI*FW1*I*PERIOD/N))
CCCC                  SIMPLE TWO FREQUENCY BEAT
C     SINL(1,I)=(COS(2.*PI*FW0*I*PERIOD/N))*(COS(2.*PI*FWI*I*PERIOD/N))
CCCC                  PM MODULATION
C     SINL(1,I)=(COS((2.*PI*FW0*I*PERIOD/N)+(((I-NXL)/NP)*2.*PI*FW1*I*
C    1PERIOD/N)))
CCCC                  FM MODULATION
C     SINL(1,I)=(COS((2.*PI*FW0*I*PERIOD/N)+(BBETA*SIN(2.*PI*FM*PERIOD
C    1*I/N))))
C     FM=5.0E+6
C     BBETA=8.0
CCCC                  LINEAR CHIRP
C     SINL(1,I)=COS((2.*PI*I*(PERIOD/N)*(FW0+(FM*(I-NXL)))))
C     FM=1.25E+5
C ***************************************************************
    3 SINL(2,I)=0.0
      DO 4 I=NXU1,N
      SINL(1,I)=0.0
    4 SINL(2,I)=0.0
C
CC CALL AUTOSCALE SUBROUTINE TO PROVIDE SCALING PARAMETER
C
      IF(II.EQ.1)GO TO 5
      GO TO 6
    5 CALL ASCALE(SINL,DINL,WORK,TEMP2,LL,LD,N,N2,SCALE,NP,TL)
      WRITE(6,903)SCALE
    6 CONTINUE
C
CC COMPUTE FOURIER TRANSFORM LENS FOCAL LENGTH
C
      EFFD=DCELL
      LFL=EFFD*SPOT/LMBDA
C
CC INPUT DIFFRACTION EFFICIENCY BANDPASS FUNCTION
C
      IF(ITRANS)9,16,9
    9 DO 10 I=1,LL
   10 BP(I)=0.0
      DO 11 I=LL,LU
   11 BP(I)=.87
      DO 12 I=LU1,N
   12 BP(I)=0.0
      GO TO 23
   16 DO 20 I=1,N
      IF(I*DELTAF-FCO)17,18,17
```

```
   17 AA=((PI/2.)*LLO*(((I*DELTAF/FCO)-((I*DELTAF/FCO)**2)))
      BB=SIN(AA)
      CC=(BB/AA)**2
      GO TO 19
   18 CC=1.0
   19 CONTINUE
   20 BP(I)=CC
   23 CONTINUE
C
C  INPUT TRANSDUCER EFFICIENCY BANDPASS FUNCTION (TOPHAT ASSUMED)
C
      DO 25 I=1,N
   25 TE(I)=1.0
C
C  INPUT THE TRUNCATED LASER WAVEFRONT
C
      IF(IWAVE)205,210,205
  205 DO 206 I=1,NDL
  206 L(I)=0.0
      DO 207 I=NDL,NDU
      FLTI= FLOAT(I)/FLOAT(N)
  207 L(I)=EXP(-4.*((DCELL/(2.*BW))**2)*((FLTI-.5)**2))
      DO 208 I=NDU1,N
  208 L(I)=0.0
      GO TO 240
  210 DO 221 I=1,NDL
  221 L(I)=0.0
      DO 222 I=NDL,NDU
  222 L(I)=1.0
      DO 223 I=NDU1,N
  223 L(I)=0.0
  240 CONTINUE
C
C  CALL THE FFT SUBROUTINE TO CONVERT THE TIME DOMAIN SIGNAL TO THE
C  FREQUENCY DOMAIN
C
      CALL FOURT(SINL,N,1,-1,0,WORK)
C
C  APPLY TRANSDUCER EFFICIENCY BANDPASS FUNCTION
C
      DO 320 I=1,N
      DD=SINL(1,I)
  320 SINL(1,I)=DD*TE(I)
C
C  CALL INVERSE FFT SUBROUTINE TO CONVERT THE FREQUENCY DOMAIN SIGNAL
C  TO THE TIME DOMAIN
C
      CALL FOURT(SINL,N,1,1,1,WORK)
```

```
C
C  SHIFT SIGNAL SPATIAL VALUES TO 3*N REGISTER FOR TIME VARIANCE
C
      DO 460 I=1,N
  460 F(I)=0.0
      DO 470 I=N1,N2
      K=I-N1+1
  470 F(I)=SINL(1,K)/N
      DO 480 I=N3,N4
  480 F(I)=0.0
C
C  APPLY TIME VARIANCE, SHIFT PRODUCT TO TEMPORARY REGISTER FOR
C  INTERACTION WITH LASER WAVEFRONT
C
      NDELAY=((TDELAY*VS)/DELTAX)
      DO 490 I=1,N
      K=N+I+NDELAY
  490 TEMP1(I)=F(K)
C
C  INTERACTION OF ACOUSTIC AND OPTICAL WAVEFRONTS
C
      DO 500 I=1,N
      SINL(1,I)=TEMP1(I)*L(I)
  500 SINL(2,I)=0.0
C
C  CALL FFT SUBROUTINE TO CONVERT THE SPATIAL INTERACTION TO THE
C  FREQUENCY DOMAIN
C
      CALL FOURT(SINL,N,1,-1,0,WORK)
      DO 600 I=LL1,LU1
      TEMP1(I)=DELTAF*I
      TEMP2(I)=((LFL*LMBDA*DELTAF)*(I-LL))/(VS)
      TEMP3(I)=SQRT(((SINL(1,I))**2)+((SINL(2,I))**2))/NP
  600 TEMP4(I)=(SQRT(((SINL(1,I))**2)+((SINL(2,I))**2))/NP)**2
C
C  APPLY DIFFRACTION EFFICIENCY BANDPASS FUNCTION
C
      DO 610 I=LL1,LU1
  610 TEMP4(I)=TEMP4(I)*BP(I)
      DO 700 JJ=1,NCOL
      K=LL+JJ
      KK=NROW+1-II
  700 D(KK,JJ)=TEMP4(K)*SCALE
  800 CONTINUE
      IF(IDB)810,876,810
  810 CONTINUE
      DO 850 I=1,NCOL
  850 Y(I)=I
```

```
      DO 860 I=1,NROW
  860 X(I)=I*20
      IF(IWAVE)870,871,870
  870 WRITE(6,900)
      WRITE(6,902)LLO
      GO TO 875
  871 WRITE(6,901)
      WRITE(6,902)LLO
  875 CONTINUE
      CALL PLT3D1(X,NROW,Y,NCOL,D,ALPHA,BETA,FF,TTL,SIZE,WK,IDN,KX,KY,NK
     1XY,LINES)
      GO TO 899
  876 CONTINUE
      DO 885 II=1,NROW
      DO 880 JJ=1,NCOL
      TEMP3(JJ)=D(II,JJ)/(SCALE)
  880 CONTINUE
      CALL DBCON(TEMP3,NCOL,N,SCALE,TL)
      DO 881 JJ=1,NCOL
  881 D(II,JJ)=TEMP3(JJ)*3.2
  885 CONTINUE
      DO 886 I=1,NCOL
  886 Y(I)=I
      DO 887 I=1,NROW
  887 X(I)=I*20
      IF (IWAVE)888,889,888
  888 WRITE(6,900)
      WRITE(6,902)LLO
      GO TO 890
  889 WRITE(6,901)
      WRITE(6,902)LLO
  890 CONTINUE
      CALL PLT3D1(X,NROW,Y,NCOL,D,ALPHA,BETA,FF,DTL,SIZE,WK,IDN,KX,KY,
     1 NKXY,LINES)
  899 CONTINUE
  900 FORMAT('0','GAUSSIAN LASER WAVEFRONT UTILIZED',/)
  901 FORMAT('0','PLANE LASER WAVEFRONT UTILIZED',/)
  902 FORMAT('0','INTERACTION LENGTH RATIO=',E12.5,//)
  903 FORMAT('0','SCALE FACTOR=',E12.5,//)
      STOP
      END
      SUBROUTINE ASCALE(DAT1,DAT2,WORK,TEMP2,LL,LD,N,N2,TSCALE,NP,TL)
      DIMENSION DAT1(2,N),DAT2(2,N),WORK(N2),TEMP2(N)
      DO 1 I=1,N
      DAT2(1,I)=DAT1(1,I)
    1 DAT2(2,I)=DAT1(2,I)
      CALL FOURT(DAT2,N,1,-1,0,WORK)
      DO 2 I=1,LD
```

```
      K=LL+I
    2 TEMP2(I)=(SQRT(((DAT2(1,K))**2)+((DAT2(2,K))**2))/NP)**2
      DO 6 I=1,LD
      TS=TEMP2(I)
      IF(TS.GE.TL)GO TO 5
      GO TO 6
    5 TL=TS
    6 CONTINUE
      X=TL
      DO 10 I=1,50
      IF(X.GT.(.25))GO TO 11
      X=10.*X
   10 CONTINUE
   11 CONTINUE
      K1=I-1
      DO 12 J=1,20
      Y=X*(20-J)*(.05)
      IF(Y.LE.(.26))GO TO 13
   12 CONTINUE
   13 CONTINUE
      K2=J
      FCT=((10.**K1)*((20-K2)*(.05)))
      TSCALE=1000.*FCT
      RETURN
      END
      SUBROUTINE DBCON(DATA,NN,N,TSCALE,TL)
      DIMENSION DATA(N)
      DO 10 I=1,NN
      DATA(I)=80.+(10.*ALOG(DATA(I)/TL))
      IF(DATA(I).LE.(0.))GO TO 6
    5 GO TO 10
    6 DATA(I)=0.0
   10 CONTINUE
      RETURN
      END
C*
//GO.PLOTPARM DD *
 &PLOT  LYNES=900  &END
```

APPENDIX C

ARBITRARY PROFILE SOLUTION DETAILS
(after Ref. 15)

The complex transmission coefficient $T(\phi)$ is defined as

$$T(\phi) = 4k^{a}_{1x}(\alpha_2 - \alpha_1)(A_{ba} - B_{ba}) \exp(-jk^{a}_{3x}L)/\mathrm{Det} \tag{C1}$$

where

$$\mathrm{Det} = (\alpha_2 A_{aa} - \alpha_1 B_{aa})(\alpha_1 A_{bb} - \alpha_2 B_{bb}) - \alpha_1\alpha_2(A_{ab} - B_{ab})(A_{ba} - B_{ba}) \tag{C2}$$

$$\alpha_1 = \frac{1}{Mk^2\epsilon_2}\{\beta^2_{-1} - \beta^2_0 + [(\beta^2_{-1} - \beta^2_0)^2 + (Mk^2_0\epsilon_2)^2]^{1/2}\}, \tag{C3}$$

$$\alpha_2 = \frac{1}{Mk^2\epsilon_2}\{\beta^2_{-1} - \beta^2_0 - [(\beta^2_{-1} - \beta^2_0)^2 + (Mk^2_0\epsilon_2)^2]^{1/2}\}, \tag{C4}$$

$$A_{\rho\sigma} = k^{a}_{2x}\left(1 + \frac{k^{\rho}_{1x}}{k^{a}_{2x}}\right)\left(1 + \frac{k^{\sigma}_{1x}}{k^{a}_{2x}}\right) \times [\exp(-ik^{a}_{2x}L) - R^{a\rho}_{21}R^{a\sigma}_{23}\exp(ik^{a}_{2x}L)], \tag{C5}$$

$$B_{\rho\sigma} = k^{b}_{2x}\left(1 + \frac{k^{\rho}_{1x}}{k^{b}_{2x}}\right)\left(1 + \frac{k^{\sigma}_{1x}}{k^{b}_{2x}}\right) \times [\exp(-ik^{b}_{2x}L) - R^{b\rho}_{21}R^{b\sigma}_{23}\exp(ik^{b}_{2x}L)], \tag{C6}$$

$$R^{\rho\sigma}_{ij} = \frac{k^{\rho}_{ix} - k^{\sigma}_{jx}}{k^{\rho}_{ix} + k^{\sigma}_{jx}} \quad \rho,\sigma = a,b, \quad i,j = 1,2,3, \tag{C7}$$

$$k^{a}_{1x} = k_0\sqrt{\epsilon_1}\cos\theta = \sqrt{(2\pi/\lambda)^2\epsilon_1 - \beta^2_0} \tag{C8}$$

$$k^{b}_{1x} = (k^2_0\epsilon_1 - \beta^2_{-1})^{1/2} \tag{C9}$$

$$k^{a}_{2x} = \{[1 - (1/2)M\alpha_1]k^2_0\epsilon_2 - \beta^2_0\}^{1/2}, \tag{C10}$$

$$k^{b}_{2x} = \{[1 - (1/2)M\alpha_2)k^2_0\epsilon_2 - \beta^2_0\}^{1/2}, \tag{C11}$$

$$k^{a}_{3x} = (k^2_0\epsilon_3 - \beta^2_0)^{1/2} \tag{C12}$$

$$k^{b}_{3x} = (k^2_0\epsilon_3 - \beta^2_{-1})^{1/2} \tag{C13}$$

M = index of Modulation of the permittivity of the Bragg cell medium

ϵ_1 = relative permittivity of air ≈ 1

ε_2 = relative permittivity of the Bragg cell medium

$\varepsilon_3 = \varepsilon_1$

θ = output angle

$k_0 = 2\pi/\lambda$

$$\beta_0 = (2\pi/\lambda)\sqrt{\varepsilon_1}\sin\theta \tag{C14}$$

$$\beta_{-1} = \beta_0 - 2\pi/d \tag{C15}$$

LIST OF REFERENCES

1. Koenig, J. A., "Problem Definition," Proceedings of the Society of Photo-Optical Instrumentation Engineers, V. 214, Acousto-Optic Bulk Wave Devices, Monterey, California, November 1979.

2. Regan, F. W., Acoustooptic Spectrum Analysis and Narrowband Interference Excision in Wideband Signal Environments, Engineer's Thesis, Naval Postgraduate School, Monterey, California, 1979.

3. Smith, D. E., Acoustooptic Spectral Excision of Narrowband Interference, Engineer's Thesis, Naval Postgraduate School, Monterey, California, 1980.

4. Korpel, A., "Acousto-optics," Applied Solid State Science, V. 3, R. Wolfe, Ed., Academic Press, 1972.

5. Hecht, D. L., "Spectrum Analysis Using Acousto-Optic Devices," Optical Engineering, pp. 461-466, September/October 1977.

6. Born, M. and Wolf, E., Principles of Optics, New York, Pergamon Press, 1975.

7. Rosenthal, A. H., "Application of Ultrasonic Light Modulation to Signal Recording, Display, Analysis and Communication," IRE Transactions on Ultrasonic Engineering, V. UE-8, pp. 1-5, March 1961.

8. Korpel, A., Adler, R., Desmares, P., and Watson, W., "A Television Display Using Acoustic Deflection of Coherent Light," Applied Optics, V. 5, pp. 1667-1674, October 1966.

9. Lambert, L. B., "Wide-Band Instantaneous Spectrum Analyzers Employing Delay-Line Light Modulators, IRE National Convention Record, V. 10, pp. 69-75, March 1972.

10. Gordon, E. I., "A Review of Acoustooptical Deflection and Modulation Devices," Applied Optics, V. 5, pp. 1629-1639, October 1966.

11. Johnson, R. V., "Temporal Response of the Acoustooptic Modulator: Physical Optics Model in the Low Scattering Efficiency Limit," Applied Optics, V. 17, pp. 1507-1518, May 1978.

12. Chu, R. E., Kong, J. A., and Tamir, T., "Diffraction of Gaussian Beams by a Periodically Modulated Layer," Journal of the Optical Society of America, V. 67, pp. 1555-1561, November 1977.

13. Chu, R. S., and Tamir, T., "Bragg Diffraction of Gaussian Beams by Periodically Modulated Media," Journal of the Optical Society of America, V. 66, pp. 220-225, March 1976.

14. Chu, R. S., and Tamir, T., "Diffraction of Gaussian Beams by Periodically Modulated Media for Incidence Close to a Bragg Angle," Journal of the Optical Society of America, V. 66, pp. 1438-1440, December 1976.

15. Chu, R. S., and Kong, J. A., "Diffraction of Optical Beams with Arbitrary Prifiles by a Periodically Modulated Layer," Journal of the Optical Society of America, V. 70, pp. 1-6, January 1980.

16. Kong, J. A., "Second-order Coupled-mode Equations for Spatially Periodic Media," Journal of the Optical Society of America, V. 67, pp. 825-829, June 1977.

17. Lindley, J. P., and Nurse, J. P., "Spectrum Analysis Using Acoustooptic Techniques,: Proceedings of the Society of Photo-optical Instrumentation Engineers, V. 128, Effective Utilization of Optics in Radar Systems, Huntsville, Alabama, September 1977.

18. Schulman, A. R., "Principles of Optical Data Processing for Engineers," NASA/GSFC Report X-521-66-434, August 1965.

19. Vatz, B. W., "Specification and Error Budgeting of Optical Signal Processors," U. S. Army Ballistic Missile Defense Advanced Technology Center, Huntsville, Alabama, Report of April 1977.

20. Hecht, D. L., "Multifrequency Acoustooptic Diffraction," IEEE Transactions on Sonics and Ultrasonics, V. SU-24, pp. 7-18, January 1977.

21. Hecht, D. L., "Acoustooptic Signal Processing Device Performance," Proceedings of the Society of Photo-optical Instrumentation Engineers, V. 180, Real Time Signal Processing II, pp. 201-211, April 1979.

22. Pinnow, D. A., "Acoustooptic Light Deflection: Design Considerations for First Order Beam Steering Transducers," IEEE Transactions on Sonics and Ultrasonics, V. SU-18, pp. 209-214, October 1971.

23. Chang, I. C., "Acoustooptic Devices and Applications," IEEE Transactions on Sonics and Ultrasonics, V. SU-23, pp. 2-23, January 1976.

INITIAL DISTRIBUTION LIST

		No. Copies
1.	Defense Technical Information Center Cameron Station Alexandria, Virginia 22314	2
2.	Library, Code 0142 Naval Postgraduate School Monterey, California 93940	2
3.	Department Chairman, Code 62 Department of Electrical Engineering Naval Postgraduate School Monterey, California 93940	1
4.	Professor John P. Powers, Code 62Po Department of Electrical Engineering Naval Postgraduate School Monterey, California 93940	5
5.	Professor H. A. Titus, Code 62Ts Department of Electrical Engineering Naval Postgraduate School Monterey, California 93940	1
6.	Commander, Naval Electronic Systems Command Naval Electronic Systems Command Headquarters ATTN: ELEX-615 Washington, DC 20360	3
7.	Department of Defense ATTN: Group R551 Fort George G. Mead, Maryland 20755	1
8.	Commanding Officer Naval Research Laboratory ATTN: Code 7924 Washington, DC 20360	1
9.	Commanding Officer Naval Research Laboratory ATTN: Code 7914C Washington, DC 20360	1

10. Professor W. H. Ku 1
Department of Electrical Engineering
408 Phillips Hall
Ithaca, New York

11. LCDR Michael J. Carmody, USN 2
6234 60th Road
Maspeth, New York 11378

Thesis
C26136 Carmody
c.1 Acoustooptical spectrum analysis modeling.

193749